Université de Montréal

Regenerative Potential of Corneal Endothelium from Patients with Fuchs Endothelial Corneal Dystrophy

par
M. Nour Haydari, MD, MSc

Département d'ophtalmologie
Faculté de médecine

Thèse présentée à la Faculté de médecine
en vue de l'obtention du grade de
DOCTORAT en Sciences biomédicales
option générale

Décembre, 2012

Université de Montréal
Faculté des études supérieures et postdoctorales

Cette thèse intitulée

Regenerative Potential of Corneal Endothelium from Patients with Fuchs Endothelial Corneal Dystrophy
Potentiel régénératif de l'endothélium cornéen du patient atteint d'une dystrophie de Fuchs

présentée par
M. Nour Haydari, MD, MSc

a été évaluée par un jury composé des personnes suivantes :

Paul Harasymowycz, MD, FRCSC; président-rapporteur
Isabelle Brunette, MD, FRCSC; directrice de recherche
Stéphanie Proulx, PhD; co-directrice
Jean Deschenes, MD, FRCSC; membre du jury
Sanjay V. Patel, MD; examinateur externe
Paul Thompson, MD, FRCSC; représentant du doyen de la FES

Résumé

La dystrophie cornéenne endothéliale de Fuchs (FECD, pour l'abréviation du terme anglais « Fuchs endothelial corneal dystrophy ») est une maladie de l'endothélium cornéen. Sa pathogenèse est mal connue. Aucun traitement médical n'est efficace. Le seul traitement existant est chirurgical et consiste dans le remplacement de l'endothélium pathologique par un endothélium sain provenant de cornées de la Banque des yeux. Le traitement chirurgical, en revanche, comporte 10% de rejet immunologique. Des modèles expérimentaux sont donc nécessaires afin de mieux comprendre cette maladie ainsi que pour le développement de traitements alternatifs. Le but général de cette thèse est de développer un modèle expérimental de la FECD en utilisant le génie tissulaire. Ceci a été réalisé en trois étapes. 1) Tout d'abord, l'endothélium cornéen a été reconstruit par génie tissulaire en utilisant des cellules endothéliales en culture, provenant de patients atteints de FECD. Ce modèle a ensuite été caractérisé *in vitro*. Brièvement, les cellules endothéliales cornéennes FECD ont été isolées à partir de membranes de Descemet prélevées lors de greffes de cornée. Les cellules au deuxième ou troisième passages ont ensuite été ensemencées sur une cornée humaine préalablement décellularisée. Suivant 2 semaines de culture, les endothélia cornéens reconstruits FECD (n = 6) ont été évalués à l'aide d'histologie, de microscopie électronique à transmission et d'immunomarquages de différentes protéines. Les endothélia cornéens reconstruits FECD ont formé une monocouche de cellules polygonales bien adhérées à la membrane de Descemet. Les immunomarquages ont démontré la présence des protéines importantes pour la fonctionnalité de l'endothélium cornéen telles que Na^+-K^+/ATPase α1 et Na^+/HCO_3^-, ainsi qu'une expression faible et uniforme de la protéine clusterine. 2) Deux techniques chirurgicales (DSAEK ; pour « Descemet stripping automated endothelial keratoplasty » et la kératoplastie pénétrante) ont été comparées pour la transplantation cornéenne dans le modèle animal félin. Les paramètres comparés incluaient les défis chirurgicaux et les résultats cliniques. La technique « DSAEK » a été difficile à effectuer dans le modèle félin. Une formation rapide de fibrine a été observée dans tous les cas DSAEK (n = 5). 3) Finalement, la fonctionnalité *in vivo* des endothélia cornéens reconstruits FECD a été

évaluée (n = 7). Les évaluations *in vivo* comprenaient la transparence, la pachymétrie et la tomographie par cohérence optique. Les évaluations post-mortem incluaient la morphométrie des cellules endothéliales, la microscopie électronique à transmission et des immunomarquage de protéines liées à la fonctionnalité. Après la transplantation, la pachymétrie a progressivement diminué et la transparence a progressivement augmenté. Sept jours après la transplantation, 6 des 7 greffes étaient claires. La microscopie électronique à transmission a montré la présence de matériel fibrillaire sous-endothélial dans toutes les greffes d'endothelia reconstruits FECD. Les endothélia reconstruits exprimaient aussi des protéines Na^+-K^+/ATPase et Na^+/HCO_3^-. En résumé, cette thèse démontre que les cellules endothéliales de la cornée à un stade avancé FECD peuvent être utilisées pour reconstruire un endothélium cornéen par génie tissulaire. La kératoplastie pénétrante a été démontrée comme étant la procédure la plus appropriée pour transplanter ces tissus reconstruits dans l'œil du modèle animal félin. La restauration de l'épaisseur cornéenne et de la transparence démontrent que les greffons reconstruits FECD sont fonctionnels *in vivo*. Ces nouveaux modèles FECD démontrent une réhabilitation des cellules FECD, permettant d'utiliser le génie tissulaire pour reconstruire des endothelia fonctionnels à partir de cellules dystrophiques. Les applications potentielles sont nombreuses, y compris des études physiopathologiques et pharmacologiques.

Mots-clés: Dystrophie cornéenne endothéliale de Fuchs, transplantation de la cornée, génie tissulaire, cellules endothéliales cornéennes, culture cellulaire, modèle félin.

Abstract

Fuchs endothelial corneal dystrophy (FECD) is a primary disease of the corneal endothelium. Its pathogenesis is poorly understood. No medical treatment is effective. Surgical treatment (the only available treatment) carries 10% of immunogenic rejection. Experimental models are needed in order to better understand the disease and to investigate potential autologous treatments (to prevent immunogenic rejection). The overall goal of this thesis is to develop an experimental model for FECD using tissue engineering. This was achieved in three steps. 1) An *in vitro* tissue-engineered FECD model was created and characterized. Briefly, Descemet's membranes from patients with late-stage FECD undergoing Descemet's Stripping Automated Endothelial Keratoplasty (DSAEK) were used to isolate and culture FECD endothelial cells. Second or third-passaged FECD endothelial cells were seeded on a previously decellularized human cornea. After 2 weeks in culture, TE-FECD corneas (n=6) were assessed using histology, transmission electron microscopy (TEM) and immunofluorescence labeling of various proteins. TE-FECD endothelium yielded a monolayer of polygonal cells well adhered to Descemet's membrane. The TE-FECD corneal endothelium expressed the function-related proteins Na^+-K^+/ATPase α1 and Na^+/HCO_3^-. Clusterin expression was faint and uniform. 2) In order to determine the best surgical procedure to transplant the TE-FECD corneas in the feline model, a DSAEK procedure was evaluated and compared to penetrating keratoplasty technique. DSAEK assessments included surgical challenges and clinical outcomes. DSAEK technique was challenging to perform in the feline model. Rapid fibrin formation was observed in all DSAEK cases (n=5). 3) The *in vivo* functionality of the TE-FECD corneas was assessed. TE-FECD corneas were grafted in the feline model (n=7) using penetrating keratoplasty procedure and observed for seven days. *In vivo* assessments included transparency, pachymetry, optical coherence tomography, endothelial cell morphometry, TEM and immunostaining of function-related proteins. After transplantation, pachymetry gradually decreased and transparency gradually increased. Seven days after transplantation, 6 out of 7 grafts were clear. Post-mortem TEM showed subendothelial

loose fibrillar material deposition in all TE-FECD grafts. The TE grafted endothelium expressed Na^+-K^+/ATPase and Na^+/HCO_3^-. This thesis demonstrates that endothelial cells from late-stage FECD corneas can be used to engineer a corneal endothelium. Compared to DSEAK, penetrating keratoplasty is a more appropriate procedure for corneal transplantation in the feline model, since the DSAEK procedure in the feline model presently yields inconsistent clinical results. Restoration of corneal thickness and transparency demonstrates that the TE-FECD grafts are functional *in vivo*. This novel FECD living model suggests a potential role of tissue engineering for FECD cell rehabilitation. Potential applications are numerous, including pathophysiological and pharmacological studies.

Keywords: Fuchs endothelial corneal dystrophy; corneal transplantation; tissue engineering; corneal endothelial cells; cell culture; feline model.

Table of Contents

List of Tables

List of Figures

List of Abbreviations

General

α: Alpha

AC: Anterior Chamber

AD: Autosomal Dominant

AQP: Aquaporin

Na^+/K^+-ATPase: Sodium-Potassium Adenosine Triphosphatase

β: Beta

CHED: Congenital Hereditary Endothelial Dystrophy

CLU: Clusterin

CV: Coefficient of Variation

DM: Descemet's Membrane

DMAEK: Descemet's Membrane Automated Endothelial Keratoplasty

DMEK: Descemet's Membrane Endothelial Keratoplasty

DSAEK: Descemet's Stripping Automated Endothelial Keratoplasty

EC: Endothelial Cells

ECM: Extracellular Matrix

EDTA: Ethylenediaminetetraacetic Acid

8-OHdG : 8-hydroxy-2-deoxyguanosine

FECD: Fuchs Endothelial Corneal Dystrophy

GAG: Glycosaminoglycans

HCEC: Human Corneal Endothelial Cells

Hg: Mercury

HM: Hand Movement

IOP: Intra Ocular Pressure

OCT: Optical Coherence Tomography

PBK: Pseudophakic Bullous Keratopathy

PCL: Posterior Collagenous Layer

pH: Potential Hydrogen

PKP: Penetrating Keratoplasty

PLL: Posterior Limiting Lamina

PPMD: Posterior Polymorphous Dystrophy

Prx: Peroxiredoxins

RER: Rough Endoplasmic Reticulum

rtPA: Recombinant Tissue Plasminogen Activator

SD: Standard Deviation

SEM: Standard Error of the Mean

TE: Tissue Engineered

TEM: Transmission Electron Microscopy

TGFβIp: Transforming Growth Factor-β-Induced Protein

TUNEL: Terminal Deoxynucleotidyl Transferase dUTP Nick End Labeling

VA: Visual Acuity

Units

%: Percent

°C: Degree Celsius

mm: Millimeter

mm^2: Millimeter Square

mg: Milligram

µg: Microgram

µm: Micrometer

nm: Nanometer

To my always beloved home; Aleppo, Syria

Acknowledgements

Deciding to have a PhD in corneal and refractive surgery was one of the most remarkable steps in my life. Looking back to the past three years I spent working like a bee in a bee hive producing honey, I've learned the true meaning of being productive, innovative, responsible and independent. None of this would be feasible without the valuable help and support of my supervisors and colleagues.

Dr. Brunette was always available and supportive. Thanks to her, I've improved my objectivity, perfection and criticism. I've also learned that great research comes from excellent ideas with potential impact. Sharing the same scientific background (Clinical Ophthalmology), I always enjoyed discussing current limitations in patient's management and what could be done to overcome these problems.

Although Dr. Proulx was in a distance (Quebec City), she was always close when needed. Thanks to her, I've learned to be well organized, straight to the point and specific. I loved working with her and I enjoyed her intelligence and her sense of humor. Her fundamental background brought me insight into the cell, making "from bench to bedside" research feasible.

I would like to thank my great team at Maisonneuve-Rosemont Hospital (HMR) Myriam Bareille, Cristina Bostan, Marie-Claude Perron, Nadia Ben Mérièm, Jeb Alden Ong, André Deveault, Angèle Halley, Ehab Elsharif, Xinling Liu, Lucie Budack and Marie-Ève Choronzey for their valuable assistance and support during my research. I really enjoyed working with them and I highly appreciate their friendship.

I would also like to thank Dr. J. Douglas Cameron, Benjamin Goyer, Olivier Roy, Olivier Rochette Drouin, Simon Laprise and Mathieu Thériault for their input in the articles; Drs. Richard Bazin, Patricia-Ann Laughrea and Marie-Ève Légaré from the Centre Universitaire d'Ophtalmologie (CUO) of the CHAUQ, Drs. Mona Harrissi-Dagher, Louis Racine and Paul Thompson from the CHUM and Dr. Johanna Choremis from HMR for their collaboration in obtaining FECD specimens. Danièle Caron, Patrick Carrier, Vivianne

Leduc, Catherine Mauger Labelle, Jeanne d'Arc Uwamaliya, Alexandre Deschambeault, Aristide Pusterla and the HMR-Rosemont and CUO operating room nurses for their technical assistance; Élodie Samson for the statistical analysis consultation; the LOEX research assistants for the histology preparations, Fayrouz Barkat for histology photography assistance; and Alain Goulet, Richard Janvier, Sylvie Roy and Steve Breault for the electron microscopy preparations and photography assistance.

This work was supported by the Canadian Institutes for Health Research (CIHR), Ottawa, ON, Canada, the FRQS ThéCell Network and the FRQS Research in Vision Network, Montreal, QC, Canada and the Fondation du CHA. I.B. is the recipient of the Charles-Albert Poissant Research Chair in Corneal Transplantation, University of Montreal, Canada.

Introduction

A century ago, the Viennese ophthalmologist Ernst Fuchs reported thirteen cases of bilateral central corneal clouding in elderly patients.[1] Subsequent investigations found that Fuchs endothelial corneal dystrophy (FECD) is caused by a primary abnormality of the corneal endothelium. The course of FECD usually spans 10 to 20 years. It becomes clinically evident in the fourth to fifth decade of life. Progressive corneal edema eventually leads to profound and painful vision loss.[2-6] The etiology of FECD is still poorly understood. Corneal edema is thought to result from decreased endothelial cell density, increased endothelial permeability and decreased endothelial pump function.[7-12] There is mounting evidence that oxidative stress,[13-15] DNA damage,[16] protein unfolding response[17] and apoptosis[18] may play a role in FECD pathogenesis.

In 2010, FECD was responsible for 28% of the 42,642 corneal grafts performed in the United-States.[19] There is no medical treatment for FECD. The current management is based on the surgical replacement of the diseased endothelium with a healthy endothelium from an eye bank cornea, either by penetrating keratoplasty (PKP) or, now more frequently, using a Descemet's Stripping Automated Endothelial Keratoplasty (DSAEK) procedure.[20] Allografts, however, carry up to 45% chances of at least one rejection episode (10% on average).[21] The most common causes of secondary corneal graft failure are endothelial failure (29%) or immunologic endothelial rejection (27%).[22]

Human corneal endothelial cells are arrested in the G1-phase of the cell cycle[23] and do not proliferate *in vivo*. However, they can proliferate *in vitro* in response to growth-promoting agents.[24-26] Previous studies in the laboratory showed that normal feline corneal endothelial cells can be cultured and can retain function *in vitro* and *in vivo*.[27-29] A previous study also demonstrated the first evidence of successful culture, without viral transduction, of corneal endothelial cells isolated from DSAEK specimens obtained from patients with FECD.[30]

Research Objectives

My first objective was to evaluate the feasibility of tissue engineering a corneal endothelium using endothelial cells from patients with FECD. Outcome parameters included endothelial cell morphometery using alizarin red and trypan blue staining, tissue integrity using regular histology, immunofluorescence labelling of function-related protein expression and ultrastructure using transmission electron microscopy.

My second objective was to determine the most appropriate surgical technique to transplant a corneal graft into the feline animal model. DSAEK procedure was evaluated. The ideal surgical technique should not cause trauma to the endothelial cells and should not induce an inflammatory reaction. Surgical challenges, clinical outcomes and postoperative complications were evaluated.

My last objective was to evaluate the functionality of a corneal endothelium tissue-engineered (TE) using corneal endothelial cells from patients with FECD cultured on a devitalized stromal carrier and transplanted in the living feline model. Outcome parameters included clinical functionality using corneal transparency, pachymetery, optical coherence tomography, endothelial cell morphometery using alizarin red and trypan blue staining, tissue integrity using histology, immunofluorescence labelling of function-related proteins and ultrastructure using transmission electron microscopy.

1 Chapter I:

The Normal Human Cornea

1.1 Anatomy of the Human Cornea

The cornea is the anterior transparent connective tissue of the eye. It represents the primary structure barrier as well as the major refractive compound of the eye. Corneal transparency, which depends on the structural anatomy and physiology of the corneal components, is essential for light perception of the retina; any distortion of the transparency will result in a decrease of the quality (i.e. aberrations) and/or the quantity (i.e. acuity) of vision.[31]

In emmetropic adults, the average white-to-white diameter of the cornea is 11.5 to 12.3 mm. The central corneal thickness ranges from 528 to 588 μm and gradually increases towards the periphery.[32]

The cornea is classically composed of five distinguishable layers. Three of them are cellular (epithelium, stroma and endothelium) and two are acellular (Bowman's and Descemet's membranes) (Figure 1).

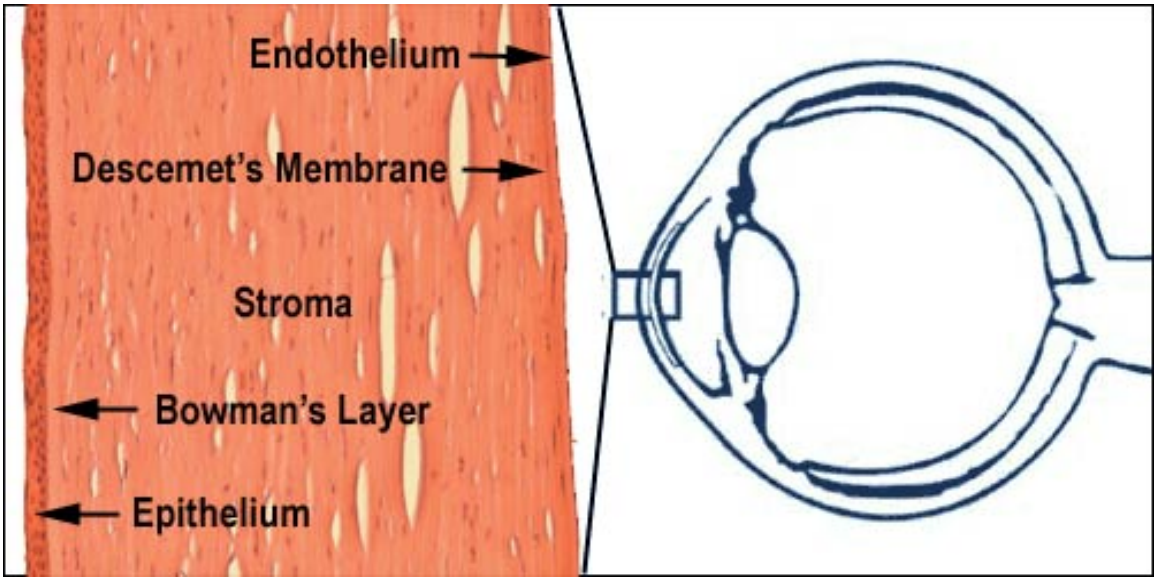

Figure 1: The five layers of the cornea (from Wilmer Eye Institute at Johns Hopkins)

1.1.1 Epithelium

The corneal epithelium forms the first barrier separating the eye from the environment. It is composed of a stratified non-keratinized squamous epithelium of 4 to 6 cell layers (40 to 50 µm in thickness). These layers are divided from posterior to anterior into: basal, wing and superficial cells. Corneal epithelial lifespan ranges from 7 to 10 days and the cells go through systematic involution, apoptosis and desquamation. This progression leads to a complete renewal of the epithelium every week.[33] The main source of corneal epithelial regeneration is the epithelial stem cells, which are located within the basal interpalisade epithelial papillae of the Palisades of Vogt at the limbus (extreme periphery of the cornea). Limbal stem cells are slow-cycling undifferentiated cells that are presupposed to undergo asymmetric division giving rise to corneal epithelial cells. Upon dividing, one daughter cell remains within the niche to replenish the stem cell population, while the other detaches from its basement membrane and becomes a transient amplifying cell (TAC) committed to differentiate. TAC cells then migrate towards the center of the cornea and start to differentiate into basal cells (Figure 2).[34]

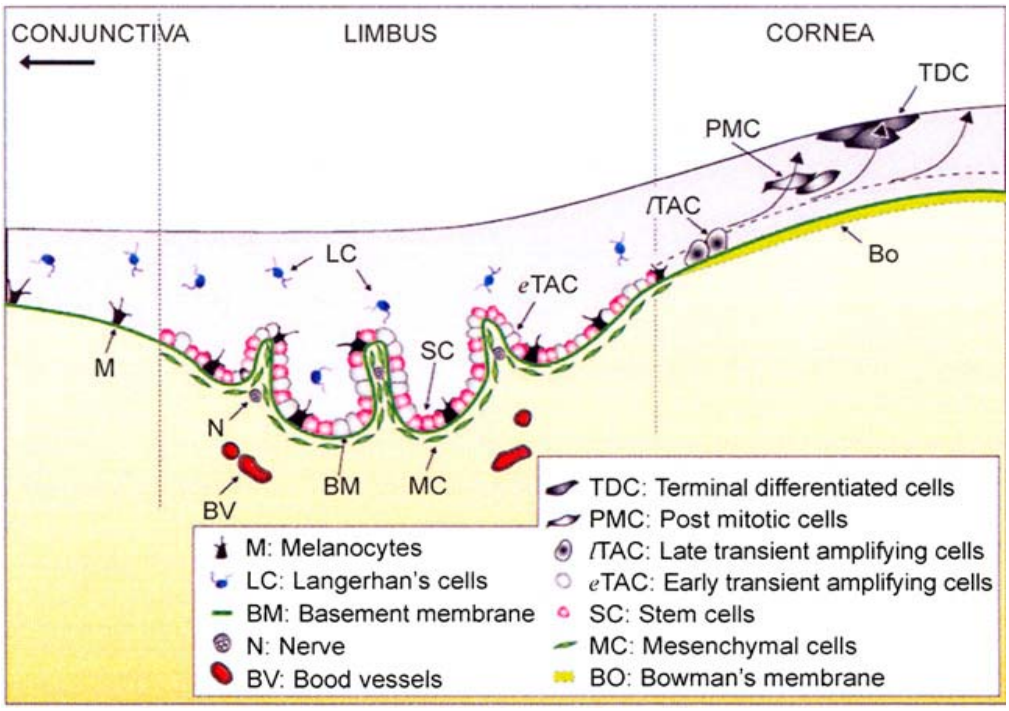

Figure 2: Limbal stem cell niche scheme.[34]

The basal cell layer consists of a single row of columnar cells (~20 µm tall) which are capable of mitosis.[35] They are the source of wing and superficial cells that are incapable of mitosis. Basal cells have lateral intercellular junctions (gap and adherent junctions) and possess hemidesmosomes to their basement membrane. They secrete their basement membrane (0.05 µm in thickness) that contains collagen type IV and laminin.[31]

Wing and superficial cells form 4 to 6 rows of cells that possess tight lateral intercellular junctions. Superficial cells have extensive apical microvilli and microplicae, which are covered by the glycocalyceal and the mucinous layers of the tear film (Figure 3).[31]

The regular thickness, the moistened status and the smooth surface of the epithelium play a role in the refractive property of the cornea. The epithelium also plays a role in protecting the underlying corneal layers from physical and chemical injuries and prevents tears from penetrating into the stroma, which could cause edema.

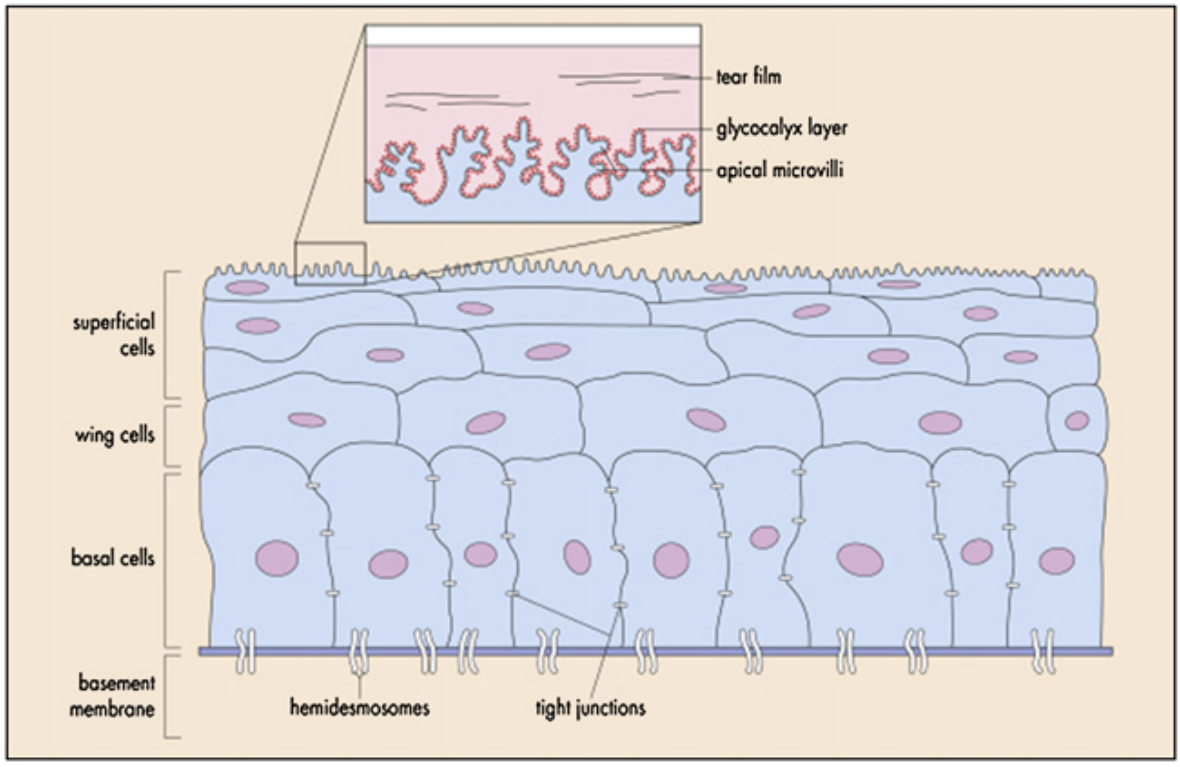

Figure 3: Corneal epithelial layers.[31]

1.1.2 Bowman's Membrane

Bowman's membrane (10-15 μm in thickness) lies posterior to the basement membrane of the epithelium. It is not a true membrane as it is an acellular condensation of collagen fibers and proteoglycans of the anterior portion of the stroma. It does not exist in many mammals (i.e. cats). Its physiological role is unclear. In cases of injury, this membrane does not regenerate and forms a scar.[31]

1.1.3 Stroma

The corneal stroma provides the volume of the structural skeleton of the cornea and constitutes 85% to 90% of its thickness. The transparency of the stroma is unique among other collagenous structures and results from the precise arrangement of the stromal collagen fibers and its extracellular matrix (ECM), which is hydrophilic and can absorb amounts of water equal to 1000 times its volume (Figure 4).[36, 37] The corneal endothelium plays a critical role in maintaining the relatively dehydrated state of the stroma, thus preserving the precise organisation of the stromal collagen fibers.

A collagen fiber is composed of parallel bundles of fibrils which bind laterally and end-to-end to form a fiber with a uniform diameter. Collagen fibers in the stroma are spaced at a regular distance and are packed in parallel to form a lamella. The stroma consists of 200 to 250 distinctive lamellae, each of which is arranged at an angle relative to the other and runs from limbus to limbus.[37] The central stroma is thinner than the peripheral one, and the collagen fibers change their direction and run circumferentially when they arrive near the limbus.[38] Posterior lamellae are more arranged and less rigid than the anterior ones. This biomechanical difference is translated clinically in a stromal edema that is more marked posteriorly, pushing on the Descemet's membrane and thus causing Descemet folds. This difference is also observed surgically: posterior lamellar dissection of the cornea has less resistance force than the anterior one.[31]

Stromal collagen fibers consist mainly of collagen type I in a triple-helix structure with significant amounts of type V collagen to achieve their uniform diameter. Collagen type VI and XII bind collagen fibers and contribute in maintaining the regularity of the

stromal structure. Keratan sulfate and chondroitin sulfate/dermatan sulfate, which are the ground substance of the stroma, play a role in regulating the hydration state and the uniform structure of the stroma.

Keratocytes, which are the main cell type of the stroma, however, occupy only 2 to 3% of its total volume. They are elongated cells that rest between collagen lamellae in a parallel manner (Figure 4). Keratocytes contain corneal crystallins that reduce cellular light scattering. They are also responsible of producing extracellular matrix (including glycosaminoglycans (GAG) and collagen molecules).[39]

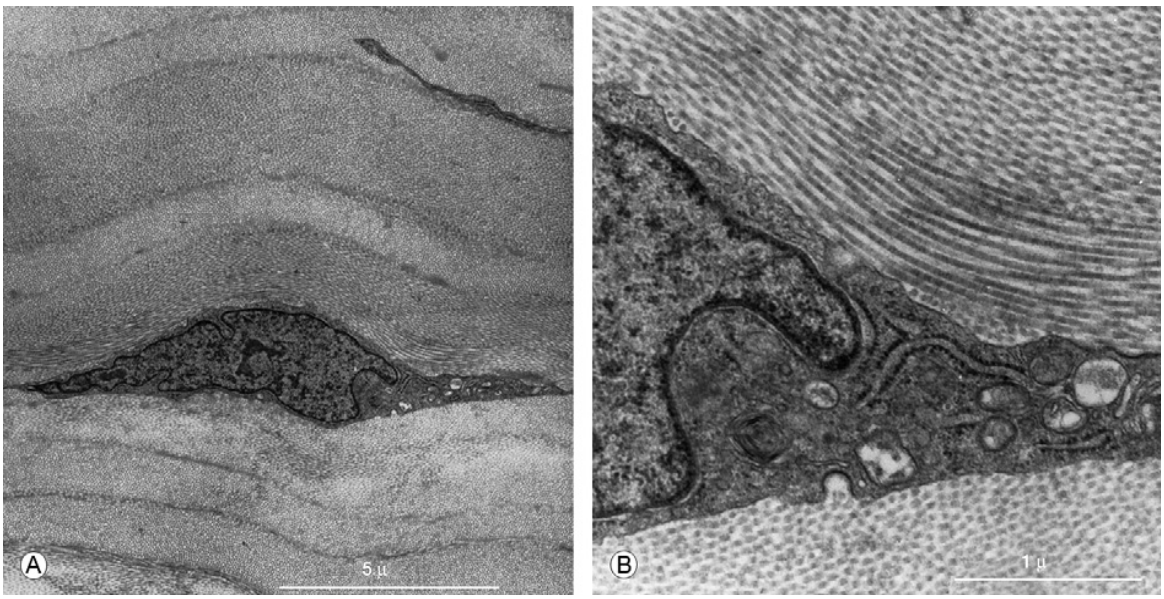

Figure 4: Transmission electron microscopy (TEM) of normal corneal stroma. (A) Stromal lamellae with embedded keratocyte. (B) Higher magnification view showing a keratocyte nuclei, rough endoplasmic reticulum, mitochondria and vacuoles. Note the precise organisation of the stromal collagen fibers.[31]

1.1.4 Descemet's Membrane

Descemet's membrane (DM) is the basement membrane of the corneal endothelium, situated between the stroma and the endothelium.

The normal DM is composed of two regular layers (Figure 5):

- Anterior banded layer: It is present in the eye of the fetus of five months of gestation. Its thickness is approximately 3 μm and it remains the same at all ages. It has wide-spaced collagen bands of 110 nm. It contains long-range arrays of vertical bands that correspond to the large, regularly spaced domains of collagen VIII. [40]
- Posterior nonbanded layer: It is secreted by the endothelial cells after birth on the posterior surface of the banded fetal portion. Its thickness increases significantly with age, averaging ~2 μm at 10 years of age and ~10 μm at 80 years of age. Over the age of 70, it is considerably thicker in females. It appears homogeneous with a finely granular quality ultrastructurally; however, banded spindles can be observed (in 5 out of 24 normal corneas observed).[41]

DM in normal adults is composed of collagen type IV (dominant), VIII and XII, laminin, perlecan, nidogen-1, nidogen-2, netrin-4, vitronectin and fibronectin.[40, 42]

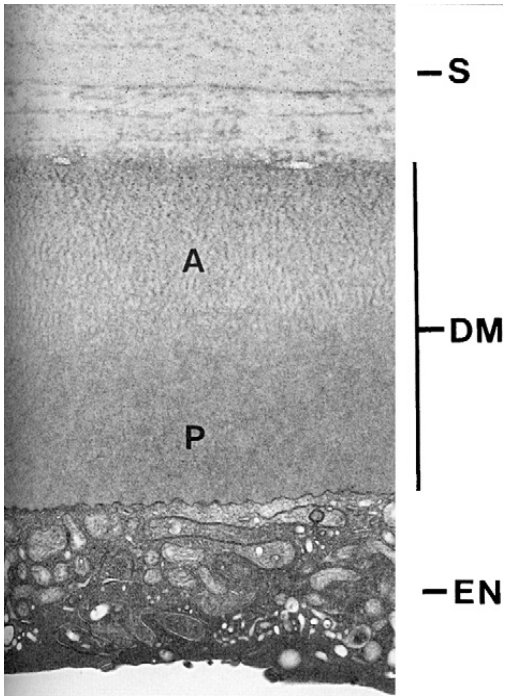

Figure 5: Transmission electron microscopy (TEM) of Descemet's membrane (DM) showing posterior stroma (S), anterior (A) and posterior (P) layers of normal DM, and endothelium (EN).[31]

1.1.5 Endothelium

Corneal specialists consider the endothelium as the soul of the cornea. In the mid 19th century, Sir William Bowman first described the microscopic structure of the monolayer endothelium as a "delicate and perishable layer".[2] In 1920, Alfred Vogt first described the hexagonal morphology of the endothelial mosaic *in vivo* using slit lamp biomicroscope.[43]

At about the sixth week of gestation, corneal endothelial cells, originating from the neural crest (neuroectoderm), migrate centrally from the rim of the optic cup to form a monolayer of cubical cells.[2] Over time, these cells flatten and start to secrete their basal membrane (DM). At birth, the endothelium is a uniform monolayer of about 10 µm in thickness and consists of ~350 000 cells (~3 000 cells/mm²) covering the entire posterior surface of the cornea and fusing with the cells of the trabecular meshwork at the periphery. DM also fuses peripherally with the trabecular beams where Schwalbe line defines the ending of DM and the beginning of the trabecular meshwork.[31]

After birth, endothelial cells keep on flattening to stabilize at 4 to 6 µm thickness at adulthood. They appear as a uniform honeycomb-like mosaic with four to nine sides, about 20µm in diameter and 250 µm² in cell area (Figure 6). Adjacent cells interdigitate, overlap and form gap and tight junctions at their lateral borders. The lateral membranes enclose a high density of Na^+/ K^+-ATPase pump sites. The individual endothelial cell contains a large oblong nucleus, numerous mitochondria (reflecting high energy demand for ion pumps), a rough endoplasmic reticulum (RER) and its ribosomes, and a prominent Golgi apparatus (indicating high protein synthesis including enzymes, structure proteins and extracellular matrix (ECM)) (Figure 5).[2, 31]

Endothelial cells do not proliferate *in vivo*. Once a cell dies, the neighbouring cells will enlarge and migrate in order to maintain the integrity of the monolayer. Endothelial cell morphometry keeps on changing throughout life. From the second to ninth decades of life, the cell density decreases from ~3300 cells/mm^2 to ~2300 cells/mm^2, the cell area increases from 290 to 450 µm², the coefficient of variation (CV) of mean cell area (polymegethism) increases from 0.22 to 0.29 and the percentage of hexagonal cells

decreases from 75% to 60% (pleomorphism), indicating that the individual endothelial cells become less uniform throughout life.[44] The central endothelial cell density decreases at an average rate of 0.6% per year in normal corneas.[45] There is no correlation between corneal thickness and endothelial cell density, cell area, coefficient of variation or cell shape. However, it has been noticed that eyes with endothelial cell density less than 500 cells/mm^2 may be at risk of developing corneal edema.[31]

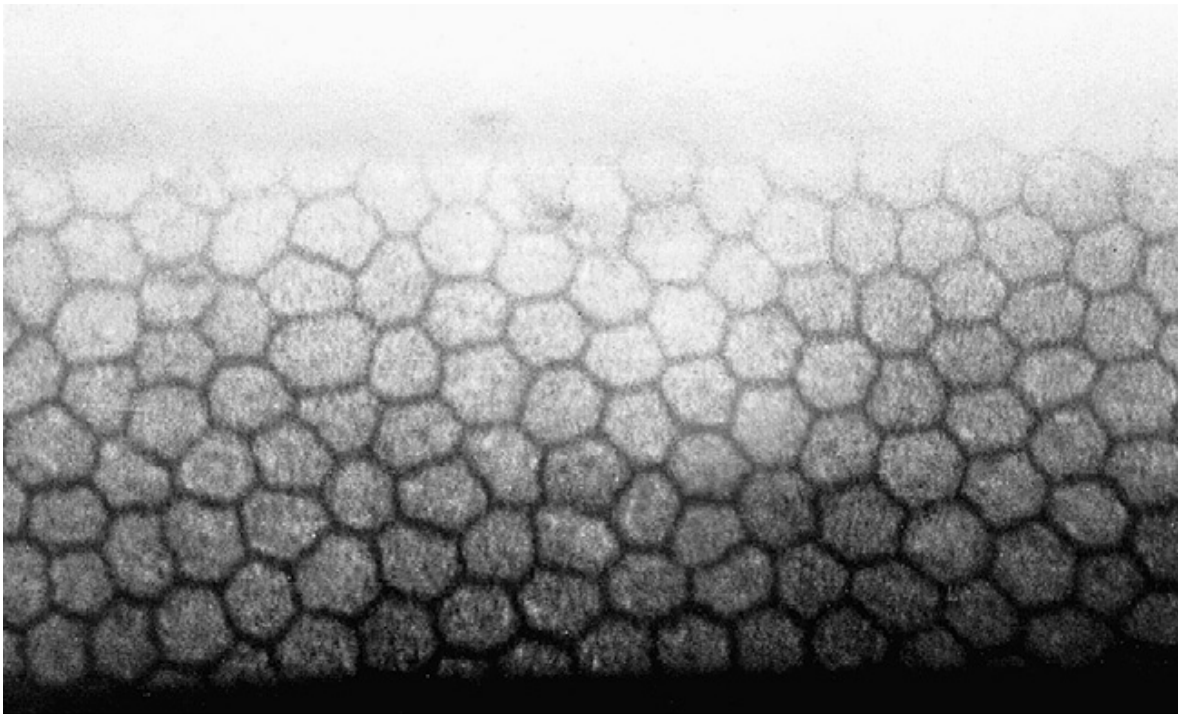

Figure 6: Specular microscopy photo of the normal corneal endothelium. Note the regular hexagonal pattern.[31]

1.2 Physiology of the Human Corneal Endothelium

1.2.1 Corneal Deturgescence

The corneal endothelium maintains corneal transparency by ensuring corneal deturgescence (a condition in which corneal stroma is relatively dehydrated (78% water content)), a process achieved through ionic pumps (Na^+/K^+-ATPase) and ion transporters such as the co-transporter Na^+/HCO_3^-,[2] while aquaporins (AQP) facilitate the flow of water in response to osmotic gradients created by those pumps.[46]

The corneal stroma imbibes fluids due to presence of glycosaminoglycans (GAG) that create an osmotic pressure (the swelling pressure 60 mmHg) which pulls fluids from the aqueous humor into the stroma providing nutrition to the keratocytes (leaky barrier of the endothelium), while the corneal endothelium actively pumps the fluid out of the stroma (pump function and AQP of the endothelium). In normal conditions, the leaky barrier of the endothelium equals its pump function. If this equivalence breaks, fluids will diffuse excessively into the stroma, disrupting the uniform collagen fiber arrangement and resulting in light scattering and corneal opacity (Figure 7).

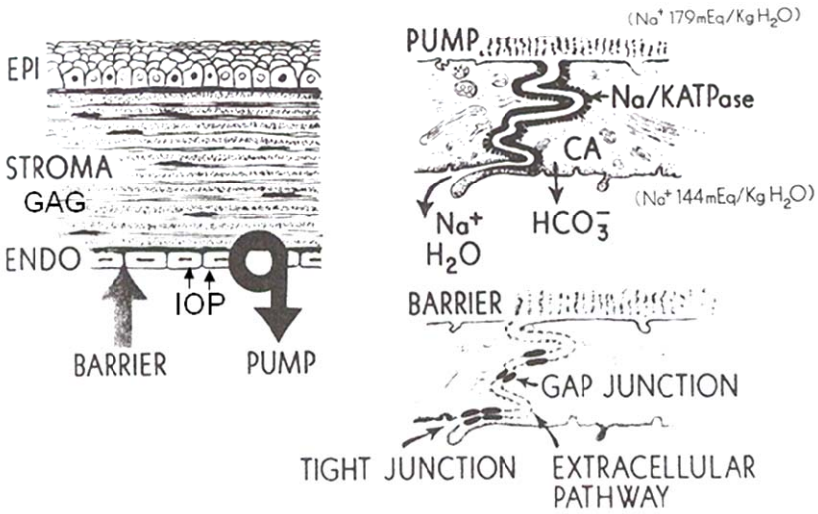

Figure 7: Drawing illustrates the pump and the barrier function of the corneal endothelium. Modified from Waring et al.[2]

1.2.2 Barrier Function of the Endothelium

The intercellular space between endothelial cells measures 25 to 40 nm. This space decreases to about 3 nm at the apical borders of the cells, where junctional complexes exist. These complexes consist of focal tight junctions (zonulae occludens) and gap junctions. They do not run continuously around the apical border of the cell; therefore, they do not form a watertight seal, allowing water and small particles to pass through the endothelium.[2]

The integrity of these junctions depends on calcium. Thus, any compound causing calcium imbalance will affect barrier function (i.e. calcium-free solutions, plasmalyte -148). Any disruption of the barrier function will lead to an increase in the leak rate over the pump rate resulting in corneal edema.[2]

1.2.3 Pump Function of the Endothelium

Endothelial pumps consist of iceberg-like enzymes embedded in the lateral plasma membrane that actively transport ions from the stroma to the aqueous humor, creating an osmotic gradient that pulls out the water from the hydrophilic stroma. Sodium/bicarbonate co-transporter actively transport sodium and bicarbonate ions into the aqueous humor, while sodium/potassium ATPase pumps actively exchange 3 sodium ions from inside the cell with 2 potassium ions from outside the cell. This pump is magnesium dependent and requires ATP to phosphorylate the enzyme. Many mitochondria populate the area near the cytoplasmic membrane to provide the ATP necessary to maintain the pump function.

Although endothelial cell density declines throughout life, sodium/potassium ATPase pump site density remains constant regardless of the age, suggesting that the remaining endothelial cells adapt to cell loss by creating new pump sites in order to maintain normal pump site density and thus pump capacity.[8]

The activity of endothelial pumps can be inhibited by a number of conditions causing corneal swelling, such as lowering of the temperature, ouabain, bicarbonate-free solutions and bromacetazolamide.[2]

1.2.4 Aquaporin Function of the Endothelium

Aquaporin (AQP) water channels are proteins that integrate in the cell's membrane to facilitate the transmembrane solute-free water transport in response to osmotic gradients. AQP1 is expressed in the corneal endothelium. Its deficiency remarkably delays restoration of corneal transparency and thickness providing evidence that water extrusion from stroma through endothelium is mediated by AQP1. However, its mechanism remains unclear.[46]

2 Chapter II:

Fuchs Endothelial Corneal Dystrophy

In 1910, the Viennese ophthalmologist Ernst Fuchs (1851-1930) first described the entity presently recognized as Fuchs endothelial corneal dystrophy (FECD) when he reported 13 cases of bilateral slowly progressive central corneal clouding in elderly patients.[1, 47] With the modest ophthalmologist's examination tools at that time, Professor Fuchs concluded that the primary defect in these cases was in the corneal epithelium; he thus entitled his paper 'Dystrophia Epithelialis Corneae'.

However, since then, several studies have shown that pathological changes in FECD result from a primary disease of the corneal endothelium. All the accompanying changes have been shown to be secondary to the process involving the endothelium.[2-6]

FECD is a common, progressive, bilateral, often asymmetric disease that leads to blindness. Its course usually spans 10 to 20 years. It becomes clinically evident at the age of forty to fifty; despite that, patients do not complain of visual symptoms for another 10 years.[2-6]

There is no efficient medical treatment for FECD. FECD accounts for 47.7% of the 23,287 corneal endothelial transplantations performed in the United States in 2011,[48] making FECD the leading indication for corneal endothelial transplantations. Allografts, however, carry up to 45% chances of at least one rejection episode (10% on average).[21] The most common causes of secondary corneal graft failure are endothelial failure (29%) and immunologic endothelial rejection (27%).[22]

2.1 Clinical Stages

Two major clinical staging systems for FECD have been described (Table 1). One of the most commonly used classification systems divides the course of FECD into four stages:[3, 6, 49]

Stage I. The patient is asymptomatic. Clinical examination shows central droplet-like excrescences at the level of DM called guttae which are considered the hallmark of FECD. Pigment dusting could also be seen at the level of the endothelium. DM appears gray and thick (Figure 8I).

Stage II. The patient starts suffering from blurred vision, glare and halos. Symptoms are worse in the morning and improve through the day. The patient may complain from foreign body sensation; however, he is free from pain. Clinical examination shows corneal guttae coalescing and spreading towards the peripheral of the cornea. Stromal edema starts posteriorly then progresses anteriorly reaching the epithelium and causing epithelial edema (Figure 8II).

Stage III. The patient complains of low vision and episodes of pain. Clinical examination shows profound stromal edema and formation of sub-epithelial bullae that can cause nerve terminal compression or can rupture, causing pain. The cornea is at risk of infection at this stage (Figure 8III).

Stage IV. The patient suffers from profound vision loss (visual acuity (VA) reaching hand movement (HM)). Pain is usually decreased. Clinical examination shows an opaque and vascularised cornea along with sub-epithelial fibrous tissue formation in response to chronic edema (Figure 8IV).

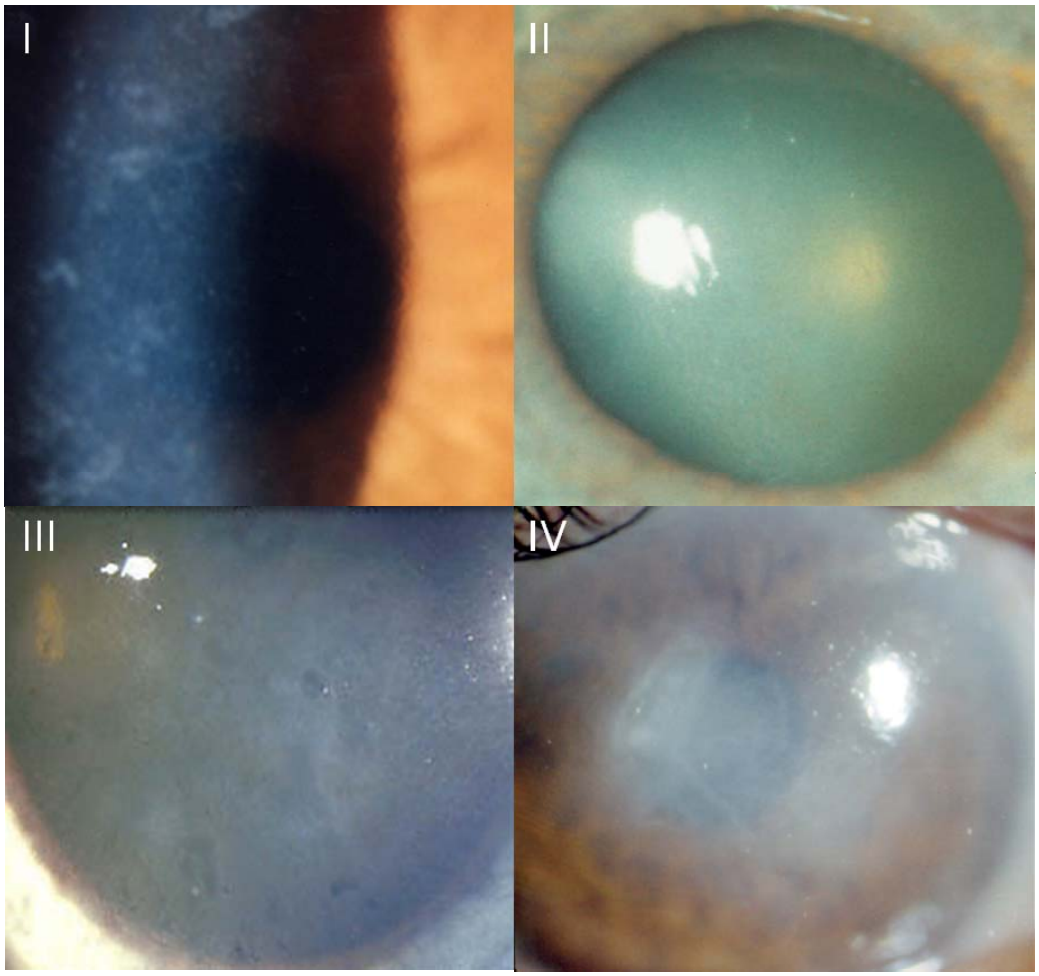

Figure 8: Clinical staging of FECD. (I) Stage I showing guttae and pigment dusting. (II) Stage II showing central corneal edema. (III) Stage III showing sub-epithelial bullae. (IV) Stage IV showing sub-epithelial fibrous tissue.

Reference	Stage I	Stage II	Stage III	Stage IV
- Waring et al.[2, 4] - Wilson et al.[5]	- Asymptomatic - Central guttae - Fine pigment dusting - DM: gray & thick	- Blurred vision, glare & halos (worse in mornings) - Stromal & epithelial edema => sub-epithelial bullae - Episodes of pain	- Patient more comfortable - VA drops - Sub-epithelial connective tissue - Peripheral corneal vascularization	-
- Adamis et al.[3] - Borboli et al.[49] - Elhalis et al.[6]	- Asymptomatic - Central guttae - Pigment dusting - DM: gray & thick	- Painless blurred vision (worse in mornings) - Stromal & epithelial edema	- Epithelial & sub-epithelial bullae - Episodes of pain	- VA drops to HM - Free of pain attacks - Subepithelial scar tissue

Table 1: Clinical classification of Fuchs endothelial corneal dystrophy.

Laing et al.[50] have described a classification of FECD based on endothelial cells and guttae appearance using specular microscopy. They have divided the severity of disease into five stages (Figure 9):

Stage I. Corneal guttae are smaller than endothelial cells.
Stage II. Corneal guttae are larger than endothelial cells.
Stage III. Corneal guttae are larger than endothelial cells and adjacent endothelial cells appear abnormal.
Stage IV. Corneal guttae coalesce and adjacent endothelial cells are difficult to identify.
Stage V. Corneal guttae coalesce and adjacent endothelial cells are completely disorganized.

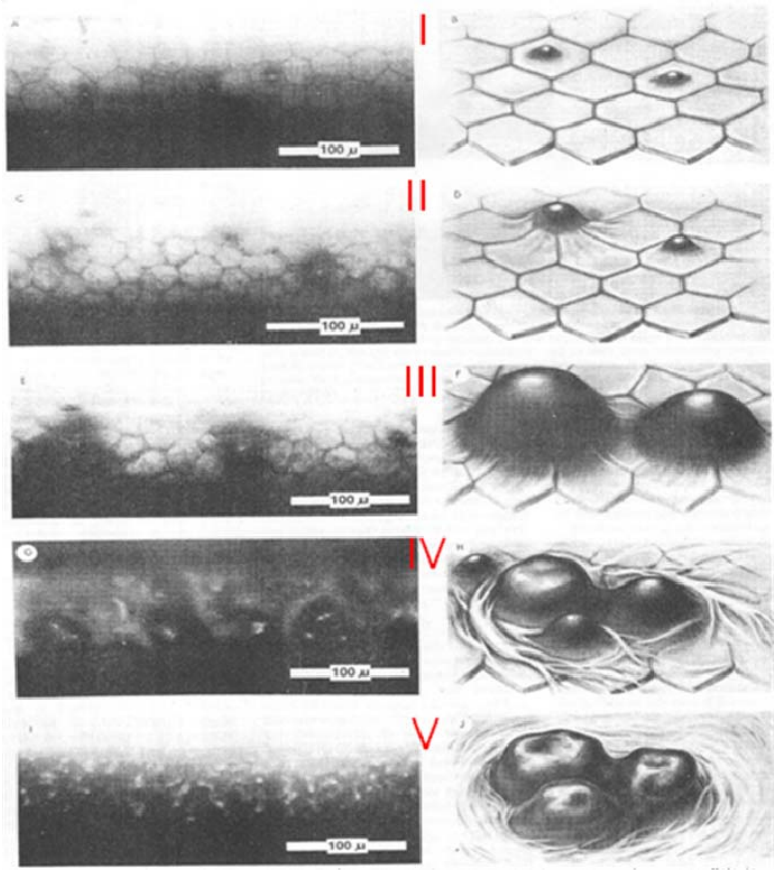

Figure 9: Specular microscopy photos and drawing illustrate Laing morphological staging of FECD.[50]

Recently, the FECD Genetics Multi-Center Study Group proposed a novel classification method depending on the shape and distribution of guttae clinically. They grade FECD from 0 to 6 on a semiquantitative scale:

Stage 0: no guttae.
Stage 1: 1 to 12 central/paracentral nonconfluent guttae.
Stage 2: more than 12 central/paracentral nonconfluent guttae.
Stage 3: 1 to 2 mm of confluent central/paracentral guttae.
Stage 4: more than 2 to 5 mm of confluent central/paracentral guttae.
Stage 5: more than 5 mm of confluent central/paracentral guttae.
Stage 6: more than 5 mm of confluent central/paracentral guttae with stromal and/or epithelial edema.

Using this classification they demonstrated a gradual increase in central corneal thickness as FECD clinically progresses.[51]

2.2 Associated Conditions

Several studies have shown an association between FECD and keratoconus,[52] age-related macular degeneration,[53] cardiovascular disease,[54] axial hypermetropia[55] and essential blepharospasm.[56] The association between FECD and open-angle glaucoma is controversial. Buxton et al. demonstrated a decrease in aqueous humor outflow in FECD patient's eyes compared to normal controls,[57] while Roberts et al. showed no impairment of the outflow facility.[58] Recently, Nagarsheth et al. demonstrated a higher prevalence of glaucoma and/or ocular hypertension in severe FECD patients compared to control subjects or unaffected family members.[59]

2.3 Differential Diagnosis

Corneal edema can be found in posterior polymorphous dystrophy (PPMD), congenital hereditary endothelial dystrophy (CHED), aphakic or pseudophakic bullous keratopathy and endothelial dysfunction due to anterior uveitis and herpes simplex keratitis.[2-4, 49]

Corneal guttae are characteristic findings in the DM of FECD; however, they can be secondary to toxins, interstitial keratitis and trauma.[2, 60, 61] They have been found neither in

PPMD nor in CHED.[62-65] Hassall-Henle bodies have an aspect similar to guttae, but they are found only in the corneal periphery. They are considered normal findings in elderly subjects and never cause corneal edema.[3, 6, 66]

2.4 Endothelial Morphology

Specular microscopy in FECD shows presence of central corneal guttae, reduced endothelial cell count, variability in cell size (polymegethism) and variability in cell polygonal shape (pleomorphism) (also see section 1.1.5)(Figure 10).[67]

Figure 10: Specular microscopy photo in FECD showing corneal guttae, polymegethism and pleomorphism.[67]

2.5 Histopathology

2.5.1 Epithelium

Transmission electron microscopy shows intracellular and intercellular edema. Surface cells retain tight junctions and intercellular desmosomes. Basal cells may detach from basement membrane due to accumulation of sub-epithelial fluid (Figure 11).[68]

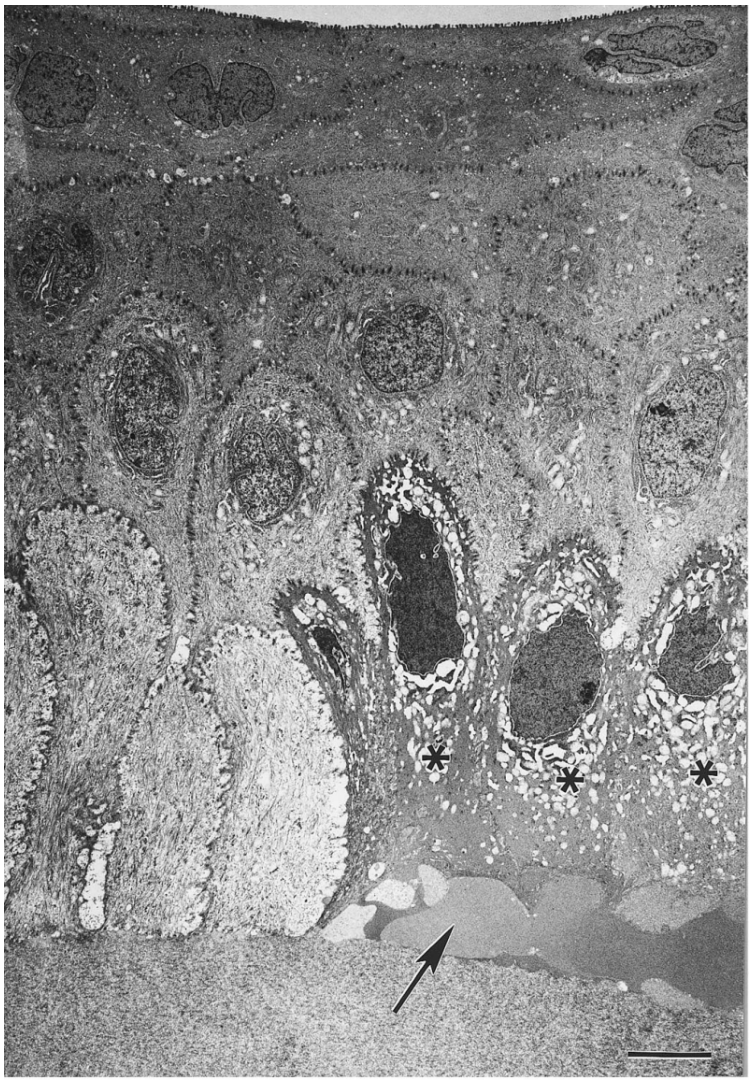

Figure 11: Epithelium in FECD. TEM is showing intercellular edema (*) and basal cell layer detachment due to sub-epithelial fluids (arrow).[68] Scale bar: 5 μm.

2.5.2 Bowman's Membrane

Bowman's membrane is usually intact or local breaks filled with connective tissue can be seen.[68, 69]

2.5.3 Stroma

Changes are seen in advanced stages of the disease including wavy collagen lamellae, wide interfibrillar spaces, degenerated keratocytes and granular or filamentous material inside or around the keratocytes. Lipid keratopathy is present in 72% of FECD (Figure 12).[69]

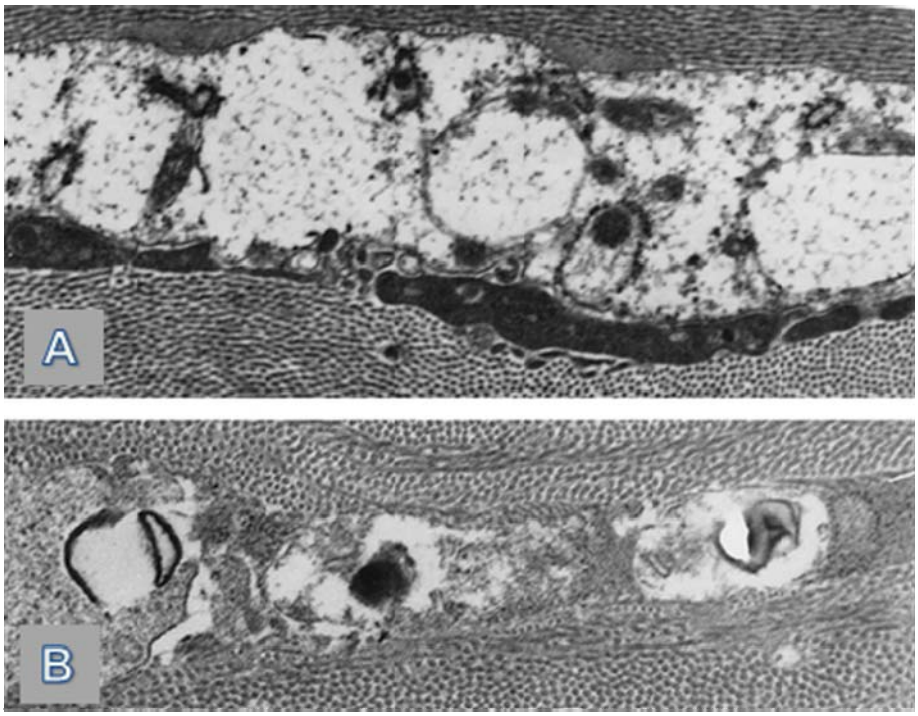

Figure 12: Stroma in FECD. TEM showing degenerated keratocytes with variable dissolution cytoplasm and loss of organelles.[69] Magnification: A: 20 000X, B: 30 000X

2.5.4 Descemet's Membrane

Kayes and Holmberg[70] studied the ultrastructure (TEM) of four corneal buttons with FECD and they noticed a large increase in DM thickness reaching 18 μm. They divided DM into 4 zones:

- Banded zone: close to the stroma, 100 nm banding.
- Nonbanded zone.
- Very regular banded zone with a periodicity of 90-125 nm that projects into the endothelium forming small hills to mushroom warts. They divided banding into: B1: usual DM fibers, B2: hexagon form, B3: fusiform spindle periodicity of 100 nm, B4: periodicity of 64 nm, F1: fibers one-half B2 size and F2 smaller fibers.
- Nonbanded zone.

In another morphological study by Iwamoto et al.[66] describing the TEM observation of 7 corneal buttons with FECD, DM was markedly thickened (2 to 4 times the normal) in 6 cases. He divided DM into five regions:

- Anterior banded region: with 100 nm banded pattern.
- Nonbanded region: without clear banding.
- Posterior banded region: It was filled with 100 nm banded materials ("warts" are formed by its partial backward protrusions).
- Border region: It was composed of groups of thin fibrils, long-spacing bundles of 100 nm periodicity with two types of banded pattern and basement membrane-like material (Figure 13A-D).
- Fibrillar region: It consisted of basement membrane-like material and collagen fibrils. Narrow fissures filled with cell debris and fibrils had been noticed (Figure 13E-F).

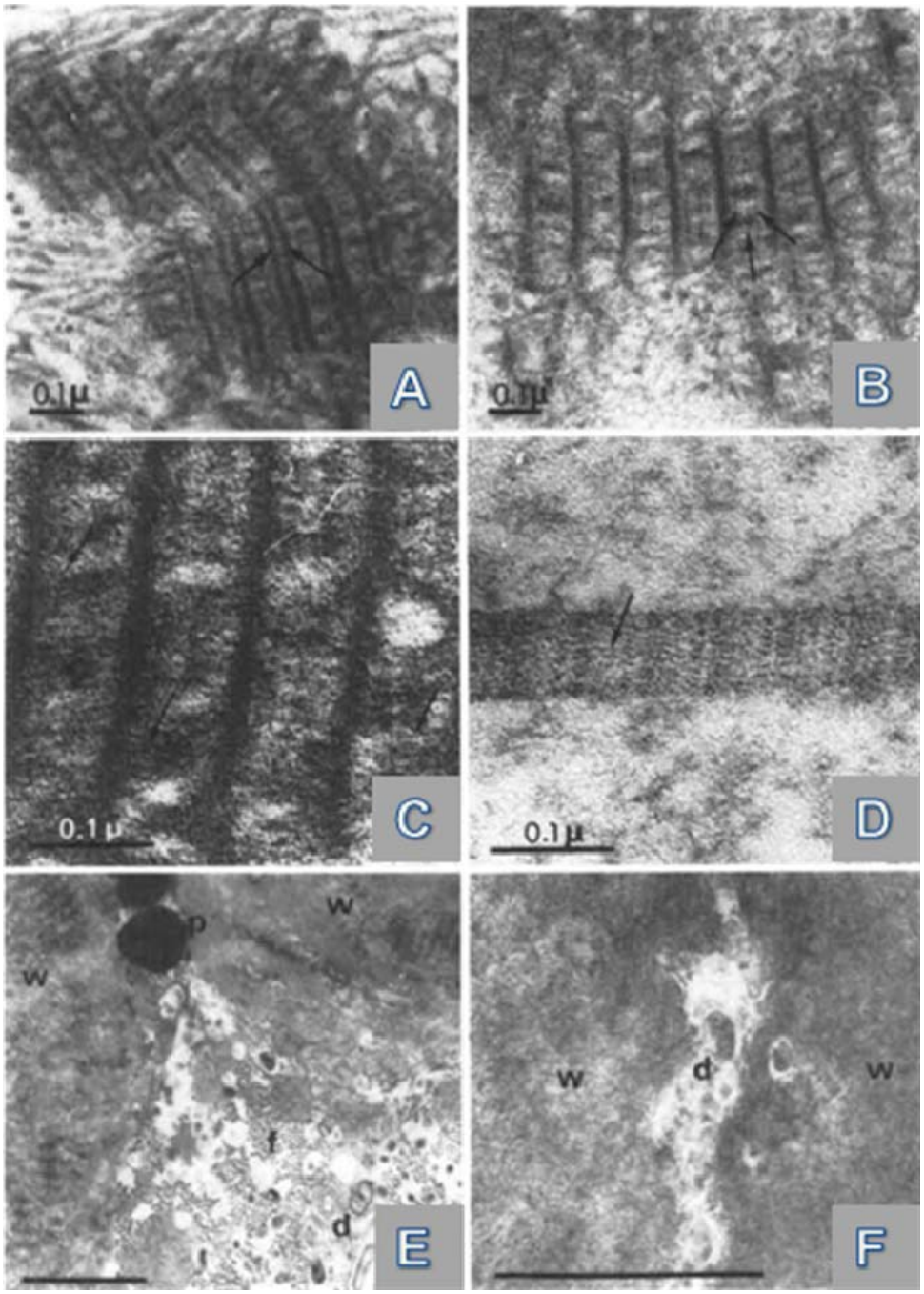

Figure 13: Border region of DM in FECD. (A-D) Striated bodies: Wide-spacing bundles. (E-F) Narrow fissure (f) filled with cell debris (d) between the warts (w).[66] Magnification; E-F: 38 000X

Bourne et al.[71] studied the ultrastructure (TEM) of DM in 11 corneal buttons with FECD (all were phakic eyes). He found that DM was composed of up to four layers:

- Anterior banded layer (fetal): It was normal in all cases showing 110 nm banding. Its thickness was 3.1 μm in average (excluding 3 cases where it was thickened).
- Posterior nonbanded layer: It was present in 2/3 of the cases and absent in 1/3, with thickness of 2.8 μm in average when present. It was composed of a framework of tiny fibrils running randomly throughout. It appeared homogeneous in general.
- Posterior banded layer: It was present in all cases, with thickness varying between 10.7 and 23.2 μm (mean 16.6). It contained 110 nm banding, banded spindle-shaped bundles, 10 to 20 nm diameter fibrils and amorphous substance. Guttae were found in this layer when present.
- Fibrillar layer: It was present in 7 corneas between the EC and the posterior banded layer. It contained 20 nm diameter fibrils randomly arranged and amorphous material. There was a statistical positive correlation between the preoperative corneal thickness and the thickness of this layer (Figure 14).

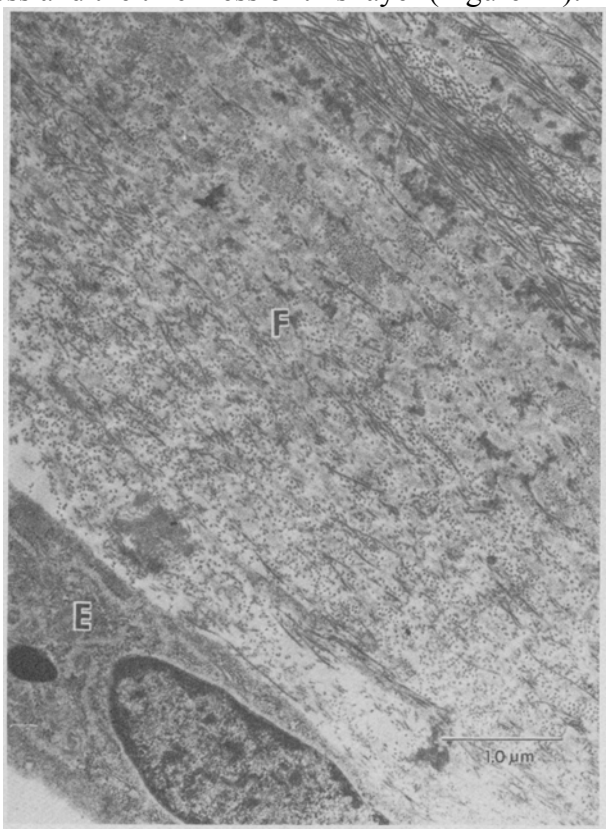

Figure 14: Fibrillar layer (F) in FECD. Fibrils (20 nm in diameter) are loosely arranged among variable amounts of amorphous material. (E) indicates endothelium.[71]

Rodrigues et al.[72] studied six corneal buttons with FECD. In light microscopy, they found that DM was thickened up to 3 times compared to normal with multiple guttata. Corneas from two patients showed oxylatan fibrils. TEM showed:

- Normal anterior: 110 nm banding (3 μm thick)
- Posterior granular portion: thinned
- Posterior collagenous layer: (16 to 38 μm thick) showed abnormal 110 nm banding, spindle-shaped 10 to 15 nm fibrils and homogenous material, with variation of the configuration of the guttata. These banded areas corresponded to the same zones stained for oxylatan fibrils.

Bergmanson et al.[68] studied the ultrastructure of one pair of corneal button with FECD and he divided the layers of DM differently:

- Posterior limiting lamina (PLL): This includes the fetal and postnatal layers, with a generalized thickening.
- Posterior collagenous layer (PCL): It was sandwiched between the EC and the PLL. It had a more granular composition than PLL. Pigment granules were occasionally observed. Guttae contained inclusion bodies of various structures; most prominent were banded or cross-striated 133 nm bodies or fibrils, while other bodies were amorphous and non-striated.

Yuen et al.[69] studied the morphology of 32 corneal buttons of patients with FECD. They found that the average thickness of DM was 17.6 μm. They also showed that the ultrastructure of Decemet's membrane was composed of up to four layers (Figure 15):

- Anterior banded layer (fetal): It was present and relatively uniform in all cases of FECD. Its thickness was 3.2 μm in average. It had wide-spaced collagen with a periodicity of 110-120 nm.
- Posterior nonbanded layer: It was present in 2/3 of the cases and absent in 1/3, with thickness of 3.2 μm in average when present. It appeared homogeneous.
- Posterior banded layer: It was present in all cases, with thickness varying from 5.8 to 32.1 μm (mean 15.9). It had wide-spaced collagen with a periodicity of 110-120 nm. In ¼ of the cases a periodicity of 60 nm was observed. The characteristic guttae of FECD were contiguous with this layer in all the cases. Their mean maximal width and height were 15.1 μm, 4.6 μm respectively.
- Fibrillar layer: It was present in 59% and absent in 41% of the cases, with average thickness of 7.8 μm when present. It was composed of a loose matrix of collagen with fibril diameters of 20-40 nm. In 1/3 of the cases, guttae were buried in this layer. In 7 cases, multiple waves of basal lamina were present along with foci of wide-spaced collagen with a periodicity of around 60 nm situated between this layer and the posterior banded layer.

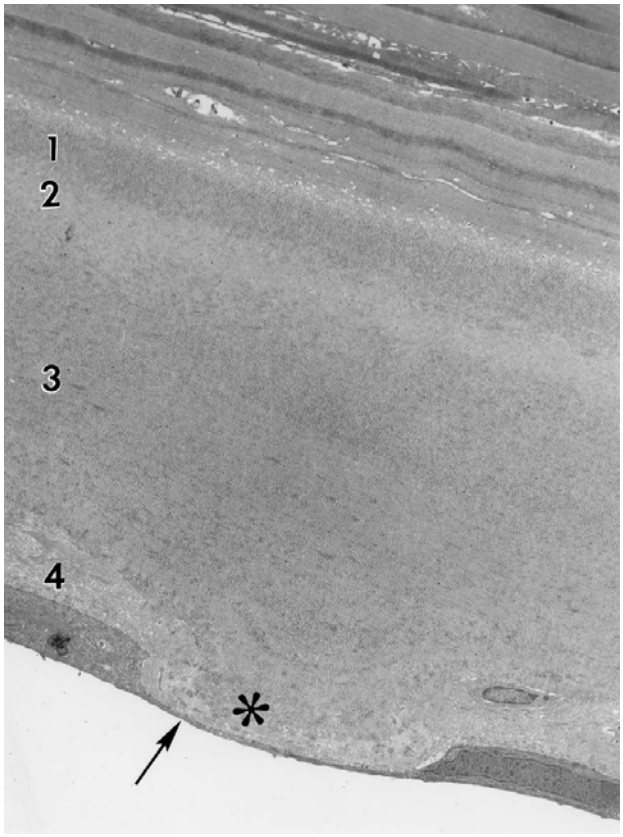

Figure 15: Descemet's membrane in FECD. 1: Anterior banded layer, 2: Posterior nonbanded layer, 3: Posterior banded layer, 4: Fibrillar layer. Guttae (asterisk) covered by attenuated endothelium (arrow).[69] Magnification: 4200X.

Zaniolo et al.[30] confirmed the ultrastructure (TEM) of DM of patients with FECD. DM was thick (up to 40.8 μm in thickness) and composed of normal anterior banded and posterior nonbanded layer as well as abnormal posterior banded and a fibrillar layer which was observed in 6 cases. Guttae were present in ten cases, varied in number, size and shape. Striated bodies of 0.11 μm spacing were present in 12 of 13 cases. Some half sized striated bodies were observed in 2 cases. Their location, thickness and length varied between cases (Figure 16).

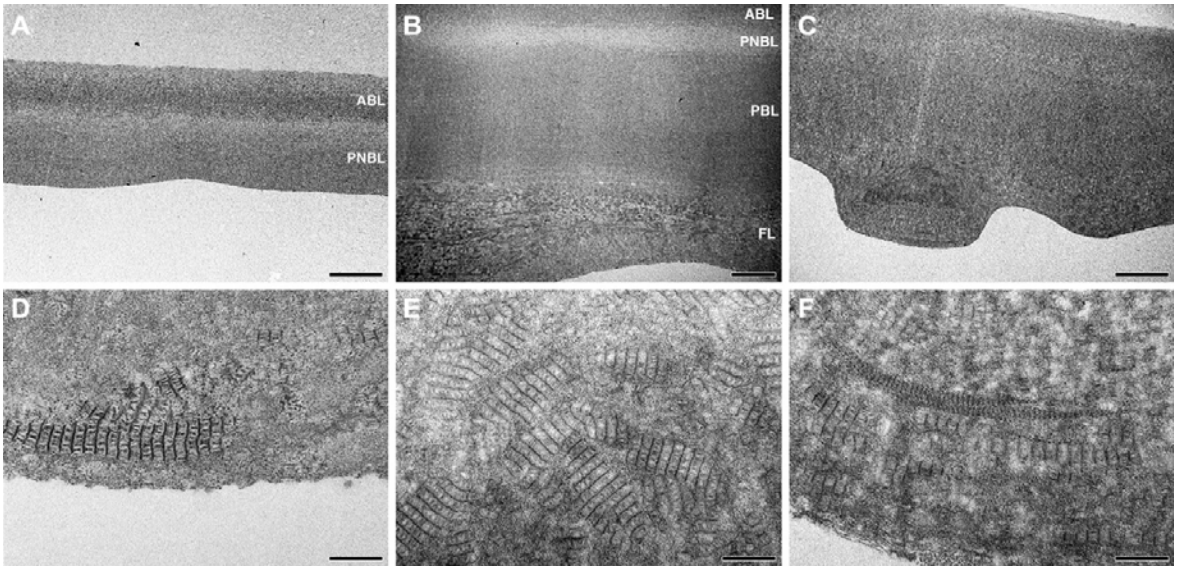

Figure 16: Ultrastructure of DM. (A) Normal DM with its two layers, an anterior banded layer (ABL) and a posterior non-banded layer (PNBL). (B-F) DM in FECD, (B) showing the presence of the abnormal posterior banded layer (PBL) and a fibrillar layer (FL), (C) showing large excrescences (guttae) in the posterior banded layer, (D) showing large striated bodies of 0.11 μm periodicity present on the edge of the posterior banded layer and perpendicular to the surface, (E) showing many large striated bodies with different orientations within guttae, (F) showing long striated bodies of 0.05 μm periodicity. Scale bars: (A-C) 5 μm, (D-F) 0.5 μm.[30]

Gottsch et al.[40] studied the ultrastructure of DM in a rare type of early-onset FECD with a L450W mutant of the COL8A2 gene and he compared it to a normal and common late-onset FECD (Figure 17):

- DM in late-onset FECD was composed of:

- Anterior banded layer.
- Posterior nonbanded layer: had a fine-grained structure that lacked this regular periodicity.
- Posterior banded layer: that had fine-grained layer containing short strips with transverse bands of about 120 nm periodicity. These strips presumably correspond to thin sections of irregular fibrous strands of structured collagen VIII.
- Fibrillar layer: thin.

- DM from the L450W COL8A2 mutant was 35 μm thick and was composed of:

- Amorphous layer: thin (1 μm)
- Anterior banded layer: thick (10 μm)
- Posterior nonbanded layer: normal
- Internal collagenous layer (ICL): 2 μm thick, characterized by wide-spaced collagen strips with 120-nm spacing, and fibrous material that corresponded to a narrow layer that stained strongly with antibodies to collagen VIII.
- Posterior striated layer: 12 μm thick, contained darker, horizontally striated material, and small, very electron-dense foci.

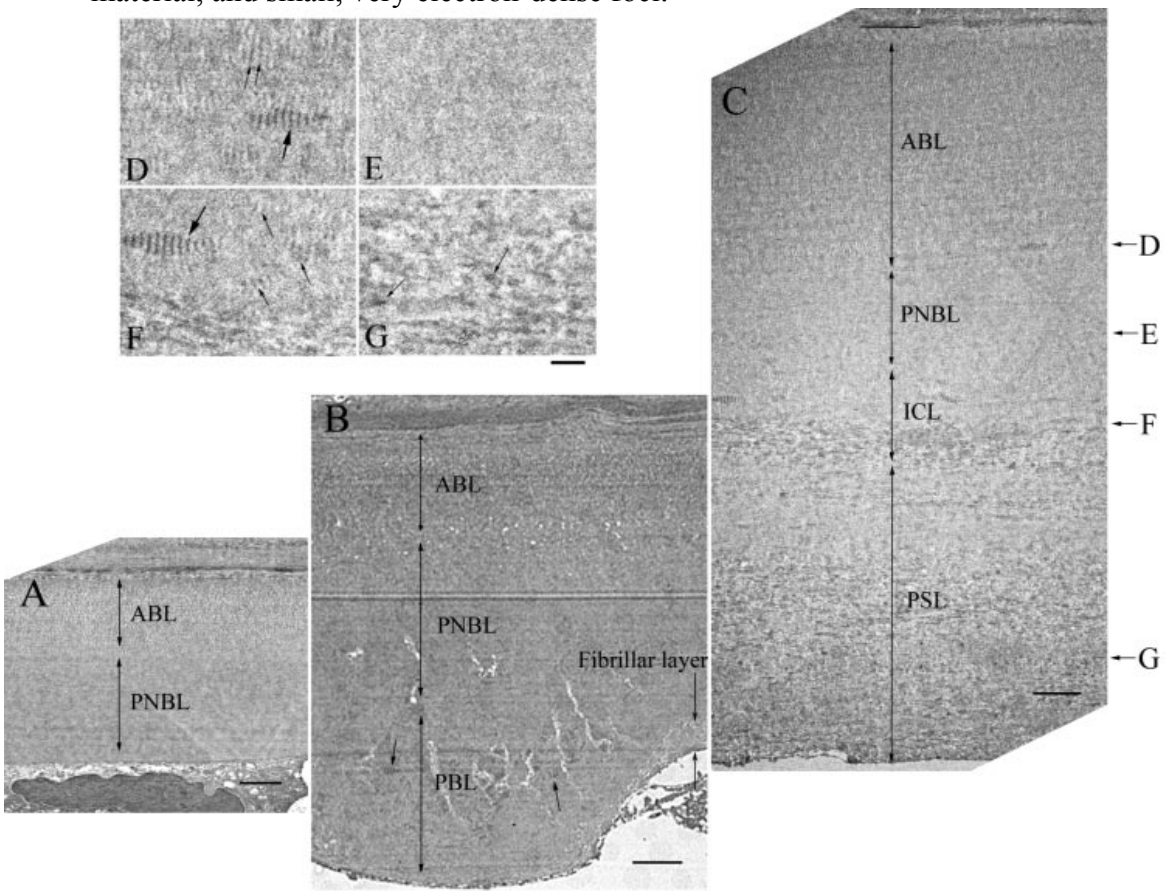

Figure 17: Ultrastructure of DM. (A) normal control, (B) late-onset FECD, and (C) early-onset FECD *COL8A2* L450W mutant. Arrows and letters, to the right of (C) indicate layers of origin for the higher-magnification images (D–G). (D) ABL. (E) PNBL. (F) ICL. (G) PSL. Bar: (A–C) 2 μm; (D–G) 500 nm.[40]

Immunohistochemistry showed that DM in early onset FECD stained positively for collagen VIII-α1 and α2 subtype in thin and thick branchlike fibers pattern respectively. Late onset FECD showed a positive staining of collagen VIII- α1 for the guttae, while α2 had a thick branchlike staining pattern (Figure 18). In early onset FECD, posterior DM had

a band of continuous staining for collagen VIII- α1 and IV, laminin and fibronectin. In late onset FECD, positive staining for collagen IV, laminin and fibronectin was observed near the posterior surface of DM and within the guttae (Figure 19).[40]

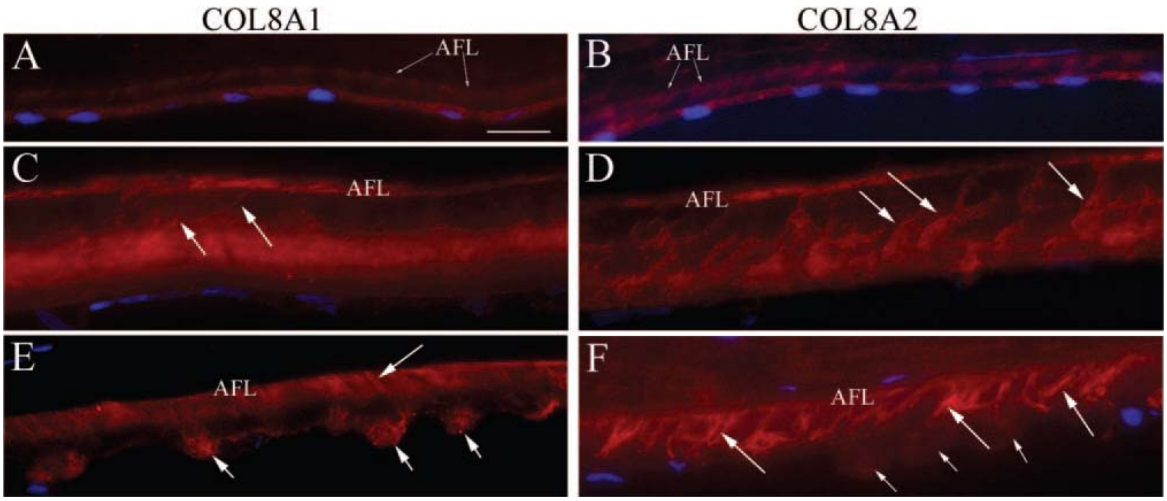

Figure 18: Collagen VIII α1 and α2 in normal and FECD corneas. (A, B) Normal cornea, showing corneal endothelial cells and DM stained with both antibodies. AFL: anterior fetal layer. (C, D) Early-onset FECD COL8A2 L450W mutant cornea. Arrows: α1 and α2 thin and thick branchlike fibers in DM, respectively. (E, F) Late-onset FECD cornea. (E) Short arrows: guttae. Long arrows: α1-labeled brushlike fibrillar structures. (F) Long arrows: α2-labeled brushlike thick fibers. Short arrows: guttae negative for α2.[40] Scale bar 20 μm.

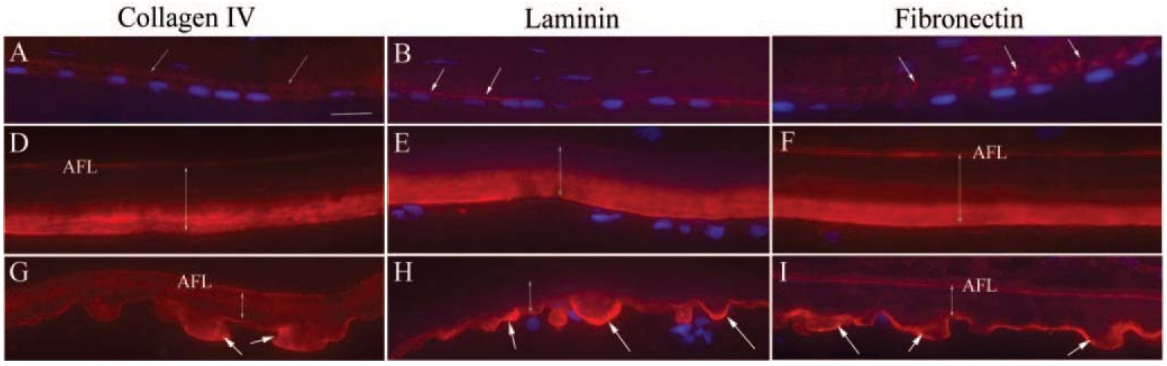

Figure 19: Collagen IV, laminin, and fibronectin. In the normal cornea (A–C), collagen IV and fibronectin with a weak linear pattern in the anterior DM (*arrows*). In early-onset FECD (D–F), thick bands in the posterior portion of DM. In the late-onset form (G–I), intense labeling in the posterior layer of the DM and guttae (arrows).[40] Scale bar: 20 μm.

However, Kenney et al.[73] studied the composition of DM in normal and FECD corneas by biochemical and immunofluorescence methods. They found that both had the same amino acid compounds and collagen types with slight discrepancy of collagen chains.

Levy et al.[74] used immunoelectron microscopy to study the DM of FECD. They found that intranodal regions of widespaced collagen stained positively for collagen VIII and negatively for collagen types I, III, V and VI, fibronectin, laminin, P component and tenascin.

Jurkunas et al.[75] studied clusterin (that has cytoprotective and antiapoptotic properties) and transforming growth factor-β-induced protein (TGFβIp) (extracellular matrix protein that mediates cell adhesion by interacting with collagen, fibronectin, and integrins) expressions. Immunocytochemistry studies of FECD showed that they were co-localized and increased in FECD DM compared to normal controls, with an increased intensity at the centers of guttae (Figure 20).

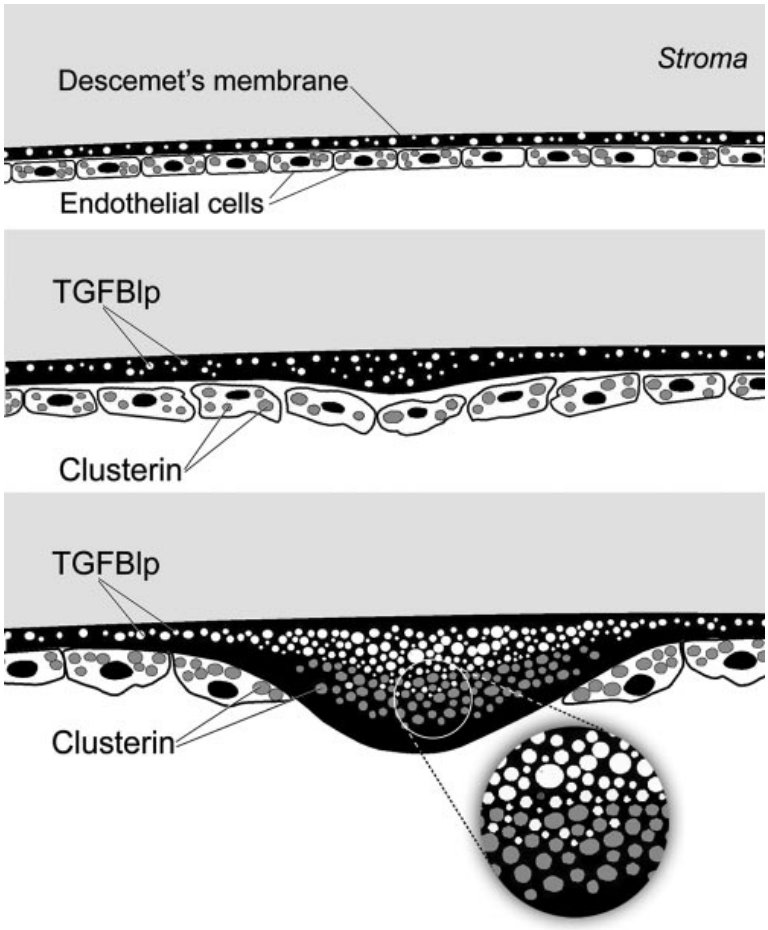

Figure 20: Clusterin and transforming growth factor-β-induced protein (TGFβIp) in DM of FECD.[75] Note their colocalization in the centers of guttae.

In conclusion, the most common way of describing DM in FECD is taken from Bourne's article.[71] DM in FECD is thicker than normal. It contains abnormal posterior collagenous layers (banded and fibrillar) that account for the increase of its thickness. However, variation in the composition does exist among the previous studies and even within each study that had a sufficient number of cases. Variation includes total thickness of DM; the thickness of each compounded layer; size, number, aspect and distribution of guttae and striated bodies (Table 2); presence and appearance of fibrillar layer. These variations in the composition could be explained by different genetic mutations responsible for this disease [40, 76] or by a different progression of the disease which may be caused by multi-factors causing stress to the endothelial cells (surgical trauma, prolonged corneal

edema). Knowing that all previous studies had obtained corneal buttons from patients who underwent corneal transplantation, we can conclude that DM was described in the end-stage of the disease. It would thus be interesting to perform a study to document the evolution of DM structure throughout the disease progression (*in vivo*); ultra high resolution optical coherence tomography (UHR-OCT) seems to be a promising tool to perform such study.[77]

Author, year	Description	Location
Yuen,[69] 2005	Wide-spaced collagen with a periodicity of 110-120 nm. In ¼ of the cases a periodicity of 60 nm was observed.	Posterior banded layer
Bourne,[71] 1982	110 nm banding, banded spindle-shaped bundles, 10 to 20 nm diameter fibrils and amorphous substance	Posterior banded layer
Bergmanson,[68] 1999	Guttae contained inclusion bodies of various structures; most prominent were banded or cross-straited 133 nm bodies or fibrils, while other bodies were amorphous and non-straited.	Posterior collagenous layer
Iwamoto,[66] 1971	Long-spacing bundles of 1000 A periodicity with two types of banded pattern and basement membrane-like material.	Posterior banded region & Border region
Kayes,[70] 1964	They divided banding into: B1: usual DM fibers B2: hexagon form B3: fusiform spindle periodicity of 100 nm B4: periodicity of 64 nm F1: fibers one-half B2 size F2: smaller fibers.	Banded zone
Zaniolo,[30] 2012	Striated bodies of 0.11 µm spacing were present in 12 of 13 cases. Some half sized striated bodies were observed in 2 cases. Their location, thickness and length varied between cases	Posterior banded
Gottsch,[40] 2005	Short strips with transverse bands of about 120 nm periodicity. These strips presumably correspond to thin sections of irregular fibrous strands of structured collagen VIII	Posterior banded layer

Table 2: Literature review of striated bodies in DM of FECD.

Corneal guttae are characteristic findings in DM of FECD. They have been found neither in PPMD nor in CHED. Abnormal posterior banded and fibrillar layers were mutual findings between FECD and both PPMD and CHED, but they were sometimes different in aspect, collagen type distribution and order in DM. Thus, these structural abnormalities are not pathognomonic of FECD. Hassall-Henle bodies also have an aspect similar to that of guttae, but a different location. [66] Similar findings were also observed in aphakic bullous keratopathy [78] and late endothelial failure.[79]

2.5.5 Endothelium

Kayes and Holmberg[70] studied the ultrastructure (TEM) of 4 corneas from patients with FECD. They found that the endothelium was thin, distorted in shape and full of vacuoles (Figure 21).

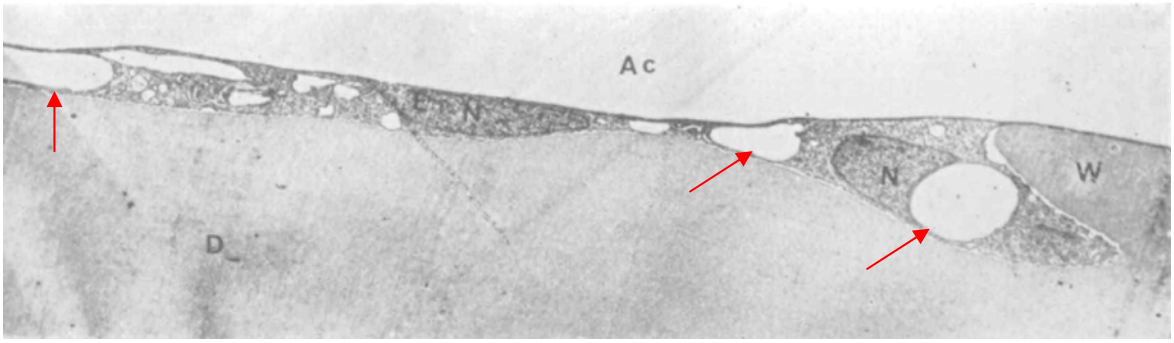

Figure 21: TEM of the endothelium in FECD showing Descemet's membrane (D), wart (W), endothelium (E), anterior chamber (Ac), nuclei (N) and large vacuoles (arrows). Magnification: 2600X.[70]

Iwamoto and DeVoe[66] studied the ultrastructure (TEM) of 7 corneas from patients with FECD. The endothelium was thin, consisting of normal appearing cells (Figure 22) and two types of abnormal cells:

- The Type 1 cell had cytoplasmic filaments, increased rough-surfaced endoplasmic reticulum (RER) and cytoplasmic processes, simulating fibroblasts (Figure 23).
- The Type 2 cell had elongated RER and lysosomes within a less dense cytoplasm, and was probably a degenerate form of the Type 1 cell (Figure 24).

Loosening of firmed attachment between the endothelial cells was a common feature. Partial discontinuity of the endothelial coverage was also seen.

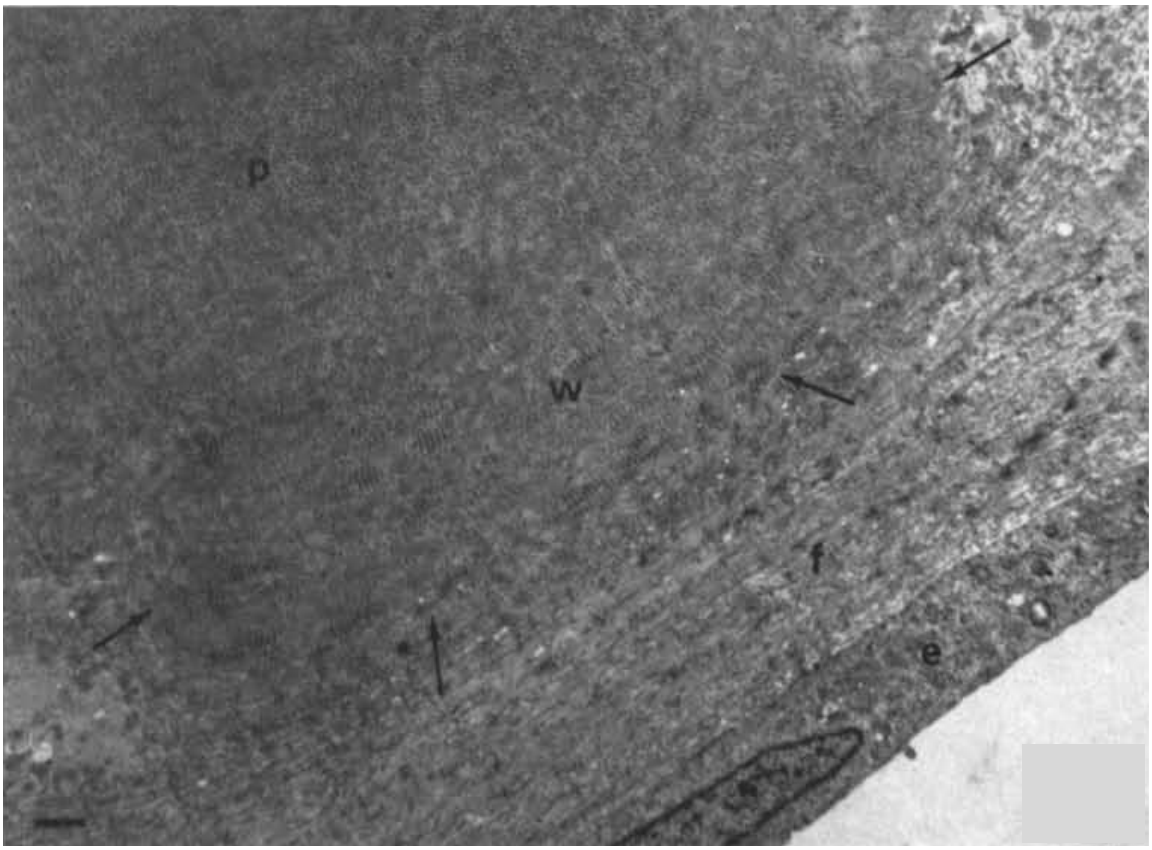

Figure 22: Ultrastructure of FECD endothelium.TEM image showing normal appearing endothelial cell (e) over fibrillar layer (f). Large wart (W) is seen surrounded by arrows and posterior banded layer (P). Magnification: X 5,600.[66]

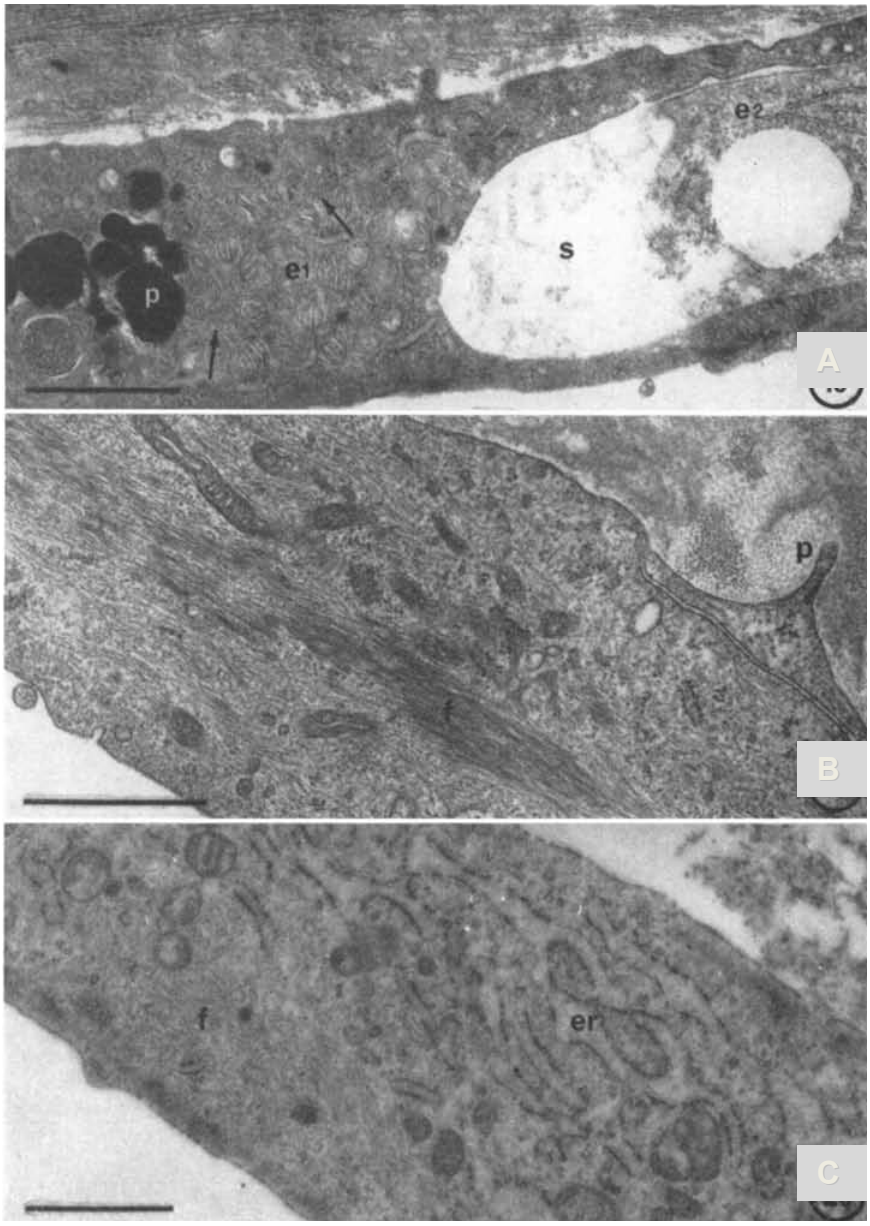

Figure 23: Ultrastructure of FECD endothelium. TEM image showing abnormal endothelial cells (Type I cell) viable-appearing fibroblast-like (A-C) characterized by (A) presence of pigment granules (p), degenerating endothelial cell (e2) leaving space (s), (B) cytoplasmic filaments (f), cytoplasmic process (p), (C) and abundant RER (er). Magnification: A: 23,000X, B-C: 22,000X.[66]

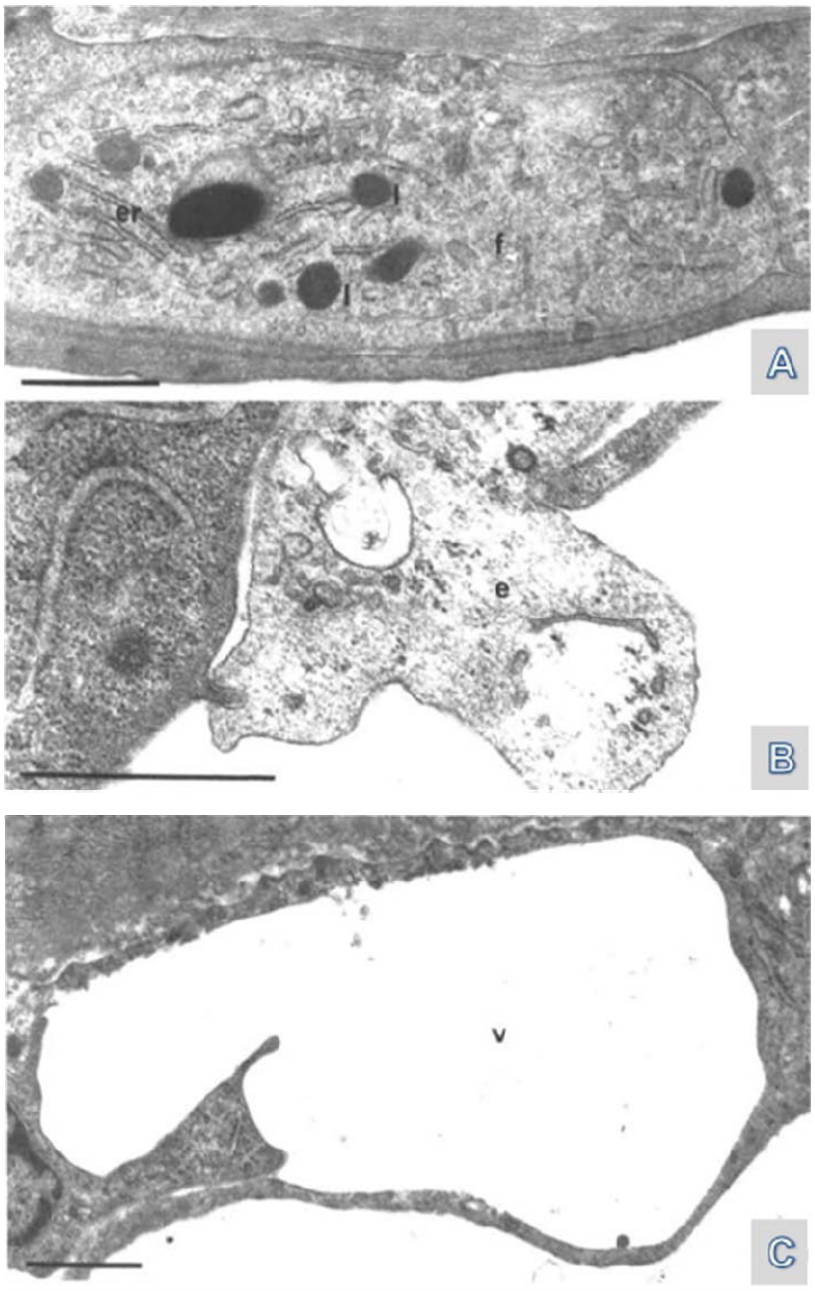

Figure 24: Ultrastructure of FECD endothelium. TEM image showing abnormal endothelial cells (Type II cell) degenerate form of type I cell (A-B) characterized by (A) elongated RER (er) lysosomes, (l) within a less dense cytoplasm, (B) degenerative endothelial cell (e) exposing to the anterior chamber, (C) vacuole (v). Magnification: A: 22,000X, B: 40,700X, C: l8,400X.[66]

Their hypothesis was that the endothelial cells in FECD become similar to fibroblasts and they start producing collagen fibrils and basement membrane-like material, forming abnormal layers of DM.

Bergmanson et al.[68] found that endothelial cell coverage was maintained while guttae progressed. Average endothelial cell thickness was 3.5 µm across the nucleus decreasing to 0.176 µm near the junction between cells and over the guttae. At these points the cells contained little or no cytoplasm between the apical and basal cell membranes, thus over considerable distances there were no organelles present. RER and mitochondriae were aggregated in the nuclear region.

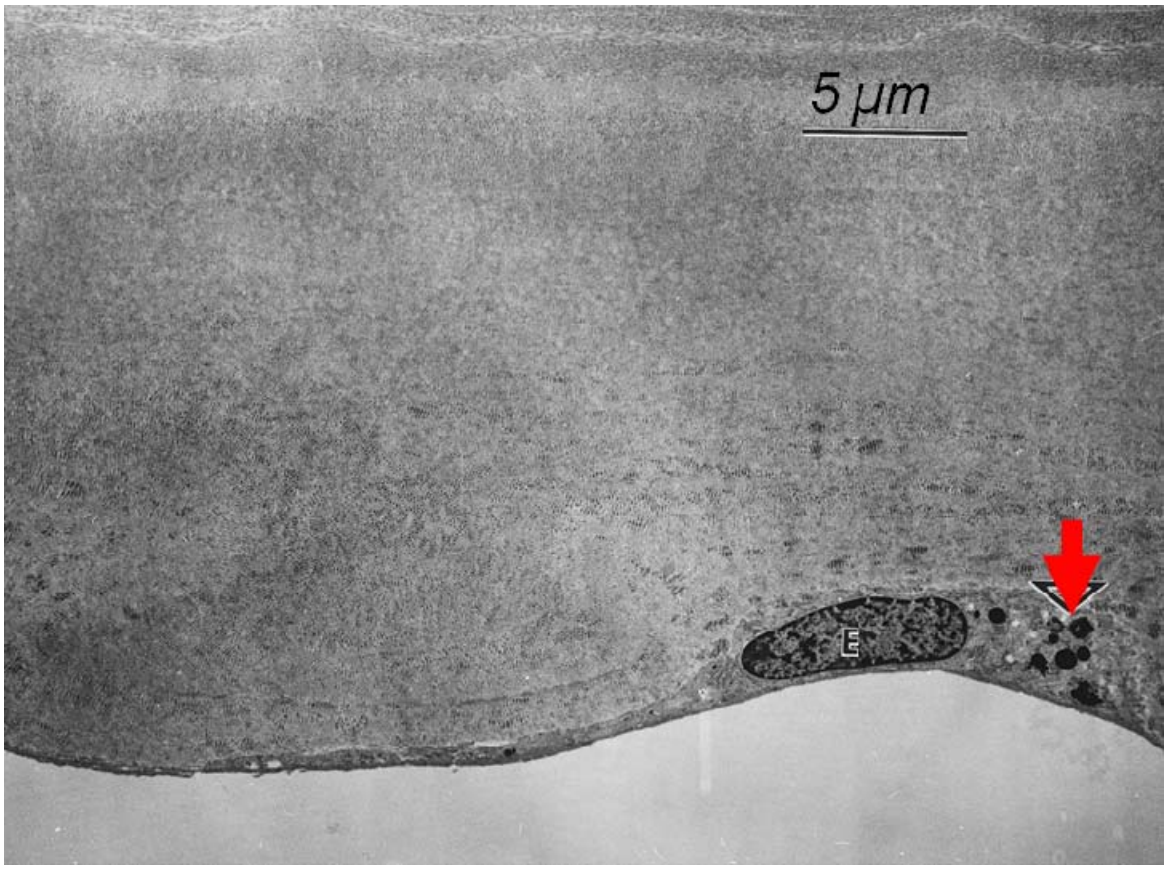

Figure 25: Ultrastructure of FECD endothelium. TEM image showing extremely thin endothelial cell over the guttae with intracellular pigment granules (arrow).[68]

The nuclei were spaced farther apart than 20 µm suggesting a reduced cell count. They were located in the valleys between the guttae, while over the guttae the cells were

extremely thin. Some nuclei had very little heterochromatin (thus pale), with a nearly spherical shape, and the surrounding cytoplasm had a degenerative and swollen appearance. Electron dense granules measuring 0.6 μm in diameter were observed within endothelial cells and occasionally in the guttae or the posterior collagenous layer (Figure 25). The endothelial cells' junctions appeared to be normal regardless of cell thickness, which led the authors to the conclusion that the endothelium still provided its normal barrier function while its fluid pump ability appeared compromised.

Yuen et al.[69] studied 32 cases of FECD using TEM. They found that endothelial cells were attenuated to atrophic (Figure 26). Large, round, melanin pigment granules were found in the endothelium of 7 cases.

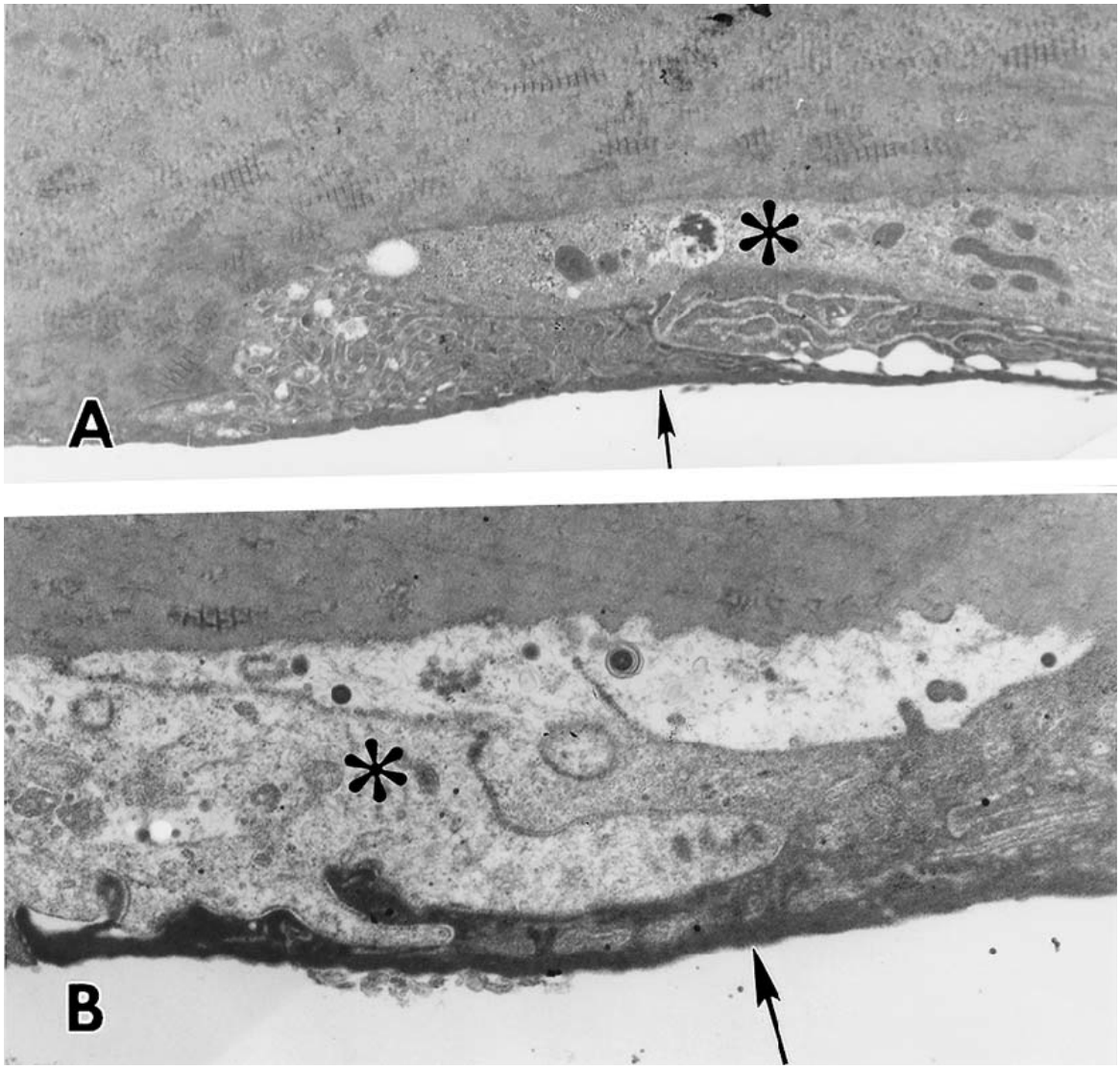

Figure 26: Ultrastructure of FECD endothelium. TEM image showing degenerative endothelial cells (asterisks) covered by intact endothelium (arrows). Magnification: A: 8,100; B: 15,000.[69]

2.6 Pathophysiology

2.6.1 Endothelial Permeability

In an *in vivo* study using slit lamp fluorophotometer, Burns et al.[7] found an increase in endothelial permeability at early FECD stages compared with age/sex matched normal controls. These results suggest that the endothelial barrier dysfunction is the earliest defect in FECD.

Few years later, Wilson et al.,[9] from the same research group, using two-dimensional scanning fluorophotometer, found no difference in endothelial permeability between patients with FECD and age/sex matched normal controls which suggests that the barrier function of the endothelium in early FECD stages is intact. The difference in conclusions between the two studies could be explained by a type I error in Burns' study and a difference in measurements methods, which were more precise in Wilson's study.

2.6.2 Endothelial Pump Function

Geroski et al.[8] showed a significant increase in pump site density in moderate guttata compared to normal controls suggesting an increase in endothelial permeability at early FECD stages that can cause a compensatory increase in endothelial pump site density, thus pump function. After this sharp initial increase, however, there is a gradual decline in pump site density correlating with severity of the disease.[10-12]

2.6.3 Aquaporin Expression

Kenney et al.[80] demonstrated a decrease in AQP1 expression in FECD endothelium compared to normal, suggesting that aquaporins may have an important role in the corneal fluid dynamics in the disease.

2.6.4 Corneal Sensitivity

Ahuja et al.[81] demonstrated a significant decrease in corneal sensitivity in FECD patients compared to normal subjects. Loss of sub-basal nerves and abnormal nerve morphology were suggested.

2.6.5 Aqueous Humor and Serum Composition

In FECD patients, there is an increased concentration of fibrinogen degradation products in both serum and aqueous humor;[82, 83] increased threonine, glutamine, and arginine; decreased asparagine, phosphoserine, and phosphoethanolamine concentration in the aqueous.[84] Significance of these findings is unclear. No difference has been found in flbrinogen-derived metabolites, ascorbate, glucose, carbon dioxide, bicarbonate and pH levels in the aqueous.[85]

2.6.6 Distribution of Chemical Elements

Alterations in Descemet's membrane were found in both guttae and non-guttae areas. Sulfur content is reduced by 40–50% and calcium content is increased with disease progression. Significance of these findings is unclear.[86]

2.6.7 Inflammation Role

Inflammation or any infectious, mechanical or toxic injury to the endothelium may play a role as a trigger in an eye genetically predisposed to develop FECD.[2, 3]

2.6.8 Apoptosis and Oxidative Stress

Apoptosis is programmed cell death. Using nucleus labelling and TUNEL (Terminal deoxynucleotidyl transferase dUTP nick end labeling) assays, the percentage of apoptotic epithelial cells, keratocytes and endothelial cell is significantly higher in FECD than normal controls.[18, 87] DNA fragmentation is also seen in the epithelium, stroma and endothelium of FECD corneas.[88]

2.6.8.1 Protein Unfolding

Protein folding is critical for cell function. Marked enlargement of RER is found in FECD endothelial cells, which is considered a sign of stress and unfolded protein response. Significant increase in levels of markers of unfolded protein response (GRP78, eIF2a and CHOP) is also found in FECD endothelial cells. Failure to alleviate RER stress by unfolded protein response can lead to cellular apoptosis.[17]

2.6.8.2 Clusterin Expression

Oxidative stress and reactive oxygen species can generate the overexpression of the clusterin (CLU) protein. CLU can help the cells to resist reactive oxygen species-mediated cellular injury.[89] CLU gene expression results in the synthesis of different forms of CLU, located in different sub-cellular compartments. Secretory CLU (sCLU) helps binding to hydrophobic molecules, clearing cellular debris and scavenging denatured extracellular proteins. Nuclear CLU (nCLU) binds Ku-proteins, which are involved in DNA repair, promoting apoptosis in stressed cells. FECD endothelial cells overexpress both sCLU and nCLU compared to normal (Figure 27).[14]

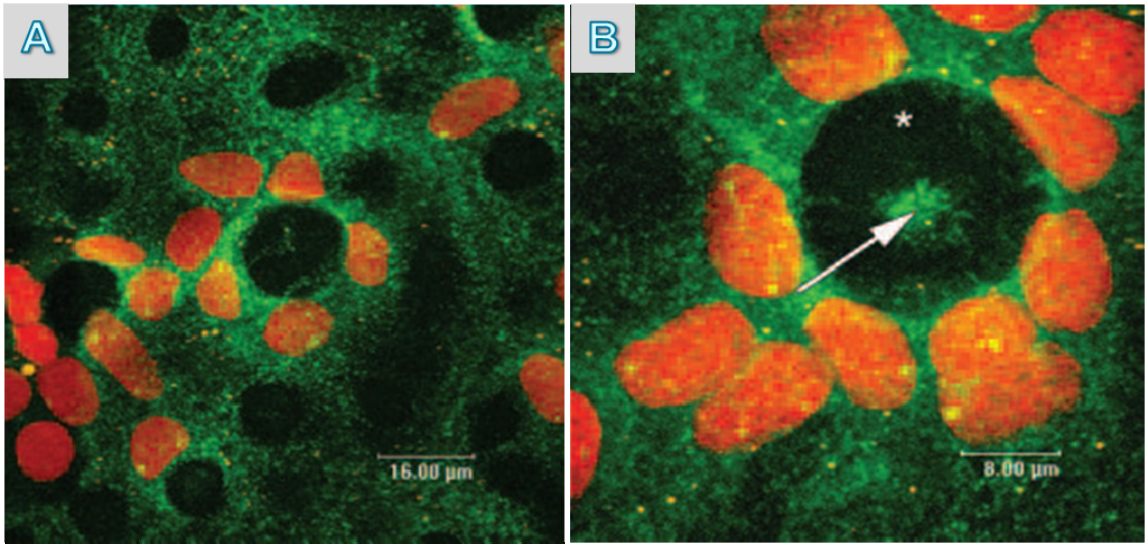

Figure 27: Clusterin expression in FECD. Endothelial cell nuclei clustered densely around the guttae with enhanced Clusterin staining at the cell membrane borders next to guttae and

inside guttae (arrow). Such a staining pattern suggests Clusterin's role in eliciting endothelial cell clustering under stress.[14] Clusterin: green, Nuclei: orange.

2.6.8.3 Transforming Growth Factor β–Induced Protein (TGFβIp)

TGFβIp is an extracellular matrix protein that mediates cell adhesion by interacting with collagen, fibronectin and integrins. There is an increase in production and modification of TGFβIp with aging in normal subjects. This increase, however, is greater in FECD. TGFβIp and CLU also co-localize in the centers of guttae.[75]

2.6.8.4 Peroxiredoxins Expression

Peroxiredoxins (Prx) are a group of antioxidants that function by removing cellular hydrogen peroxide. There is a significant decrease in Prx-2, -3 and -5 in FECD endothelium compared to normal suggesting a reduction in the ability of FECD endothelial cells to resist oxidant-induced damage.[15]

2.6.8.5 Mitochondria and DNA Damage

ATP production or utilization may play a role in the pathogenesis of FECD. Cytochrome oxidase is a key enzyme in the respiratory chain. There is a reduction of cytochrome oxidase activity in the central area of FECD endothelium, along with a decreased number of mitochondria.[90]

8-hydroxy-2-deoxyguanosine (8-OHdG) is an oxidative DNA damage marker. There is an increase in 8-OHdG levels in FECD endothelial cells compared to normals. Oxidative DNA damage in FECD co-localizes with mitochondria (Figure 28). There is also a co-localization of apoptosis and oxidative DNA damage in FECD endothelium compared to normal and pseudophakic bullous keratopathy (PBK) endothelium.[13] Normal endothelial cells are resistant to oxidative-stress-induced apoptosis *ex vivo.* While in FECD endothelial cells, there is an increase in p53 levels (p53 has many mechanisms of anticancer function, apoptosis initiation and genomic stability) leading to increased susceptibility to oxidative-stress-induced apoptosis (Figure 29). Therefore, p53 is presumed to play a central role in

cell death seen in FECD.[16] Figure 30 sumarizes the pathogenesis of FECD as proposed by Jurkunas et al.[13]

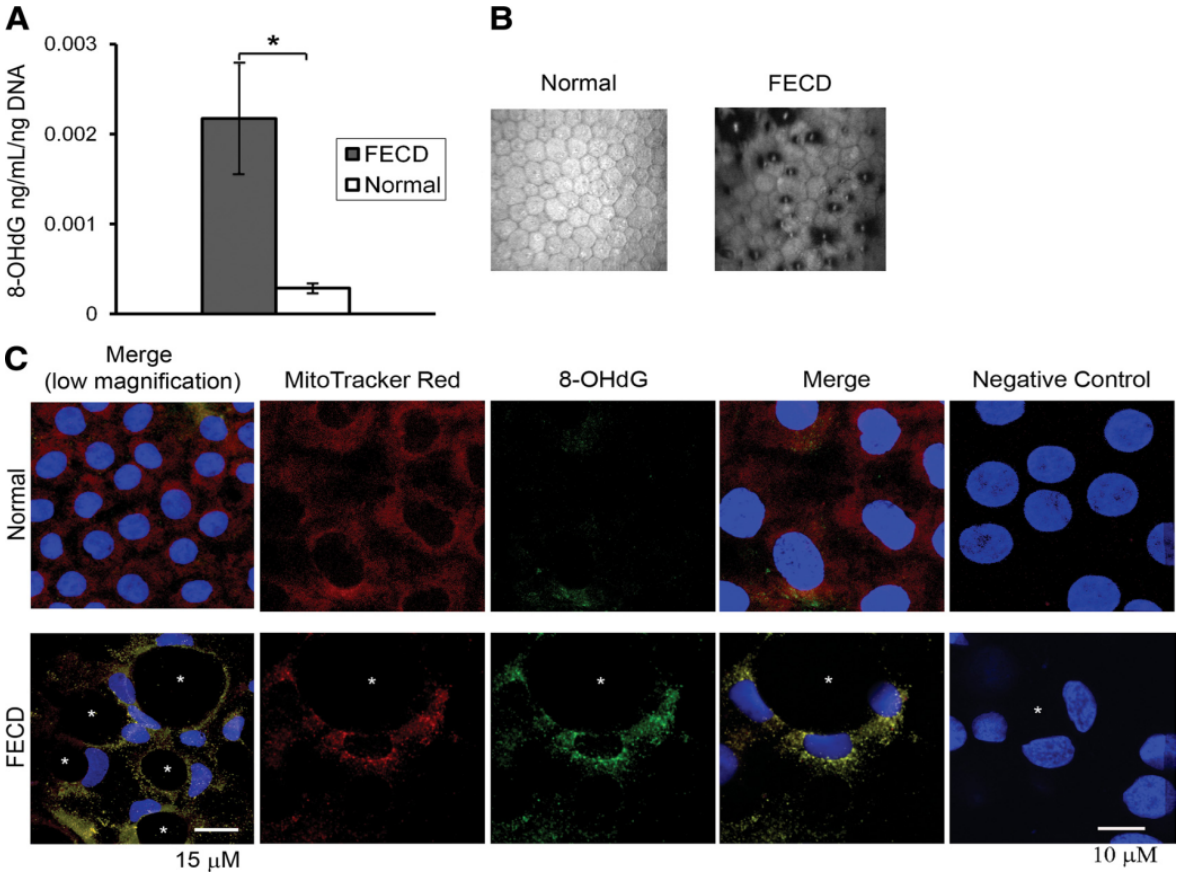

Figure 28: Oxidative DNA damage and its colocalization with mitochondria in FECD endothelium. (A) ELISA showing higher concentration of 8-OHdG per nanogram DNA from patients with FECD and normal, *p=0.006. (B) *In vivo* confocal microscope images of normal and FECD endothelium. (C) Showing increased immunostaining of FECD endothelium with 8-OHdG (green) and its colocalization with mitochondria (red) compared with normal endothelium. Nuclei are in blue. Asterisks indicate guttae.[13]

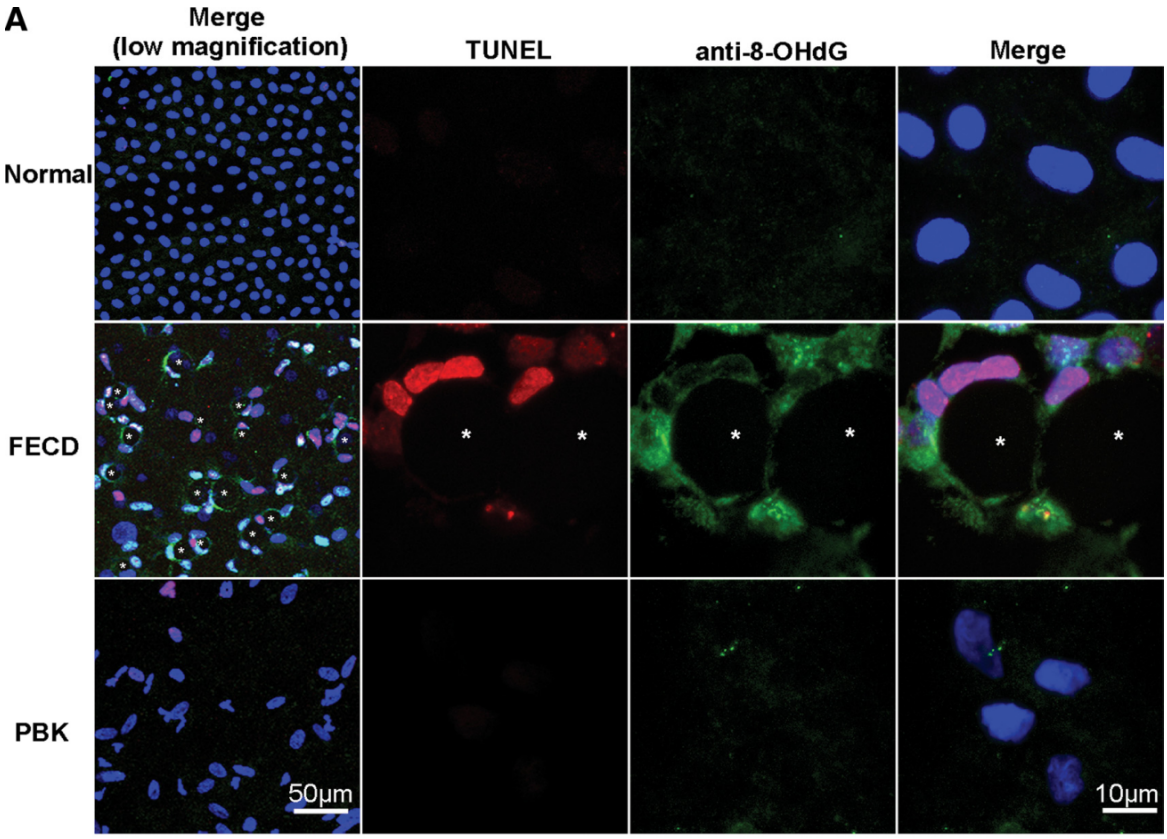

Figure 29: Apoptosis and oxidative DNA damage in normal, FECD and PBK endothelium. This figure demonstrates an increased apoptosis (TUNEL in red) and its colocalization with oxidative DNA damage (anti-8-OHdG in green) in FECD endothelium. Nuclei are in blue. Asterisks indicate guttae.[13]

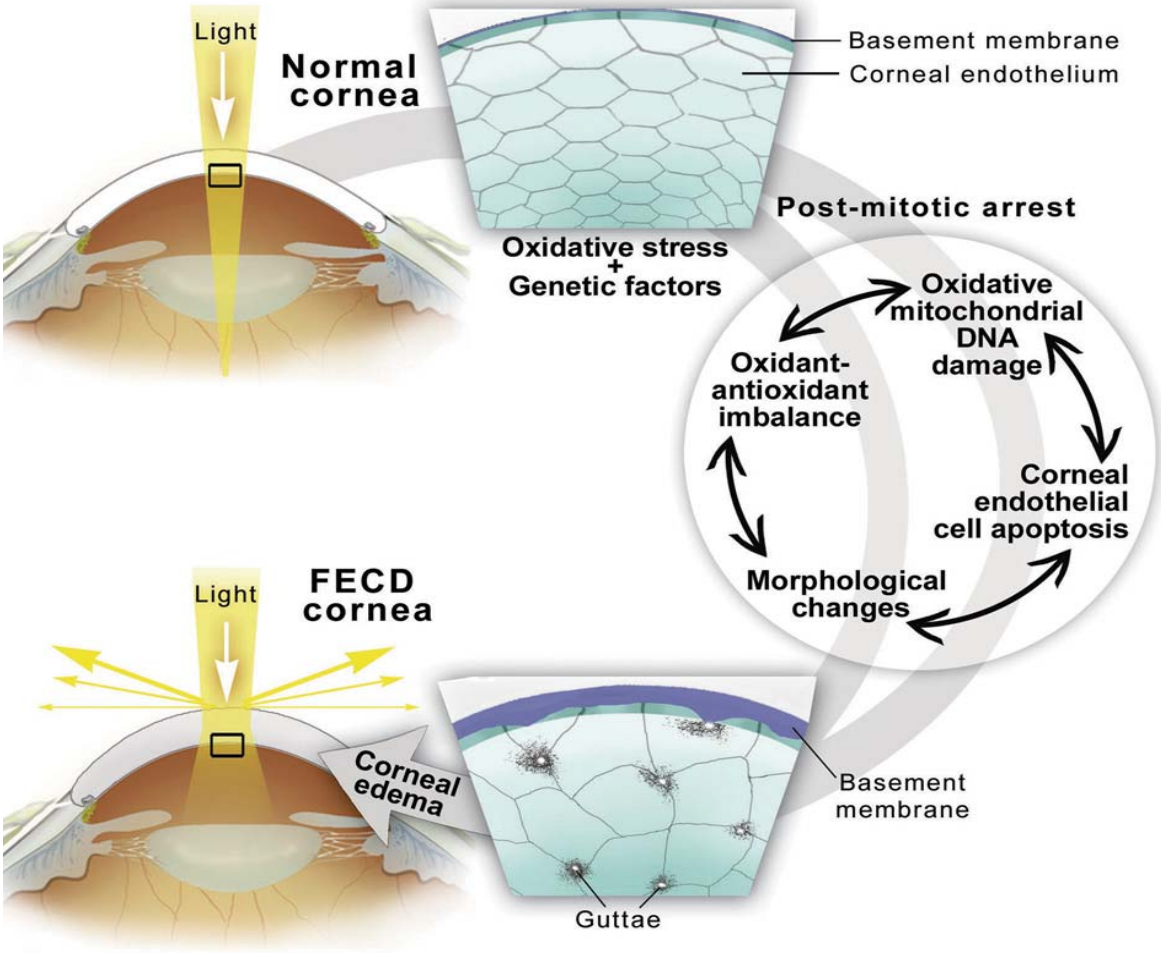

Figure 30: Summary of FECD pathogenesis as proposed by Jurkunas et al.[13]

2.7 Inheritance

FECD is an inherited disease that usually follows an autosomal dominant pattern with a high degree of penetrance and variable expressivity.[91-93] Females are more severely affected than males but not more frequently.[94] Increased severity in women may also suggest a hormonal role in the pathophysiology of FECD.

2.7.1 International Committee for Classification of Corneal Dystrophies (IC3D)

The new IC3D classification of corneal dystrophies includes FECD in three categories depending on the characterization of the gene defect (Table 3).[6, 95]

Category I includes a well-defined corneal dystrophy where both of gene and specific mutation have been identified. Early-onset FECD mapped to COL8A2 (FECD1) falls in this category.[96]

Category II includes a well-defined corneal dystrophy that has been mapped to one or more specific chromosomal loci but the gene has not been identified. Familial FECD (FECD 2) falls in this category.

Category III includes a well-defined corneal dystrophy where the chromosomal locus has not been identified. A large number of familial FECD cases fall in this category.[97]

	Mode of Inheritance	Gene Locus	Gene	Mutations
Early-onset FECD				
FECD1 (OMIM*)	AD**	1p34.3-p32.3	COL8A2	Q455K L450W Q455V
Late-onset FECD				
FCD1 / FECD2 (OMIM)	AD	13pTel-q12.13	Unknown	
FCD2 / FECD3 (OMIM)	AD	18q21.2-q21.32	Unknown	
FCD3 / FECD5 (OMIM)	AD	5q33.1-q35.2	Unknown	
FECD4 (OMIM)	?	20p13-p12	SLC4A11	E399K G709E T754M c.99-100delTC
	Complex	7, 15q, and X	Unknown	
	AD	1(53cM) 17q(107-126cM)	Unknown	

*Online Mendelian Inheritance in Man[112] ** Autosomal dominant

Table 3: Summary of FECD defective genes and their mutations.[6]

2.8 Current Treatment

The management of FECD depends on its clinical stage:

Stage I: treatment is not necessary.

Stage II: topical hyperosmotic agents (5% NaCl solution) or hairdryer could be used to facilitate corneal dehydration.

Stage III: loosely fit, high water content soft contact lenses could be used to relieve pain caused by recurrent erosions.

Intraocular pressure-lowering agents, even if the intraocular pressure is normal, could be used. Carbonic anhydrase inhibitors, however, should be avoided as they may interfere with the Na^+-K^+ATPase pump. There is no evidence that the use of steroids would help in FECD.[98]

When medical management is no longer adequate, corneal transplantation becomes the only available option. The current management is based on the surgical replacement of the diseased endothelium with a healthy endothelium from an eye bank donor, either by PKP where full thickness of the cornea is replaced or, now more frequently, using a DSAEK procedure, where only the diseased posterior part of the cornea is replaced.[20]

2.9 Limitations of Current Knowledge and Management of FECD

Many factors contribute in our lack of knowledge of the mechanism of FECD. Most of the studies conducted to investigate the pathogenesis of Fuchs were performed at the clinical end-stage due to the infeasibility of obtaining a biopsy of the cornea from an asymptomatic patient (at early stages of the disease). FECD spans up to 20 years; the timeline of disease is missing. For example, what is the role of the accumulation of abnormal DM and of guttae formation in endothelial cell dysfunction and survival? And what is the significance of the fibrilar layer in DM?

Lack of knowledge of FECD pathogenesis along with lack of experimental models contributes to the absence of effective medical treatment.

Surgical management is not perfect either. Corneal endothelial allograft transplantation yields a 10% average rate of immunologic rejection (range 0% to 45% for

follow-ups ranging from 6 to 21 months).[21] There is a 17% cumulative probability of endothelial graft rejection at four years in patients with FECD without ocular co-morbidities. Graft rejection in these eyes is known to result in significant endothelial cell losses, thus graft failure.[99]

Corneal endothelial tissue engineering may carry a potential solution to these problems. By creating an *in vitro* and *in vivo* model of the disease, its pathogenesis could be better understood and potential treatments could be tested. In addition, transplantation of functional TE corneas to the same patient (autograft) would allow the elimination of allograft rejection.

3 Chapter III:

Tissue Engineering of the Corneal Endothelium

Human corneal endothelial cells are believed to be incapable of proliferation *in vivo.* They are arrested in the G1-phase of the cell cycle.[23] Once cell degenerates for any reason (i.e. aging, toxins, trauma or disease) the neighboring cells will enlarge and migrate in order to maintain the integrity of the monolayer, leading to a decrease in cell density and, eventually, endothelial failure.

Human corneal endothelial cells retain their capacity of proliferation *in vitro* in response to growth promoting agents,[25, 26] which makes tissue engineering of a corneal endothelium feasible. The tissue engineering procedure, however, consists of several steps including cell isolation, cell culture and tissue carrier. Techniques and materials vary greatly between different laboratories.

The ideal tissue engineered cornea should be nontoxic, free of transmitting diseases, genetically stable, immunologically compatible and having long term functioning stability and high cell survival rate. It also needs to be compatible with current surgical techniques for transplantation. Patients have to obtain superior benefits with this tissue engineered graft in order to replace current native graft transplantation.

In this chapter, I will briefly review corneal endothelial tissue engineering. I will be focusing on our laboratory success in isolating and culturing endothelial cells from patients with Fuchs endothelial corneal dystrophy.

3.1 Corneal Endothelial Cell Isolation Techniques

Risk of contamination of corneal endothelial cell culture with stromal keratocytes is a challenge.[100, 101] The most common method to overcome this challenge is to peel off Descemet's membrane (DM) (carrying endothelial cells) from its stromal bed. Endothelial cells are then detached from DM using either ethylenediaminetetraacetic acid (EDTA), [26, 102] collagenase,[103] trypsin,[104] or dispase.[105]

The isolation method that we use in our lab is based on Zhu and Joyce technique.[26] For human subjects (i.e. patients with FECD), endothelial cell specimen is obtained as

follows: At the time of DSAEK, a blunt-tipped, reverse Sinskey hook is used to score the diseased Descemet's membrane (DM), which is then peeled off and removed from the eye through a 2.75 mm limbal incision using an angled tying forceps. The anterior chamber being maintained by balanced salt solution (BSS; Alcon Canada Inc., Mississauga, ON, Canada) irrigation. The specimen is put in Optisol-GS (Bausch and Lomb, Rochester, NY) and sent on ice to the laboratory for cell isolation (Figure 31). For PKP, the full thickness corneal specimen is sent in Optisol-GS and DM is stripped in the laboratory.

For eye bank donor corneas (Québec Eye Bank, Montréal, and Banque d'yeux du Centre universitaire d'ophtalmologie (CUO), Québec, QC, Canada), endothelial cell specimen is obtained as follows: Central Descemet's membrane is stripped using a circular biopsy punch (Acuderm, Dormer Laboratories, Toronto, ON, Canada) and fine forceps.

Descemet's membranes are incubated overnight at 37^{o}C in growth medium. After centrifugation, they are incubated one hour in 0.02% ethylenediaminetetraacetic acid (Sigma, Oakville, ON, Canada) and the loosened cells are gently detached from DM by passing several times through a flamed-polished pipet. Cells are then centrifuged and resuspended in fresh medium. This isolation method was proposed to avoid fibroblast contamination.[26]

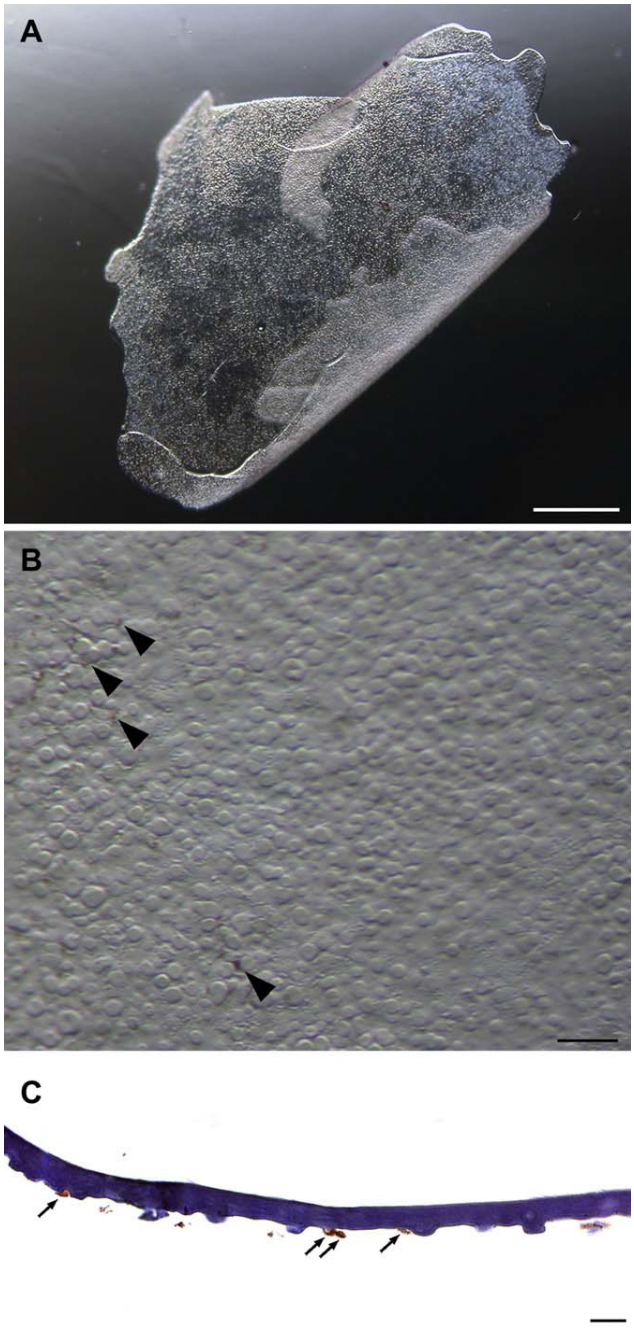

Figure 31: Central corneal DM-endothelium of a 58 year-old female with Fuchs endothelial corneal dystrophy (A). Higher magnification of the specimen showing multiple guttae and pigmentation (arrowheads) (B). Histology of the DM before cell isolation (C) showing multiple guttae and a few scarce cells (arrows). This specimen successfully initiated a culture. Scale bars: (A) 1 mm, (B) 100 µm, C) 20 µm.[30]

3.2 Corneal Endothelial Cell Culture Methods

As mentioned before, corneal endothelial cells retain their proliferative capacity when isolated and incubated in serum and growth media. Many growth supplements were tested in order to enhance the proliferative capacity of the endothelial cells and maintain their morphology. Peh et al.[106] published a review describing different growth medium formulas optimized from different laboratories (Table 4). The goal of adding growth supplements is to enhance proliferation and to help maintaining endothelial morphology.

Author	Basal medium	Serum (%)	Growth factors and supplements
Blake et al.[107]	MEM	10%	5 μg/mL insulin 5 μg/mL transferrin 5 ng/mL sodium selenite 150 μg/mL ECGS 50 μg/mL gentamicin 100 U/mL penicillin 100 µg/mL streptomycin 0.25 µg/mL amphotericin B
Yue et al.[108]	MEM	15%	200 mM glutamine 2% essential amino acids 1% nonessential amino acids 10 μg/mL gentamicin 1.2 μg/mL amphotericin B
Miyata et al.[109] and Amano[110]	DMEM	15%	30 mg/L L-glutamine 2.5 mg/L fungizone 2.5 mg/L doxycycline 2 ng/mL bFGF
Pistsov et al.[111]	M199	20%	4 mM glutamine 200 μg/mL ECGS 100 μg/mL penicillin 100 μg/mL streptomycin
Zhu and Joyce[26]	Opti-MEM-I	8%	20 ng/mL NGF 5 ng/mL EGF 20 μg/mL ascorbic acid 200 mg/L calcium chloride 100 µg/mL pituitary extract 50 μg/mL gentamicin 1Xantibiotic/antimycotic 0.08% chondroitin sulfate

Engelmann and Friedl[112, 113]	F99 Ham's F12 and M199 (1:1 ratio)	2%–5%	20 μg/mL ascorbic acid 20 μg/mL bovine insulin 2.5 μg/mL transferrin 0.6 µg/mL sodium selenite 10 ng/mL bFGF
Li et al.[103]	SHEM Ham's F12 and DMEM (1:1 ratio)	5%	0.5% DMSO 2 ng/mL EGF 5 μg/mL insulin 5 μg/mL transferrin 5 ng/mL selenium 0.5 μg/mL hydrocortisone 1 nM cholera toxin 50 μg/mL gentamicin 1.25 μg/mL amphotericin B
Ishino et al.[105]	DMEM	10%	2 ng/mL bFGF 50 U/mL penicillin 50 μg/mL streptomycin
Choi et al.[114]	EGM-2 endothelial growth medium	10%	SingleQuots (Lonza, Switzerland) consisting: VEGF EGF bFGF IGF Ascorbic acid Hydrocortisone Gentamicin Amphotericin B

Table 4: Growth medium supplements used to culture human corneal endothelial cells. ECGS, endothelial cell growth supplement; bFGF, basic fibroblast growth factor; NGF, nerve growth factor; EGF, epidermal growth factor; DMSO, dimethyl sulfoxide; VEGF, vascular endothelial growth factor; IGF, insulin-like growth factor; SHEM, supplemented hormonal epithelial medium; MEM, minimum essential medium; DMEM, Dulbecco's Modified Eagle Medium. Modified from Peh et al.[106]

We use the formula described by Zhu and Joyce,[26] which was optimized for human endothelial cell culture. Our growth medium consists of OptiMem-I (Invitrogen, Burlington, ON, Canada), 8% fetal bovine serum (HyClone, Logan, UT), 5 ng/ml human epidermal growth factor (Austral Biologicals, San Ramon, CA), 20 ng/ml nerve growth factor (Biomedical Technologies, Stoughton, MA), 100 µg/ml bovine pituitary extract

(Biomedical Technologies), 20 µg/ml ascorbic acid (Sigma), 200 mg/L calcium chloride (Sigma), 0.08% chondroitin sulfate (Sigma), 25 µg/ml gentamycin sulfate (Schering, Pointe Claire, QC, Canada) and 100 IU/ml penicillin G (Sigma).

Our laboratory has validated this formula for normal human endothelial cell culture and we have demonstrated for the first time that human endothelial cells obtained from patients with FECD can be cultured using this formula without the need of transfecting oncogenes.[30]

We have reported a culture success rate of 62% for FECD endothelial cells and 58% for normal endothelial cells. 66% of cultured FECD endothelial cells have an endothelial morphology (rounded and slightly elongated cells) while the remaining have fibroblast-like morphology (thin and very elongated cells). For normal endothelial cell culture, 42% have endothelial morphology (Figure 32). Both cells of endothelial and fibroblastic-like morphology express keratins 8 and 18 (K8/18) (Figure 33), confirming the absence of contamination with fibroblasts in culture.[115] Donor's old age and presence of fibrillar layer of DM are the main factors affecting initiation of endothelial cell culture with an endothelial morphology. On the other hand, donor gender, presence of guttae, pigmentation and corneal edema, and specimen size do not seem to affect successful culture.

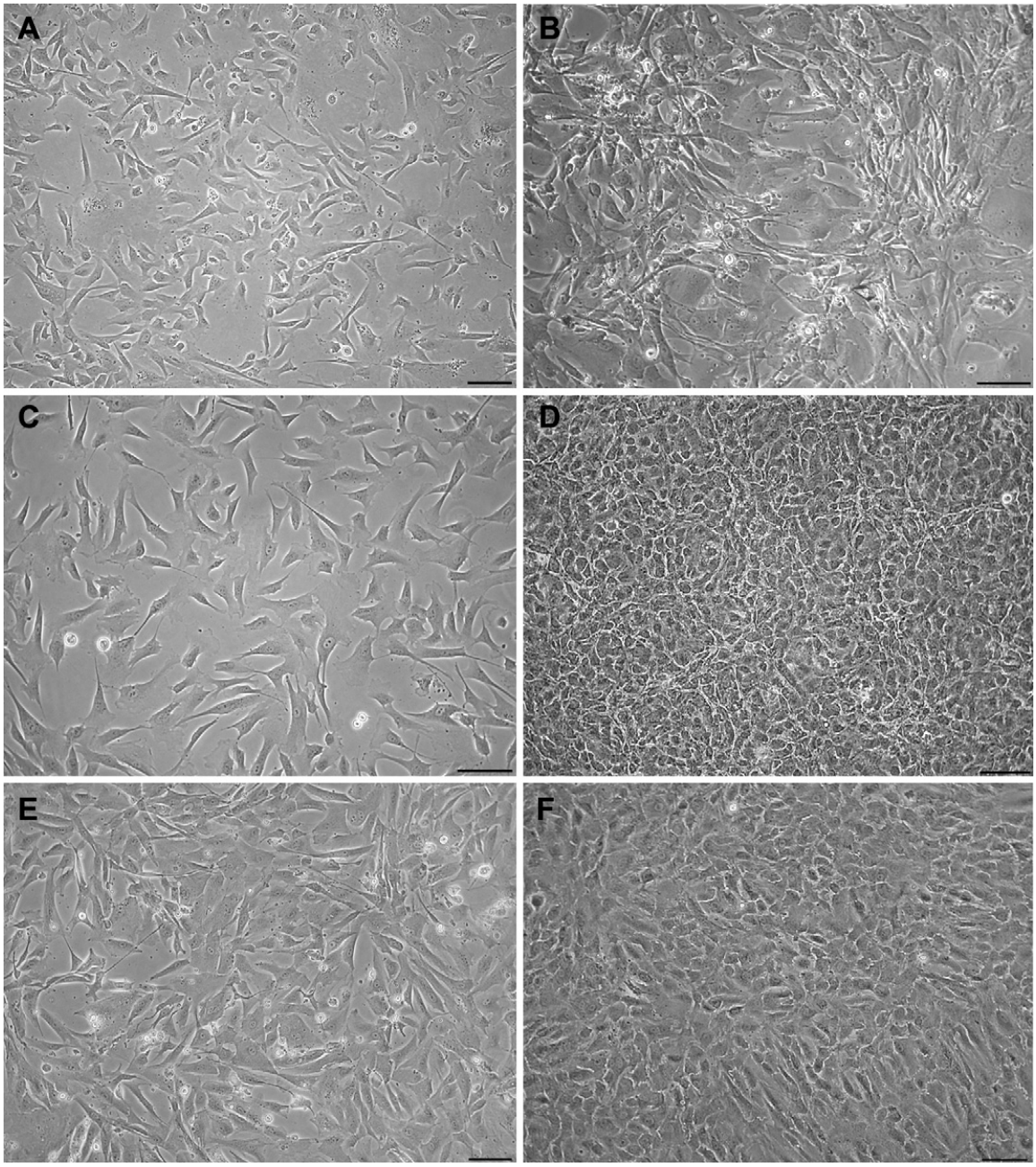

Figure 32: Culture of corneal endothelial cells and their morphology. (A-D) Show FECD endothelial cells. (E-F) Show normal endothelial cells. (A) Shows endothelial-like morphology of a primary FECD (P0) culture. (B) Shows mixed morphology of FECD corneal endothelial cells of another primary culture (P0). (C) Shows second-passaged FECD cells of the same population in A. (D) Shows third-passaged FECD cells of the same population in A and C. The culture formed a monolayer of polygonal cells. (E) Shows

culture of normal corneal endothelial cells in P0. (F) Shows confluent third-passaged culture of normal corneal endothelial cells. Scale bars 100 μm.[30]

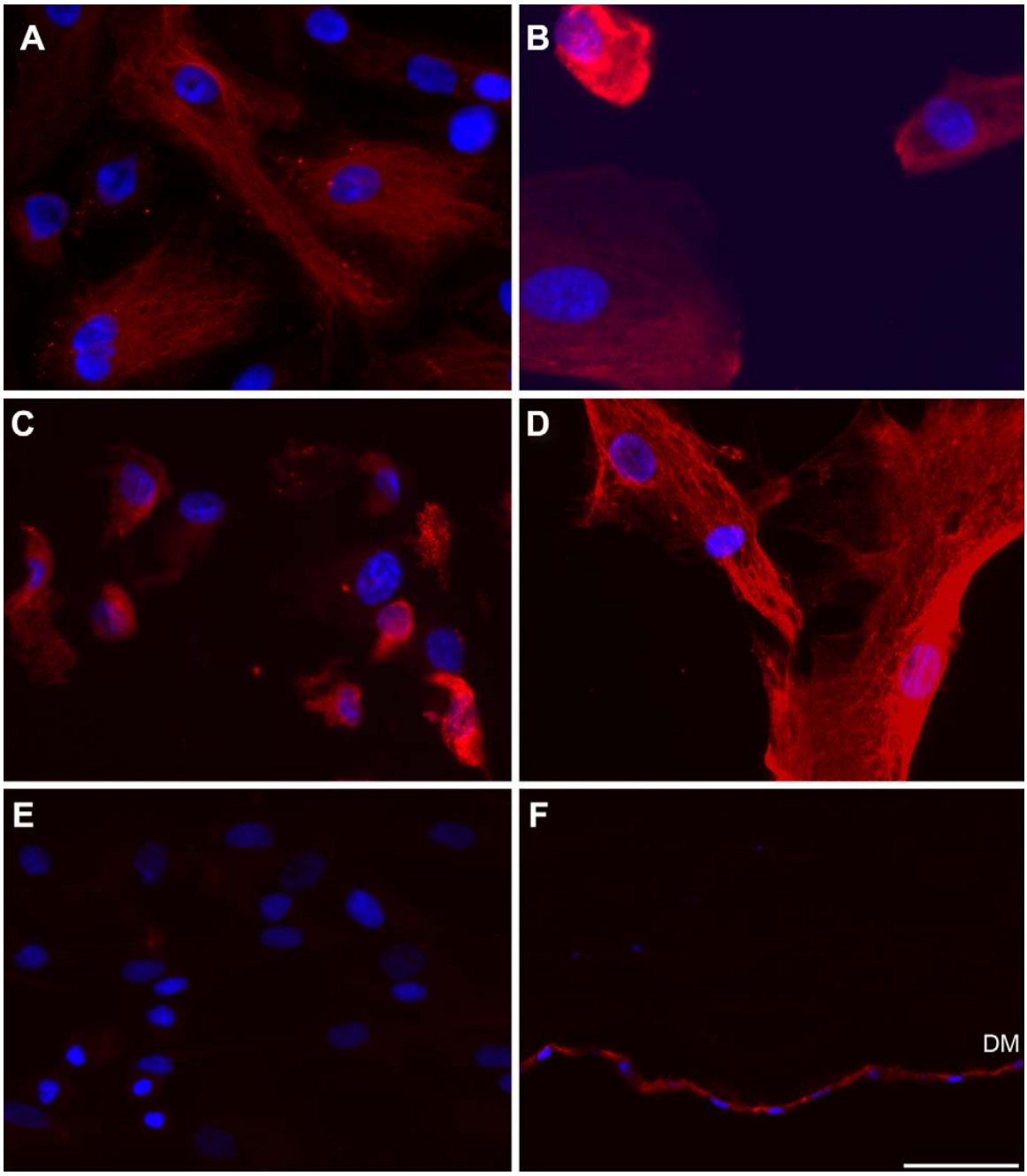

Figure 33: Keratins 8 and 18 (K8/18) expression. (A-B) Show cultured FECD corneal endothelial cells with endothelial (A) and fibroblast-like morphology (B). (C-D) Show cultured normal corneal endothelial cells of endothelial morphology (C) and fibroblast-like

morphology (D). (E) Shows cultured corneal stromal fibroblasts. (F) Shows native normal cornea. K8/18 (red) was expressed in both cultured and native corneal endothelial cells (A-D, F) and was absent in both cultured and native corneal stromal cells (E-F). Nuclei were stained with Hoechst (blue). Scale bars: 50 μm.

3.3 Endothelial Cell Carriers

Cultured endothelial cells need a support in order to be transplanted *in vivo*. Several carriers have been proposed. Thin carriers (such as Descemet's membrane,[116] amniotic membranes,[105] gelatin membranes,[117] anterior crystalline lens capsule[118] and silk fibroin membranes[119]) are soft and hard to manage. Transplanting them *in vivo* without damaging the fragile endothelial cells is a challenge. More rigid carriers (such as hydrogel lenses[120] and cross-linked collagen[121]) may not follow the curvature of the host cornea, thus they are more susceptible to detach.[122]

Native stromal carriers mimic the current native allograft transplantation. However, they carry a high risk of contamination with epithelial cells and keratocytes in culture as well as a risk of immunological rejection when transplanted *in vivo*.[100]

In order to avoid the undesirable effect of native cell presence, a devitalized stromal carrier has been proposed. Elimination of native stromal cells can be performed by one freeze (-80°C)/thaw cycle,[123] three freeze (-20°C)/thaw cycles (technique used by our laboratory)[27, 29] or chemically using ammonium hydroxide.[102]

3.4 Tissue-Engineered Corneal Endothelium Approaches

Restoration of normal vision is the ultimate goal of tissue engineering of a cornea. Thus, the transparency outcome of the TE corneas is highly important. *In vitro* and *ex vivo* assessments usually include tissue integrity, endothelial morphometry and function-related protein expression. Beside these characterizations, the *in vivo* assessments include mainly corneal transparency and thickness, which indicate the real functionality of the TE cornea. Several approaches have been proposed to tissue-engineer a corneal endothelium:

Patel et al.[124] used an innovative method where superparamagnetic microspheres (SPMs) were incorporated into cultured human endothelial cells. The cells were then transplanted into a human anterior segment *ex vivo* model with the aid of an external magnetic field. They showed that the endothelial cells formed a confluent monolayer over the bare stroma; however, their attachment was not uniform. A similar successful approach was also demonstrated by Mimura et al.[125]

Amano et al.[126] seeded cultured human endothelial cells on denuded human corneas. The TE endothelium aspect was comparable to native cornea (in histology, morphology and ultrastructure). The TE endothelium showed active pump function.

Proulx et al.[28] used the self-assembly approach to produce tissue-engineered corneas using all three corneal cell types (epithelial, stromal and endothelial cells). Endothelial cells formed a monolayer of tightly packed cells well adhered to the TE stroma. The TE endothelium expressed function-related proteins.

Previous studies in our laboratory showed that normal feline corneal endothelial cells can be cultured on a devitalized human stromal carrier. The TE cornea showed a monolayer of tightly packed polygonal cells well adhered to DM.[27] The TE corneal endothelium expressed function-related proteins. These TE corneas can retain function and maintain corneal transparency when transplanted in the feline eye.[29]

Wencan et al.[127] used the basement membrane of human amniotic membranes as a carrier to transplant cultured feline endothelial cells in the feline animal model. After culture, endothelial cells formed a continuous confluent monolayer. Six weeks after transplantation, grafts were clear and corneal thickness was slightly greater than that before transplantation.

Koizumi et al.[128] used collagen type I carrier to transplant cultured monkey endothelial cells in the monkey animal model. Endothelial cells formed a confluent monolayer of closely attached hexagonal cells that expressed function-related proteins. After transplantation, the graft's transparency increased and central corneal thickness decreased suggesting a functioning TE endothelium.

Honda et al.[129] used native human corneal disk as a carrier where cultured human corneal endothelial cells were seeded and then transplanted in the rabbit model. After transplantation, the edema of the TE cornea decreased and transparency recovered gradually. The transplanted endothelium expressed function-related proteins.

In conclusion, several successful attempts were conducted to tissue-engineer a functional corneal endothelium by various approaches. However, none of them used dystrophic/diseased corneal endothelial cells. Transplantation of TE allografts would not solve the problem of rejection. The ideal graft to avoid rejection is the autogenic graft.

4 Chapter IV:

Tissue Engineering of a Corneal Endothelium Using Cells from Patients with Fuchs Endothelial Corneal Dystrophy: *1st Article (The First Objective: In Vitro Characterization)*

Tissue Engineering of a Corneal Endothelium Using Cells from Patients with Fuchs Endothelial Corneal Dystrophy

(Manuscript submitted in Tissue Engineering, Revised version sent in November 2012)

4.1 AUTHORS

*Benjamin Goyer, B.Sc.,[1] *†M. Nour Haydari, M.D., M.Sc.,[2] Olivier Rochette Drouin, M.Sc.,[1] Olivier Roy,[1] Mathieu Thériault, M. Sc.,[1] Simon Laprise,[1] Isabelle Brunette, MD, FRCSC,[2] Stéphanie Proulx, Ph.D.[1,3§]

*Equal contributors

†MN Haydari had a major contribution in this study including vital stainings, light and transmission electron microscopy observations and morphometric data analysis. He also participated in the writing the manuscript and answering some of the questions raised by the reviewers.

4.2 AFFILIATIONS

[1]Centre LOEX de l'Université Laval, Génie tissulaire et régénération- Centre de recherche FRQS du Centre hospitalier *affilié* universitaire de Québec, Québec, QC, Canada

[2]Centre de Recherche de l'hôpital Maisonneuve-Rosemont, Montréal, QC, Canada and Département d'ophtalmologie, Université de Montréal, Montréal, QC, Canada

[3]Département d'ophtalmologie et d'oto-rhino-laryngologie – chirurgie cervico-faciale, Faculté de médecine, Université Laval, Québec, QC, Canada

[§]**Corresponding author:** Stéphanie Proulx, Ph.D.

4.3 ABSTRACT

The future of regenerative medicine involves the production of tissues using the patient's own cells. Autologous cells are not rejected by the patient's immune system and are therefore better suited for permanent tissue replacement. Engineering tissues using diseased cells, however, is a significant challenge, because autologous engineered tissues need to be functional before their implantation back into the patient. The goal of this study was to assess the feasibility of engineering a corneal endothelium using the corneal endothelial cells excised from eyes of patients with end-stage Fuchs endothelial corneal dystrophy (FECD) at the time of their corneal transplantation. Two types of corneal endothelium were engineered, namely a corneal endothelium generated from FECD corneal endothelial cells and a corneal endothelium generated from healthy eye bank corneal endothelial cells. In both cases, cultured corneal endothelial cells were seeded on the Descemet's membrane of a devitalized human stromal carrier. The tissue-engineered corneas were kept in culture for 1 to 3 weeks. They were then studied by morphometric analyses of flat mounts stained with alizarin red or fixed for histology, transmission electron microscopy and immunofluorescence microscopy. Both types of corneal endothelium (tissue-engineered from FECD or healthy corneal endothelial cells) formed a monolayer of tightly-packed cells that adhered well to Descemet's membrane. FECD and healthy tissue-engineered endothelial cells expressed similar levels of the function-related proteins Na^+/K^+-ATPase α1 and sodium-bicarbonate co-transporter (Na^+/HCO_3^-). They similarly expressed keratins 8 and 18 (K8/18) and did not express alpha-smooth muscle actin (α-SMA). Clusterin expression was faint and uniform in both groups. To the best of our knowledge, this is the first report on the feasibility of engineering a tri-dimensional human tissue from diseased cells. Potential applications of this engineered tissue show promise for the treatment of this eye blinding disease.

4.4 INTRODUCTION

The cornea is constituted of an epithelium, a stroma and an endothelium. The corneal endothelium consists of a monolayer of flatt ened cells facing the anterior chamber of the eye.[130, 131] Its main role is to maintain corneal transparency by ensuring stromal dehydration, a process achieved through ionic pumps (Na^+/K^+ATPase, Mg^{2+}-ATPase)[132] and ion transporters such as the co-transporter Na^+/HCO_3^-.[133] Corneal endothelial cell dysfunction results in stromal hydration and loss of corneal transparency, leading to blindness.[2]

Endothelial failure can result from a number of conditions, the two most frequent etiologies being Fuchs endothelial corneal dystrophy (FECD) and surgical traumatism (post-cataract surgery complications), which were respectively responsible for 47.7% and 19.2% of the 23,287 corneal endothelial transplantations performed in the United States in 2011.[48] There are currently no non-surgical therapeutic alternatives to corneal transplantation for corneal endothelial failure. Corneal endothelial allograft, however, yields a 10% average rate of immune rejection (range: 0% to 45% for follow-ups ranging from 6 to 21 months).[21] Li *et al*. recently reported a 17% cumulative probability of endothelial graft rejection at four years in patients with FECD without ocular co-morbidities. Graft rejection in these eyes is known to result in significant endothelial cell loss.[99]

Tissue engineering offers the option of generating a new and highly functional corneal endothelium made from autologous cells, which would allow to circumvent the two main causes for endothelial graft failure, namely immune rejection and endothelial cell attrition. The challenge with tissue engineering a corneal endothelium starts at the cell culture level. In the living eye, corneal endothelial cells are arrested in the G1-phase of the cell cycle and do not proliferate.[23] When isolated and cultured in the presence of growth promoting agents, however, these cells are capable of limited proliferation.[24, 26] Our group has reported on the successful culture of corneal endothelial cells.[28, 134] We have used these cultured cells to engineer a corneal endothelium,[27] which was shown to be highly functional

at one week when transplanted in a living animal eye.[29] Engineering a corneal endothelium for autologous transplantation also implies harvesting autologous cells to initiate the culture. Our group has demonstrated the feasibility of engineering a corneal endothelium from a small size endothelial biopsy harvested from healthy feline corneas.[100] In the case of FECD, the challenge is two-fold, as endothelial cell density is severely decreased and the remaining cells are sick. However, preliminary results by our group have shown that the central corneal endothelial cells harvested in human patients at the time of corneal transplantation for end-stage clinical FECD still retain proliferative capacities.[30]

This paper shows the feasibility of engineering a corneal endothelium using corneal endothelial cells from patients with end-stage clinical FECD. To the best of our knowledge, this is the first report on the characterization of an ocular tissue engineered from diseased ocular cells.

4.5 MATERIALS AND METHODS

This study was conducted according to our institutions' guidelines and the Declaration of Helsinki. Six specimens from six patients with end-stage clinical FECD were used in this study (three women and three men, aged 58 to 77 years, mean ± SD = 68 ± 8 years). The diseased Descemet's membranes were harvested at the time of corneal transplantation, as described previously.[30] Native human corneas without endothelial diseases (hereafter called "healthy") and unsuitable for transplantation in human subjects, were obtained from our local eye bank (Banque d'Yeux du Centre universitaire d'ophtalmologie (CUO)). These healthy corneas were used for immunostaining of native corneas (three corneas from two donors, aged 74 and 77), for isolation and culture of healthy corneal endothelial cells (two corneas from two donors, aged 47 and 68) and as carriers for the engineering of corneal endothelia (ten corneas from ten donors, aged 54 to 84 years, mean ± SD = 69 ± 10 years).

4.5.1 Devitalisation of the Human Stromal Carriers

The eye bank corneas were devitalized using three freeze-thaw cycles,[27] then stored at -20°C until used (range: 17 to 620 days, mean ± SD = 88 ± 106 days). On the day of reconstruction, they were thawed, rinsed to remove the dead cells, and observed under a stereomicroscope (Nikon SMZ800, Mississauga, ON, Canada). Corneas in which Descemet's membrane was detached were discarded.

4.5.2 Isolation and Culture of Corneal Endothelial Cells from Healthy and FECD Corneas

All corneal endothelial cells were isolated using the technique described by Zhu and Joyce (2004).[26] Briefly, Descemet's membranes were peeled off and incubated overnight in growth medium at 37°C. After centrifugation, they were incubated 1 h in 0.02% EDTA (Sigma, Oakville, ON, Canada), and the loosened cells were detached from the Descemet's membrane by several passes through a flamed-polished pipet. Cells were then centrifuged and resuspended in fresh medium consisting of OptiMem-I (Invitrogen, Burlington, ON, Canada), 8% fetal bovine serum (HyClone, Logan, UT), 5 ng/mL human epidermal growth factor (Austral Biologicals, San Ramon, CA), 20 ng/mL nerve growth factor (Biomedical Technologies, Stoughton, MA), 100 μg/mL bovine pituitary extract (Biomedical Technologies), 20 μg/mL ascorbic acid (Sigma), 0.08% chondroitin sulfate (Sigma), 25 μg/mL gentamicin sulfate (Schering, Pointe-Claire, QC, Canada) and 100 IU/mL penicillin G (Sigma). Cells were plated on dishes covered with FNC coating mix (containing fibronectin, collagen and albumin; Athena Enzyme Systems, Baltimore, MD).

Population doubling was determined by the common logarithm of the number of cells in the growth dishes at the end of a period of growth divided by the number of viable cells plated in the growth dishes multiplied by 3.33.

4.5.3 Tissue-Engineered Human Corneal Endothelium

Tissue engineering of the corneal endothelium was performed as per our previously published protocol.[29] Briefly, devitalized human corneas were placed in the bottom of a six-

well plate, with the denuded Descemet's membrane facing up. Endothelial cells isolated from healthy eye bank corneas (n=3, initial cell seeding of $2.8x10^5 \pm 0.1x10^4$ cells) and FECD specimens (n=6, initial cell seeding of $2.0x10^5 \pm 8.2x10^4$ cells) were seeded on top of the denuded Descemet's membrane and allowed to adhere for 4 h before immersion in culture medium. They were further cultured for 1 to 3 weeks (healthy corneal endothelial cells: from 9 to 16 days, mean ± SD = 11 ± 2 days; FECD corneal endothelial cells: from 8 to 20 days, mean ± SD = 13 ± 3 days). A flow diagram of the tissue engineering protocol is presented in Figure 34.

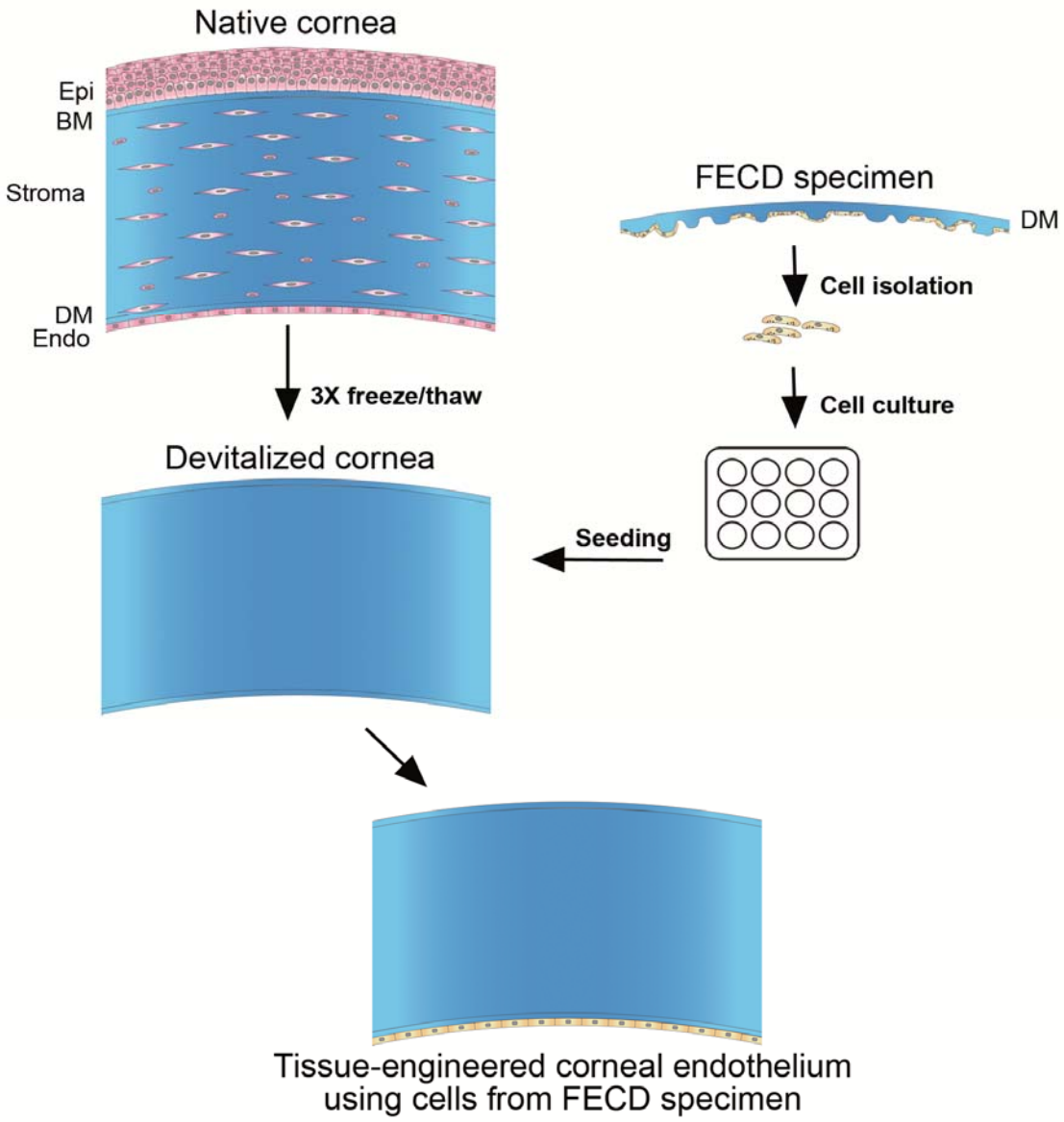

Figure 34: Schematic representation of the tissue engineering protocol. Healthy eye bank corneas were devitalized following three freeze-thaw cycles and used as carriers for the engineering of a corneal endothelium using cultured cells isolated from FECD specimens. The same protocol was also used to engineer a corneal endothelium using healthy cells from normal eye bank corneas (not shown).

4.5.4 Tissue Fixation

Each tissue-engineered cornea was divided into four parts. One quarter was used for alizarin red staining for endothelial cell density assessments. One quarter was fixed in 3.7% formaldehyde (ACP Chemicals, Montreal, QC, Canada) for histology. One quarter was embedded in Optimal Cutting Temperature compound (Somagen, Edmonton, AB, Canada), frozen in liquid nitrogen and stored at -70°C for ulterior immunofluorescence staining. The last quarter was fixed in 2.5% glutaraldehyde and processed for transmission electron microscopy.

4.5.5 Corneal Endothelial Cell Density

Cell density of the tissue-engineered corneal endothelium was calculated as described.[29] Briefly, the surface was stained for 45 seconds with the intercellular stain alizarin red S (0.2%; Sigma) then rinsed and photographed (Nikon SMZ800). Using the KSS-409SP software (version 2.10), endothelial cell densities were determined and morphometric analyses were performed. Different fields were randomly selected for each tissue-engineered endothelium. The percentage of hexagonal cells was used as an index of pleomorphism and the coefficient of variation in cell area was used as a measure of polymegethism.[67, 135] Data were statistically evaluated with the unpaired student's t-test using the Prism software (version 5.0). P-values less than 0.05 were considered statistically significant.

4.5.6 Histology and Electron Microscopy Analysis

For histology, the tissue fixed in formaldehyde was processed for paraffin embedding. Sections (5 μm) were stained with Masson's trichrome and analyzed by light microscopy. For transmission electron microscopy, the tissue fixed in glutaraldehyde was washed in cacodylate buffer, post-fixed in 1% osmium tetraoxide, stained with 0.5% uranyl acetate dehydrated in a graded series of ethanol solutions, and embedded in Poly/Bed 812. Thin sections were processed and visualized using a JEOL JEM-1230 transmission electron

microscope (Tokyo, Japan) at 80 kV. Thickness measurements were made using AxioVision 4.8.1 (Carl Zeiss, Toronto, ON, Canada).

4.5.7 Indirect Immunofluorescence Analysis

Indirect immunofluorescence was performed as previously described.[29] Cryosections (5 μm) were fixed for 10 minutes at -20°C using acetone (90%, EMD, Mississauga, ON, Canada) and immunostained with anti-Na^+/K^+-ATPase α1 (clone 9A-5; Sigma), a rabbit anti- Na^+/HCO_3^- (Abcam, Cambridge, MA), and a guinea pig anti-cytokeratin 8/18 (clone GP11; ARP, Waltham, MA) as primary antibodies. Others cryosections were fixed for 10 minutes at -20°C using methanol (100%, Fisher Scientific, Ottawa, ON, Canada) and immunostained with a mouse anti-alpha smooth muscle actin (α-SMA; clone 1A4, Dako, Burlington, ON, Canada). For clusterin immunostaining, cryosections were fixed for 10 minutes at -20°C using ethanol (99%, Commercial Alcohols, Brampton, ON, Canada), permeabilized with Triton-PBS 1% (v/v) for 10 minutes and immunostained with a mouse anti-clusterin-α/β (H-330, Santa Cruz Biotechnology, Santa Cruz, CA). Goat anti-guinea pig, donkey anti-mouse and chicken anti-rabbit IgG antibodies conjugated with Alexa 594 (Invitrogen) were used as secondary antibodies. Sections were incubated with antibodies diluted in phosphate buffered saline containing 1% bovine serum albumin (Sigma), at room temperature for 2h (for clusterin) or 45 min (for all other primary antibodies) and 30 min for secondary antibodies. Negligible background was observed for controls (primary antibodies omitted). Cell nuclei were counterstained with Hoescht reagent 33258 (Sigma). Fluorescence was observed using a Nikon Eclipse TE-2000U inverted microscope.

4.6 RESULTS

4.6.1 Isolation and Culture of Healthy and FECD Corneal Endothelial Cells

Figure 35 shows the central Descemet membrane taken from a healthy cornea (Figure 35A) possessing a monolayer of hexagonal cells (Figure 35B) overlying a thin and

uniform Descemet's membrane (Figure 35C). FECD specimens showed the classic signs of this dystrophy, including the presence of numerous excrescences (guttae) and pigmentation (Figure 35A-C). Histology of the Descemet's membranes rarely showed the presence of endothelial cells, a result of both the dystrophy and the surgery necessary for their retrieval. However, the few endothelial cells that remained were able to generate a cell culture (Fig. 3).[30](Figure 36).[30]

At primary culture, some of the isolated FECD cells showed cytoplasmic pigment granules (Figure 36D). These pigmented cells did not proliferate, and no pigmented cells were found in any of the passaged cultures (Figure 36E-F). After reaching confluence, FECD (Figure 36E-F) and healthy corneal endothelial cells (Figure 36B-C) adopted the typical endothelial polygonal morphology.

FECD and healthy corneal endothelial cells also showed similar cell counts and population doubling times. After one passage, the mean FECD cell count was $4.7x10^5 \pm 3.1x10^5$ cells (range: $3.3x10^4$ to $1.1x10^6$ cells), corresponding to a 2.1 population doubling in 4 ± 1 days. The mean cell count for healthy corneal endothelial cells was $5.0x10^5$ cells $\pm 2.2x10^5$ cells (range: $3.0x10^5$ to $7.0x10^5$ cells), corresponding to a 1.9 population doubling in 5 ± 1 days.

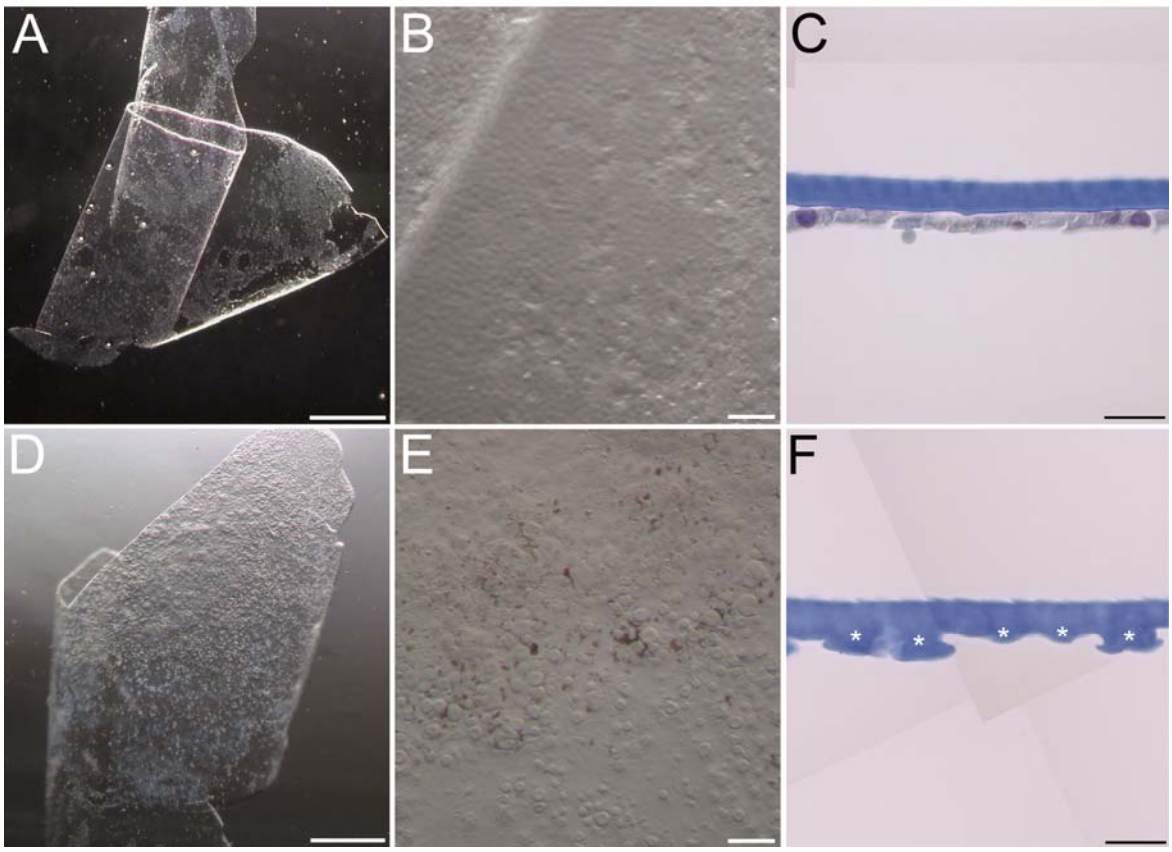

Figure 35: Descemet's membrane from healthy Eye bank corneas and from patients with Fuchs endothelial corneal dystrophy. A) Central Descemet's membrane taken from a healthy Eye bank cornea. B) Higher magnification of (A) shows the corneal endothelium as well as some areas of endothelial damage. C) Histology cross-section shows a uniform Descemet's membrane along with a monolayer of corneal endothelial cell. D) Specimen from a patient with Fuchs endothelial corneal dystrophy upon receipt, as seen through a stereomicroscope. E) Higher resolution of the specimen shown in (A). Note the presence of multiple guttae and pigmentation. F) Histology of a Descemet's membrane from a patient with Fuchs endothelial corneal dystrophy. Note the thickened Descemet's membrane and the presence of excrescences (guttae) typical of this dystrophy (star). The trichrome Masson's staining gives a purple coloration to cells and a blue coloration to collagen. Scale bar: (A, D) 1 mm, (B, E) 100 µm, (C, F) 20 µm.

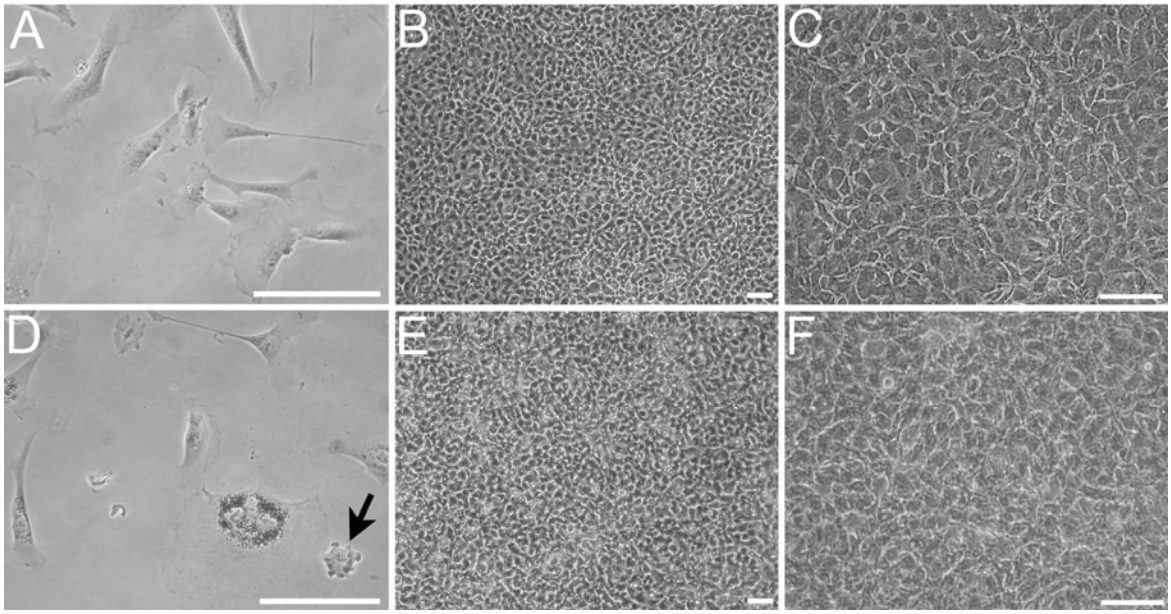

Figure 36: Culture of corneal endothelial cells from healthy corneas and from patients with clinical end-stage Fuchs endothelial corneal dystrophy. A) Sub-confluent corneal endothelial cells in primary culture (P0). B) Confluent third-passage endothelial cells from healthy cornea. C) Higher magnification of (B) shows that endothelial cells form a monolayer of polygonal cells. D) FECD corneal endothelial cells in primary culture (P0). Arrow shows a pigmented cell with blebs, a characteristic sign of apoptosis. E) Confluent third-passage corneal endothelial cells from FECD. F) Higher magnification of (E) shows that confluent FECD cells also adopt the typical endothelial polygonal morphology. Scale bars: 100 μm.

4.6.2 Tissue-Engineered Corneal Endothelium

The freeze-thaw cycles allowed destruction of all native cells (Figure 37A). Endothelial cells cultured on the devitalized carrier entirely resurfaced the denuded Descemet's membrane, forming a monolayer of tightly packed cells (Figure 37B-C).

Alizarin red confirmed the complete coverage by polygonal cells (Figure 38A and B). Some small intercellular gaps were present. Cell density in the tissue-engineered FECD corneal endothelium was 581 ± 241 cells/mm^2 (range: 235 to 1038 cells/mm^2, n=17 counts of 6 tissue-engineered corneas) whereas the corneal endothelium tissue-engineered with

healthy cells was at 782 ± 63 cells/mm^2 (range: 689 to 868 cells/mm^2, n=6 counts of 2 tissue-engineered corneas) (Figure 38C). The difference in cell density between the two groups was not statistically significant (p-value = 0.0598). The percentage of 6-sided cells and the coefficient of variation in cell area were also similar between the two groups (respective p-values of 0.5056 and 0.3564). The tissue-engineered FECD corneal endothelium contained cells with a higher average cell area; however, the difference was not statistically significant (p-value = 0.0581).

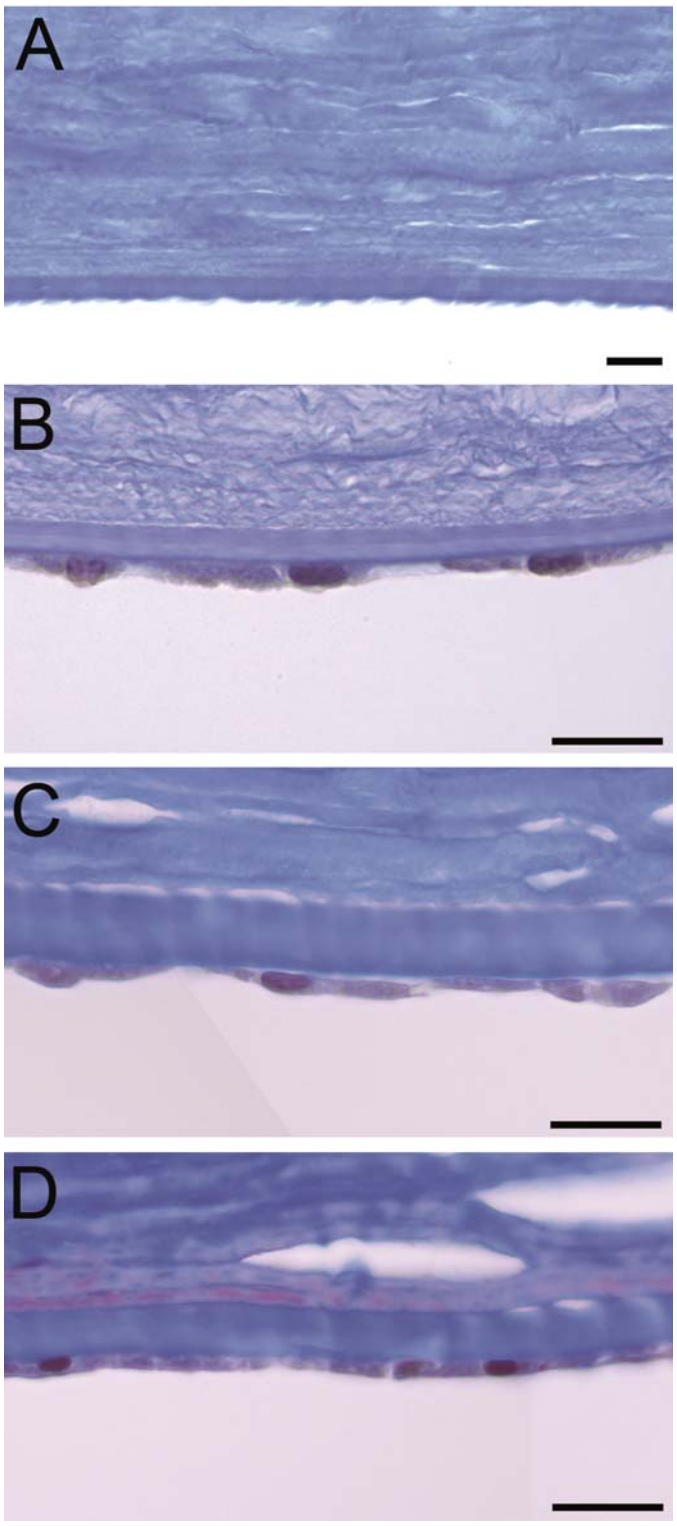

Figure 37: Histology cross-sections. Trichrome Masson's staining. This staining gives a purple coloration to cells and a blue coloration to collagen. A) Devitalized human cornea

before cell seeding. Note the absence of cells in the stroma (s) and on Descemet's membrane (DM). B) Corneal endothelium tissue-engineered using cells from patients with Fuchs endothelial corneal dystrophy. C) Corneal endothelium tissue-engineered using healthy cells from an eye bank cornea. D) Native human eye bank cornea. Scale bar: 20 μm.

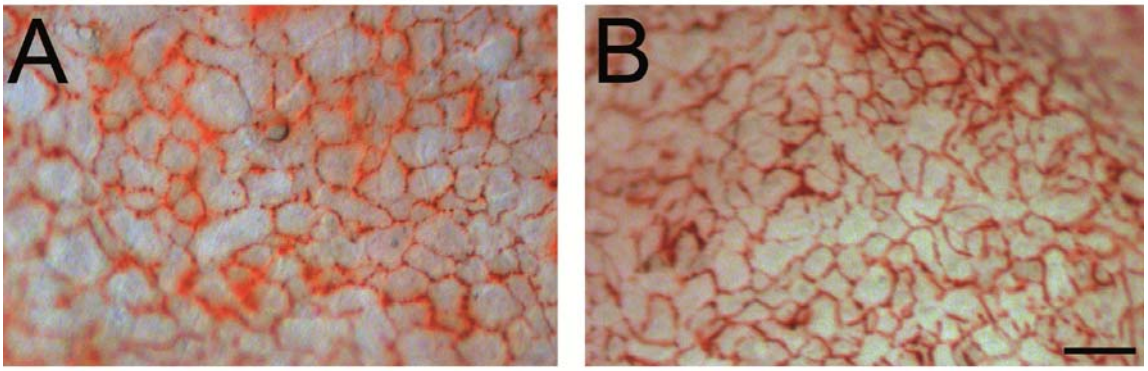

C

Morphometric analysis

	TE-FECD N=6 n=17	TE-Healthy N=2 n=6	p-value
Cell density (cells/mm²)	581 ±241	782 ±63	0.0598
6-sided cells (%)	46 ±6	44 ±10	0.5056
Average cell area (μm²)	2047 ±913	1287 ±106	0.0581
Area min (μm²)	425 ±239	318 ±34	0.2927
Area max (μm²)	5030 ±1946	3358 ±472	0.0527
SD	940 ±416	567 ±84	
CV	47 ±7	44 ±5	0.3564

Figure 38: Endothelial cell coverage and density. A, B) Alizarin red staining of an endothelium tissue-engineered with FECD (A) and healthy (B) corneal endothelial cells. High cell coverage of the carrier is shown, with only narrow acellular areas stained with alizarin red between adjacent cells, indicating still-incomplete attachment between cells. C) Morphometric analysis. Alizarin red images were analysed using the KSS-409SP software available in specular microscopes used in Eye banks, which calculates cell density, cell morphology, cell area, standard deviation of cell area and coefficient of variation. Results

are presented as mean ±SD. TE: Tissue-engineered, FECD: Fuchs endothelial corneal dystrophy, SD: standard deviation of cell area, CV: coefficient of variation. Scale bar: 100 µm.

4.6.3 Ultrastructure

A normal Descemet's membrane is thin and uniform and composed of an anterior banded layer and a posterior non-banded layer (Figure 39A). One typical finding in late-stage FECD is the presence of an abnormal fibrillar layer in Descemet's membrane (Figure 39B and C). No fibrous material was deposited by the endothelial cells on top of the native Descemet's membrane Figure 39E and F). Transmission electron microscopy showed a single layer of endothelial cells in close proximity to Descemet's membrane in the native (Figure 39D) as well as in both types of engineered tissues (Figure 39E and F). The mean thickness of the engineered FECD endothelium was 3.2 ±0.9 µm (range: 1.4 µm to 4.8 µm; n=30 counts of 5 tissue-engineered corneas), and the mean thickness of the engineered endothelium using healthy cells was 4.7 ±1.3 µm (range: 3.0 µm to 6.6 µm; n=12 counts of 2 tissue-engineered corneas). Lysosomes, mitochondria, rough endoplasmic reticulum and Golgi apparatus were observed in both types of tissue-engineered corneal endothelium. Cells were in close proximity to each other (Figure 39G). Small intercellular gaps were sometimes observed between neighbouring cells (Figure 39H and I).

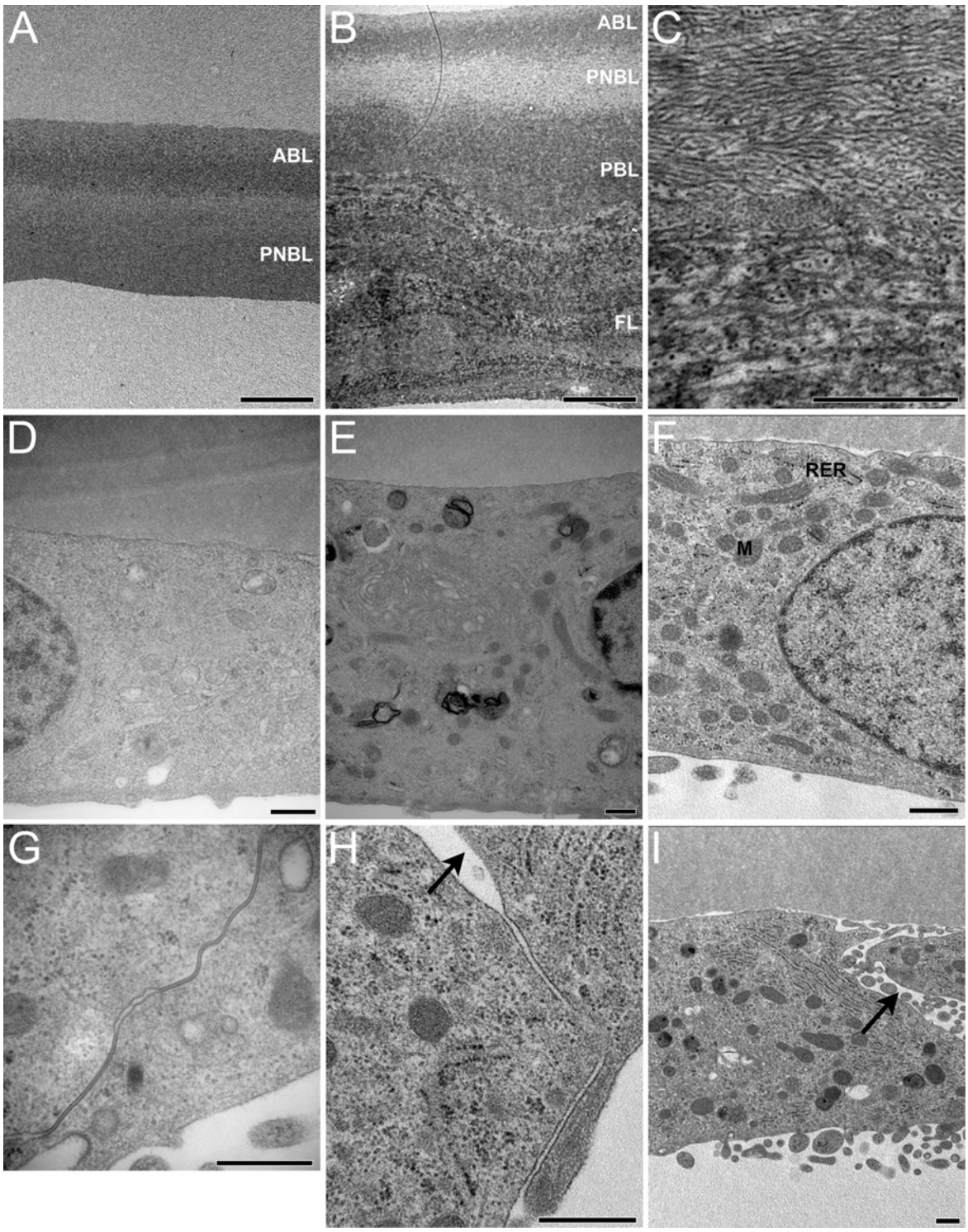

Figure 39: Ultrastructure. A) The Descemet's membrane of a healthy Eye bank cornea is composed of an anterior banded layer (ABL) and a posterior non-banded layer (PNBL). B)

Transmission electron microscopy image of a late-stage FECD Descemet's membrane showing the presence of two abnormal layers, the posterior banded layer (PBL) as well as a thick fibrillar layer (FL). C) Higher magnification of the fibrillar layer. D) Transmission electron microscopy image of the endothelium of a native human eye bank cornea. E) Transmission electron microscopy image of a corneal endothelium tissue-engineered using cells from a healthy cornea. F) Transmission electron microscopy images of a corneal endothelium tissue-engineered using cells from a FECD specimen. Rough endoplasmic reticulum (RER) and mitochondria (M) are easily visible. G-I) Cell-cell junctions in a corneal endothelium engineered using healthy cells (G) or FECD cells (H-I). Intercellular gaps where sometimes observed between cells (arrows). Scale bars: (A, B) 5 μm, (C) 1 μm, (D-I) 0.5 μm.

4.6.4 Endothelial Phenotype

Both types of tissue-engineered corneal endothelial cells expressed keratins 8 and 18 (K8/18). Expression was stronger in engineered tissues than in native corneas (Figure 40C). Absence of α-SMA was also noted in both engineered and native corneal endothelium (Figure 40).

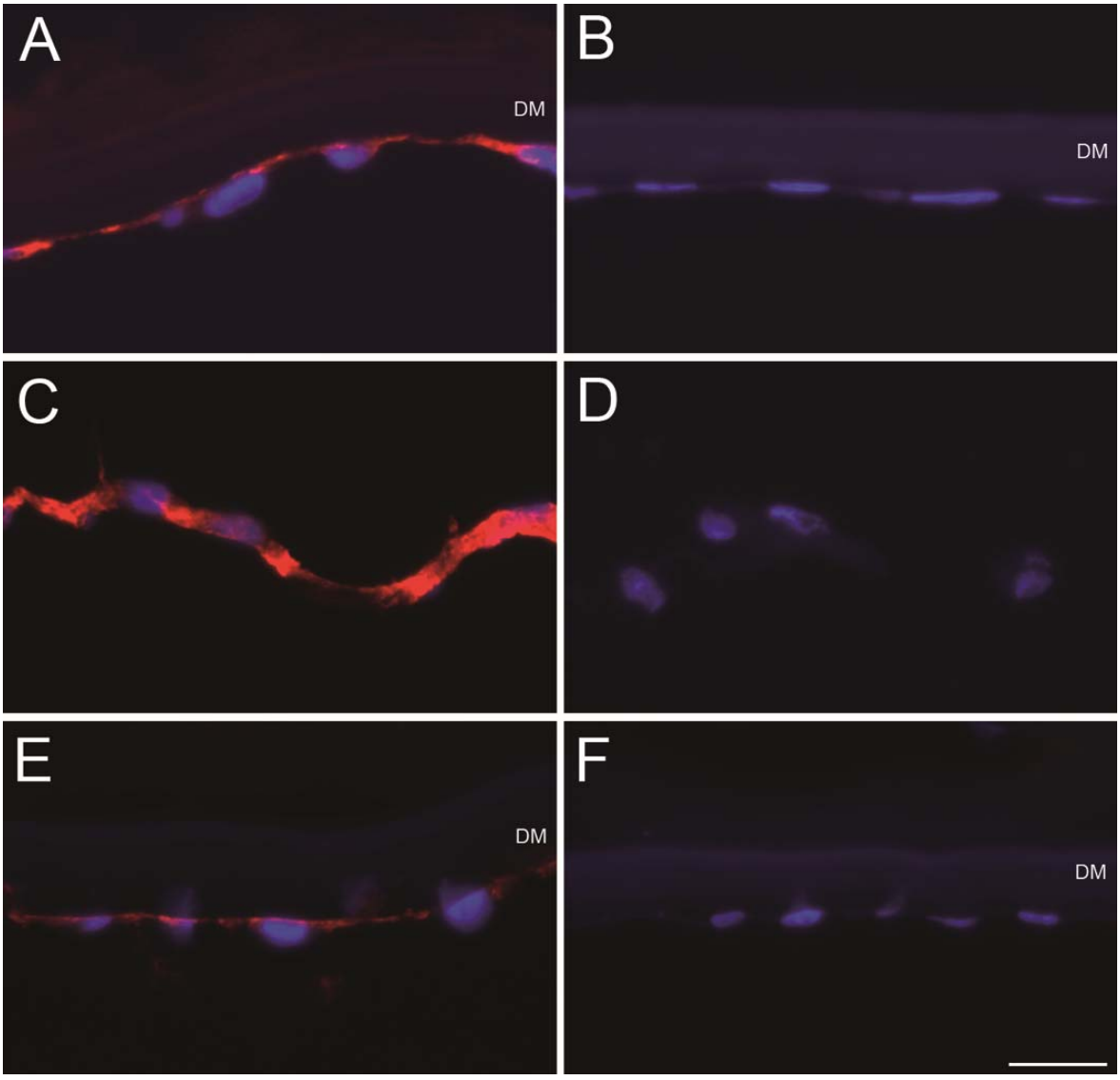

Figure 40: Keratins 8 and 18 (K8/18) and α-smooth muscle actin (α-SMA) protein expression. Immunofluorescence staining (red) of K8/18 (A, C, E) and α-SMA (B, D, F) in a corneal endothelium tissue-engineered using cells from FECD corneas (A, B), in a corneal endothelium tissue-engineered using cells from a healthy cornea (C, D), and in a native human eye bank cornea (E, F). Nuclei are counterstained with Hoechst (blue). The corneal endothelium is detached from Descemet's membrane in C and D. DM: Descemet's membrane. Scale bar: 20 μm.

4.6.5 Function-Related Proteins

As shown in Figure 41, Na^+/K^+-ATPase α1 protein expression was localized to the cell membrane. Expression was more intense in the native cornea than in the engineered tissues. Na^+/HCO_3^- protein expression was diffuse, uniform and found throughout the cell. This co-transporter's expression had a similar intensity in engineered and native tissues.

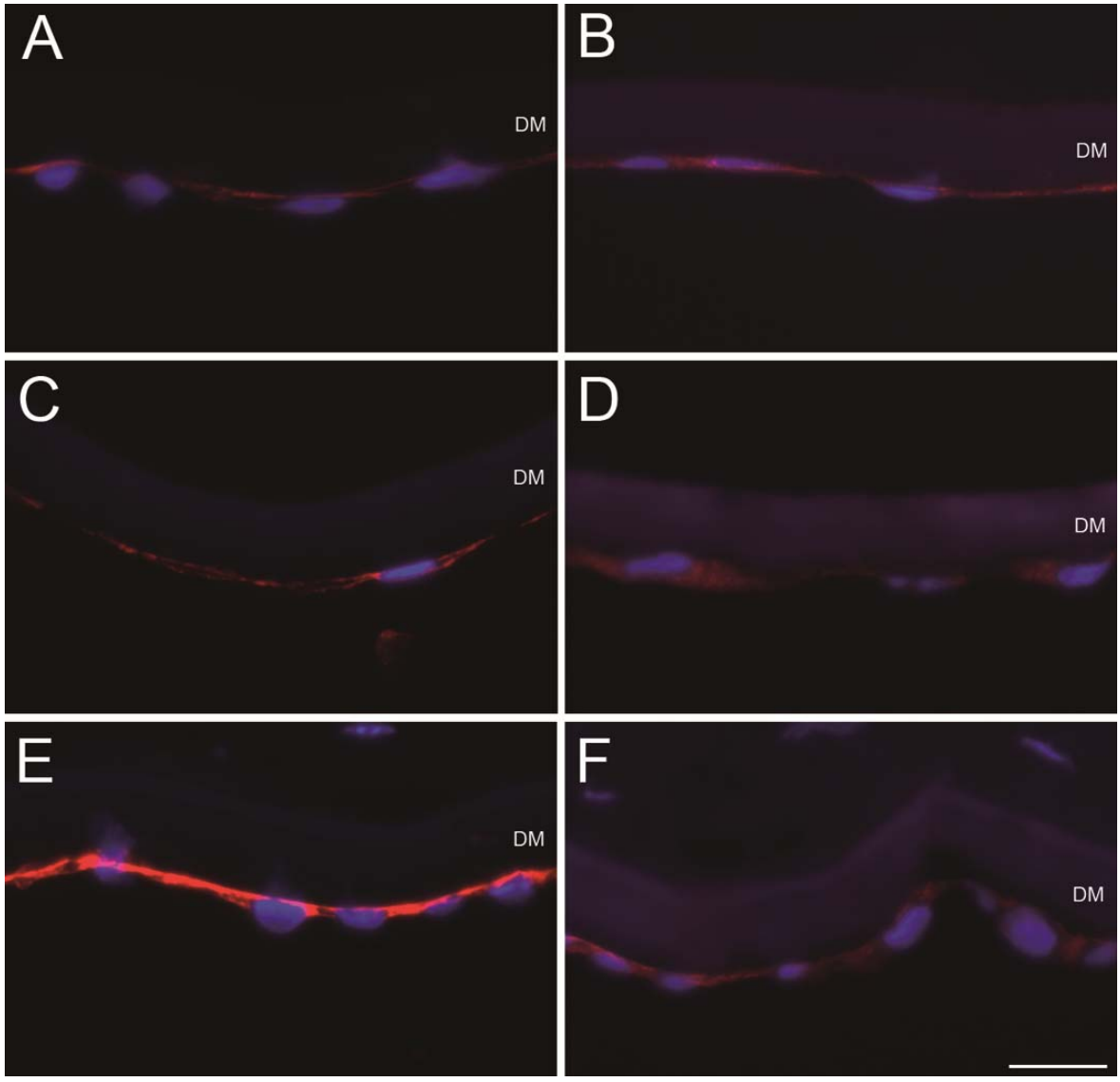

Figure 41: Na^+/K^+-ATPase α1 and Na^+/HCO_3^- protein expression. Immunofluorescence staining (red) of Na^+/K^+-ATPase α1 (A, C, E) and Na^+/HCO_3^- (B, D, F) in a corneal endothelium tissue-engineered using cells from a FECD specimen (A, B), in a corneal

endothelium tissue-engineered using cells from a healthy cornea (C, D), and in a native human eye bank cornea (E, F). Nuclei are counterstained with Hoechst (blue). DM: Descemet's membrane. Scale bar: 20 μm.

4.6.6 Clusterin Expression

Immunostaining of the glycoprotein clusterin was also performed (Figure 42). A faint, uniform clusterin staining was present in the cytoplasm of engineered and native corneal endothelial cells.

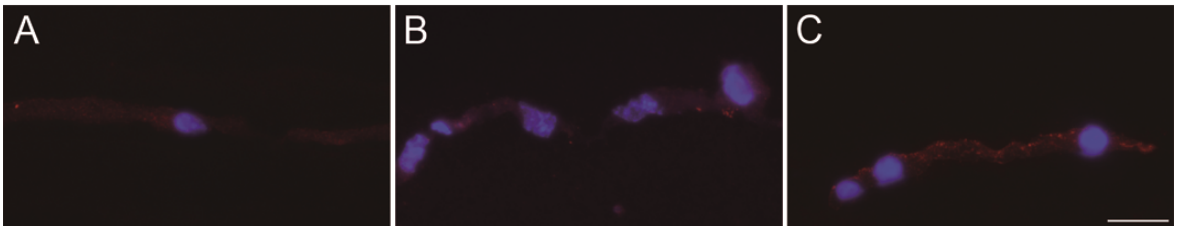

Figure 42: Clusterin protein expression. Immunofluorescence staining (red) of the glycoprotein clusterin in a corneal endothelium tissue-engineered using cells from a FECD specimen (A), in a corneal endothelium tissue-engineered using cells from a healthy cornea (B), and in a native human eye bank cornea (C). Nuclei are counterstained with Hoechst (blue). The corneal endothelium is detached from Descemet's membrane in all three images. Scale bar: 20 μm.

4.7 DISCUSSION

In this study we demonstrated the feasibility of engineering a human corneal endothelium using cultured cells from healthy and FECD corneas seeded on devitalized tridimensional corneal carriers. We showed that the two types of corneal endothelium engineered either from FECD or from healthy human endothelial cells formed a regular monolayer of tightly-packed polygonal cells that adhered well to the Descemet's membrane carrier. The expression of K8/18 and lack of expression of α-SMA confirmed the corneal endothelial nature of these cells and the absence of stromal fibroblasts that can sometimes contaminate endothelial cell cultures.[115] In both groups (tissue-engineered from FECD or healthy cells), endothelial cells expressed the function-related proteins Na^+/K^+-ATPase α1

and Na^+/HCO_3^-. They also showed similar expression levels of clusterin, a glycoprotein previously reported to be upregulated in FECD.[14, 75] No deposition of fibrillar material was observed ultrastructurally under the corneal endothelium engineered using FECD cells.

The corneal endothelia engineered with healthy and FECD cells were similar at all levels analyzed (morphology, cell density, ultrastructure, protein expression). The lack of indicators of FECD *in vitro* could be explained by a number of reasons: ***i)*** Pigment granules: The presence of pigment granules within endothelial cells is typically found in FECD.[68, 136] There are no reports on corneal endothelial cells being able to synthesize pigment granules, and *in vitro* formation of pigment granules was not observed in this study. It has previously been proposed that the pigments granules found in the endothelial cells come from phagocytized pigment granules originating from the iris pigment epithelium.[137] The absence of pigments in the tissue-engineered endothelium could simply be explained by the absence of an active source of pigments, such as the iris epithelium. ***ii)*** Cell selection: Cell culture may have induced selection of the healthiest cells or the ones less affected by the disease. In the native corneal endothelium, K8/18 is not expressed by all cells[115] and its level of expression varies between cells, as seen in Figure 40E. K8/18 expression was higher in cultured cells (Figure 40A and C) than in the native tissue, suggesting that K8/18-expressing cells were favored by cell culture. Furthermore, FECD cultures presented a higher rate of cell apoptosis than the healthy cells in the early culture stages, especially among pigmented cells, suggesting early attrition of the most severely diseased cells in favor of the most robust cells. ***iii)*** Culture time: FECD is a slowly progressive corneal disease that becomes clinically evident in adults over age 40.[136] In this study, characterization of the FECD cells was performed after 1 to 3 weeks of culture, which may not have been long enough to observe FECD pathogenesis. ***iv)*** Dynamic *in vivo* conditions: Intraocular pressure and flow of aqueous humor, which are absent in our *in vitro* culture conditions, may be required for the development of FECD pathogenesis. ***v)*** Oxidative stress: Previous studies have shown that FECD cells are more susceptible to oxidative stress-induced apoptosis than normal cells.[13, 16] In our culture conditions, the growth media contained antioxidants (serum, ascorbic acid) and medium was changed three times a week to remove oxygen reduction products generated by normal respiratory

metabolism. Absence of induced acute oxidative stress (by adding reactive oxygen species such as hydrogen peroxide for example) in our tissue-engineered model may also explain the similarity between healthy and FECD tissue-engineered corneal endothelia. ***vi)*** Healthy Descemet's membrane: In FECD, Descemet's membrane's structure is abnormal. It is thicker, with additional abnormal layers, thick excrescences (guttae) and striated bodies.[30, 66, 68-71] Descemet's membrane is secreted by corneal endothelial cells throughout life and secretion of an abnormal Descemet's membrane would result from endothelial dysfunction. However, cell-extracellular matrix signals interact both ways (inside-out signaling) and the abnormal Descemet's membrane could send signals to the endothelial cells that further contribute to the pathology. Consequently, removing the endothelial cells from the diseased Descemet's membrane and seeding these cells on a healthy Descemet's membrane may facilitate restoration of a healthier corneal endothelial phenotype.

Devitalized eye bank corneas have been previously used by our laboratory for the engineering[27] and the transplantation[29] of an allogeneic corneal endothelium to show its short-term functionality. This living model will allow the comparison of the *in vivo* functionality of the human tissue-engineered corneal endothelium engineered using both healthy and FECD cells. The long-term goal would be to use these engineered tissues to replace the patient's dysfunctional endothelium. Corneal transplantation is never performed in both eyes at the same time. FECD is a bilateral often asymmetrical disease,[2, 3, 5, 6] which increases even more the delay between surgeries in the first and second eyes. Cells harvested at the time of the first surgery could be cultured and frozen until needed for the second eye or if a regraft is required in the first eye. A technique of corneal biopsy could also be developed in order to apply this technique to the first eye. A biopsy constitutes a realistic approach knowing that a FECD specimen as small as 2 mm^2 is sufficient to generate enough cells to engineer a fully endothelialized corneal button. [30]

The successful engineering of a tissue using dystrophic cells also paves the way for *in vitro* pharmacologic testing or gene therapy treatments, in order to engineer healthy tissues that could be transplanted back into the patient.

4.8 ACKNOWLEDGMENTS

This work was supported by the Fondation du CHA (S.P.), the Canadian Institutes of Health Research (CIHR I.B., S.P.), the FRQS ThéCell Network and the FRQS Research in Vision Network. I.B. is the recipient of the Charles-Albert Poissant Research Chair in Corneal Transplantation, University of Montreal, Canada.

The authors would like to thank Drs. Richard Bazin, Patricia-Ann Laughrea and Marie-Ève Légaré from the Centre Universitaire d'Ophtalmologie (CUO) of the CH*A*UQ, Drs. Mona Harrissi-Dagher, Louis Racine and Paul Thompson from the CHUM and Dr. Johane Choremis from HMR for their ongoing collaboration in obtaining the specimens; Myriam Bareille, Danièle Caron, Patrick Carrier, Marie-Eve Choronzey, Alexandre Deschambeault, Marie-Claude Perron, Jeanne d'Arc Uwamaliya, the CUO and the HMR-Rosemont operating room nurses for their technical assistance; Alain Goulet, Richard Janvier and Sylvie Roy for the electron microscopy preparations; and the LOEX research assistants for the histology preparations.

DISCLOSURE STATEMENT

No competing financial interests exist.

5 Chapter V:

Animal Models and Corneal Transplantation Techniques (The Second Objective: DSAEK in the Feline Model)

5.1 Animal Models

Transplanting the tissue-engineered endothelium *in vivo* allows the ultimate confirmation of its functionality. The choice of an animal model depends on the anatomical and physiological similarities to humans, per and post transplantation challenges, as well as model availability and hosting costs.

High availability, low cost and easy handling are the main advantages of mouse, rat and rabbit models. On the other hand, small eye size of mouse and rat and the capacity of rabbit endothelial cells to proliferate *in vivo*[138-140] limit their use in the *in vivo* assessment of tissue-engineered corneas. The pig model is characterized by its anatomical and physiological corneal similarities to humans.[100] It is also highly available. However, previous studies in our laboratory demonstrated that penetrating keratoplasty in the pig model is challenging and shows suboptimal functional results.[141] The monkey model is considered very close to the human model.[100] It has been used to host tissue-engineered corneas that showed optimal functional results.[122, 142-144] However, limited availability and high hosting cost of this model in North America limit its use.

The feline model is a well-established model for the assessment of new surgical and medical managements involving the cornea. It has been used in comparative microscopic studies of the corneal anatomy,[145] constructing tissue-engineered corneal endothelium on a devitalized human cornea,[27] transplanting cultivated corneal endothelial cells on the basement membrane of human amniotic membrane,[127] devising new preservation models for the corneal grafts,[146] assessing rejection mechanisms[120, 147, 148] and assessing innovative methods that would halt corneal rejection.[149, 150] Like in humans,[23, 24] feline corneal endothelial cells do not replicate *in vivo*,[138, 151, 152] contrary to regenerative corneal endothelial cells of animals such as rats [153] and rabbits.[138-140] Mechanisms of corneal endothelium repair by enlargement and migration of cells appear to be the same in cats[138, 152, 154] and in humans.[2, 155, 156] Moreover, human and cat exhibit morphological similarities, suggesting that developments in tissue-engineered corneal endothelium in the feline model

would be readily transferable to human. Some of the comparable particularities, in human and cat respectively, are the endothelial cell counts (between 3022-3464 [157-159] and 2300-2900 [145, 151, 160-162] cells/mm^2), the endothelial cell area (between 317-324 [157, 159] and 348-357 [159, 161] μm^2) and the central corneal thickness (between 534-564 [163, 164] and 545-650 [145, 162, 165, 166] μm). The large corneal diameter of the cat's cornea (15.5-18[160, 167] mm) permits full size grafts, using the same instrumentation and techniques as for human subjects. These large grafts also yield large amounts of tissue for extensive postmortem analyses. Xenografts are well tolerated and the human-to-cat xenograft model of corneal transplantation demonstrated endothelial cell loss and other clinical findings similar to human allografts.[146, 148] However, the feline model is less available and more expensive than other models (such as pig, rat and rabbit). For posterior lamellar keratoplasty, the feline model is relatively intolerant to air in the anterior chamber,[168] and large corneal diameter relatively limit intraocular maneuvers during surgery.

5.2 Transplantation Techniques in the Feline Model

The ideal surgical technique to transplant a tissue-engineered corneal endothelium is characterized by minimal trauma to the newly-made endothelium, quick rehabilitation and less postoperative complications (i.e. intraocular inflammation) that could affect the clinical outcomes.

5.3 Penetrating Keratoplasty (PKP)

Penetrating keratopasty (PKP) (full thickness transplantation) is a well-established procedure in the feline model.[127, 169, 170] PKP, however, has undesirable complications. The sensory innervations of the graft is severed over 360 degrees by the full thickness cut, thereby resulting in poor healing of anaesthetized corneas. Suture-related problems are numerous. As these sutures loosen, they become exposed and leave the graft amenable to infection, ulceration, vascularization and rejection. Full thickness vertical wounds are unstable. Indeed, graft dehiscence can occur with minor trauma in as late as several years after surgery.

In 2009, Proulx et al.[29] reported the first evidence that cultured endothelial cells seeded on a devitalized stromal carrier can recover an active pump function and can restore and maintain normal corneal thickness and crystal-clear transparency over a 7-day observation period after transplantation using a PKP technique in the living feline model. Eighteen cats were enrolled in the study: eleven cats received tissue-engineered allogeneic grafts; one cat received autologous native graft; three cats received allogeneic native grafts; one cat received xenogeneic human native graft; two cats received stromal carrier only (without endothelial cells). PKP surgery was uneventful in all cases. Nine of the 11 tissue-engineered grafts and all native grafts were clear 7 days after PKP. One of the unclear tissue-engineered grafts had an almost complete detachment of Descemet's membrane, which was noticed at the time of surgery. The other unclear graft had a positive vitreous pressure during surgery and intra-operative formation of fibrin membrane strands. The postoperative follow-up had also more inflammatory reaction than usually observed, with fibrin participates on both graft and recipient. Anterior chamber was calm except a mild and transient flare, a few cells, and a fine fibrin membrane residual from surgery in seven cases. Neither corneal neovascularization nor immunologic reaction was observed in any graft during the observation period.

5.4 Descemet's Stripping Automated Endothelial Keratoplasty (DSAEK)

The philosophy of lamellar keratoplasty is to replace only the diseased tissue while leaving the healthy tissue in place for greatest functional outcome. In 1998, Gerrit Melles described the first experimental corneal endothelial keratoplasty.[171, 172] In 2000, Mark Terry performed the first posterior keratoplasty in the United States.[173, 174] Since then, DSAEK became the most popular technique for posterior lamellar transplantation, as confirmed by the Eye Bank Association of America (10-fold increase from 2005 to 2007).[175]

The remarkable advantages of DSAEK over PKP include: preservation of the host corneal surface, with no incisions or sutures; elimination of suture-related complications,

rendering a corneal surface that is smoother and almost astigmatism-free; faster wound healing and earlier refractive stability with no need for suture removal.

5.4.1 GOAL

The goal of this study was to assess the feasibility of DSAEK in the feline model (unpublished data). The conclusion of this study determines and justifies the surgical technique that is used to transplant the tissue-engineered FECD grafts.

5.4.2 MATERIALS AND METHODS

All experiments were conducted in accordance with the Declaration of Helsinki. The research protocols were approved by the Committee for Animal Protection of the Maisonneuve-Rosemont Hospital (Montreal, QC, Canada).

Five healthy animals were obtained from a certified supplier. Ophthalmic examination included slit lamp examination (Haag-Streit, Bern, Switzerland), intraocular pressure measurement with a hand held veterinary tonometer (Tonovet, TV01; Tiolat Oy, Helsinki, Finland) and central corneal pachymetry (Ultrasound Pachymeter SP 3000; Tomey, Nagoya, Japan). One eye per animal was randomly assigned to surgery.

One cat received a tissue-engineered (TE) cornea using allogeneic endothelial cells (case 1). One cat received a tissue-engineered cornea using autologous endothelial cells (case 2). Three cats received a xenogeneic human native cornea (cases 3, 4 and 5). Functional outcome was assessed for 7 days.

Corneal tissue engineering was performed as described previously.[27] Briefly, feline corneal endothelial cells were isolated and cultured. Native human corneas unsuitable for transplantation in humans were used as a carrier. These human corneas were devitalized through three freeze -20^{o}C/thaw cycles. The carrier was seeded with the cultured feline corneal endothelial cells and cultured for 2-3 weeks to allow the reconstruction of a compact endothelial monolayer.

5.4.2.1 Surgery

Preoperative pharmacological dilation of the pupil was achieved using tropicamide 1% (Mydriacyl, Alcon Canada, Mississauga, Canada), phenylephrine 2.5% (Mydfrin, Alcon Canada, Mississauga, Canada), and cyclopentolate (Cyclogyl minims, Chauvin, Kingston-Upon-Thames, England) 1 drop of each every 5 minutes.

Surgeries were performed under general anesthesia. Anesthesia was induced and maintained by inhalation of 4-5% and 2% of Isoflurane, respectively. Atracurium (0.25 mg/kg, followed by 0.1 mg/kg every 20–30 minutes as needed) was used to induce paralysis of the extraocular muscles as well as to prevent the third eyelid prolapse. The ocular area was disinfected with a 0.5% Povidone-Iodine solution (Proviodine solution 1%, Rougier Pharma, Ratiopharm, Canada), along with one drop being added to the inferior fornix. Lieberman lid speculum was inserted.

A limbal 2.5 mm incision was made at the limbus and the anterior chamber was filled with viscoelastic (Healon, AMO, Santa Ana, CA). The recipient bed was prepared by the stripping of Descemet's membrane and its endothelium[176] and the viscoelastic agent was rinsed with BSS. The donor button was then cut with a semi-automated microkeratome (ALTK-Cbm, Moria, Antony, France) using a 300 micron foot-plate and a Hannah Punch (Moria, Antony, France). A drop of Healon was added on the endothelial surface of the posterior lamellar graft, which was then folded in two, in a proportion of 60% top and 40% bottom and inserted in the anterior chamber through the 5 mm limbal incision. The graft was centered using a reversed Sinsky and stabilized against the recipient bed using an air bubble for 30 minutes. The endothelial pump of the newly transplanted endothelium allowed the donor disk to adhere to the recipient cornea, thus eliminating the need for corneal sutures. The air bubble was then totally removed since the feline model is relatively intolerant to air in the anterior chamber.[168]

5.4.2.2 Postoperative Management

Following surgery, all animals received dexamethasone (1.2 mg in 0.3 ml), tobramycin (10 mg in 0.25 ml) and cefazolin (55 mg in 0.25 ml) in the form of

subconjunctival injections, and tobramycin 0.3% and dexamethasone 0.1% ointment (Tobradex, Alcon). An Elizabethan collar was gently tied around the animal's neck to protect the operated eye. Animals were examined daily following surgery to check for graft transparency, signs of infection, inflammation, wound dehiscence or other complications.

5.4.3 RESULTS

5.4.3.1 Surgery

Stripping of Descemet's membrane was challenging. The strong adherence of DM to the underlying stroma, especially at the center of the cornea, made it impossible to detach the DM and endothelial layers as a single unit. DM adherence was such that pulling on it induced significant traction and distortion to the entire cornea with subsequent severe corneal edema. Surgical manoeuvres were limited in general by the depth of the anterior chamber and the steepness of the corneal curvature in the feline eye. Rapid and severe fibrin formation was noticed filling the entire anterior chamber. The fibrin strands condensed and attached firmly to the graft once inserted, which made graft unfolding after insertion, air bubbling and graft-to-host attachment more challenging and traumatic than when DSAEK is performed in humans.

5.4.3.2 Clinical Outcome

5.4.3.2.1 DSAEK case 1 (TE cornea using allogeneic endothelial cells):

Seven days after transplantation, graft was semitransparent with evident epithelial and stromal edema. Recipient stromal edema with intra-stromal haemorrhage was observed between the limbic wound and the graft. Central corneal thickness was impossible to measure. Mild cells and flare were observed in the anterior chamber along with fibrin strands attaching to the graft's edge (Figure 43).

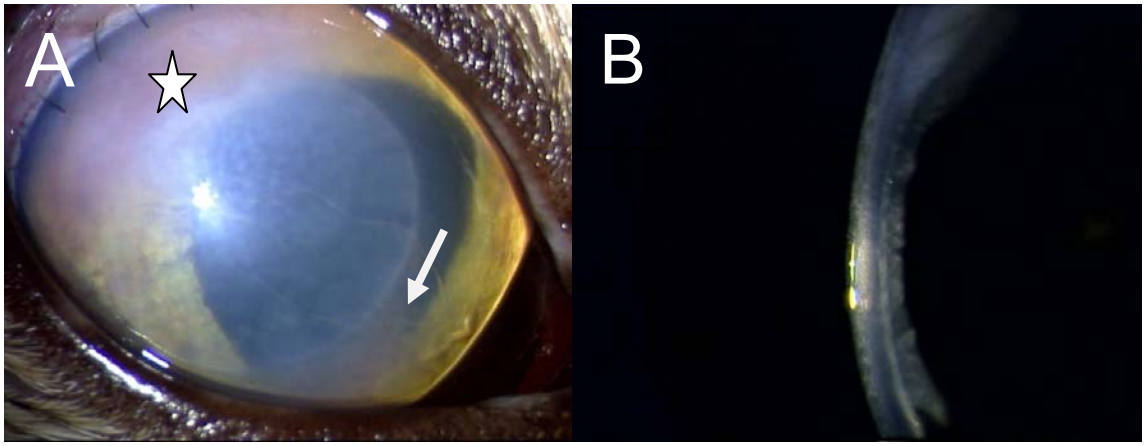

Figure 43: First DSAEK case; Slit lamp photos seven days after transplantation (final exam) showing semitransparent graft, recipient edema with intra-stromal haemorrhage (star) and fibrin strands attaching to the edge of the graft (arrow) (A); and graft edema (B).

5.4.3.2.2 DSAEK case 2 (TE cornea using autologous endothelial cells):

Four days after transplantation, graft was opaque with evident epithelial and stromal edema. An 80% graft detachment was observed. Cells (+3) and flare (+3) were observed in the anterior chamber along with fibrin strands attaching to the graft (Figure 44).

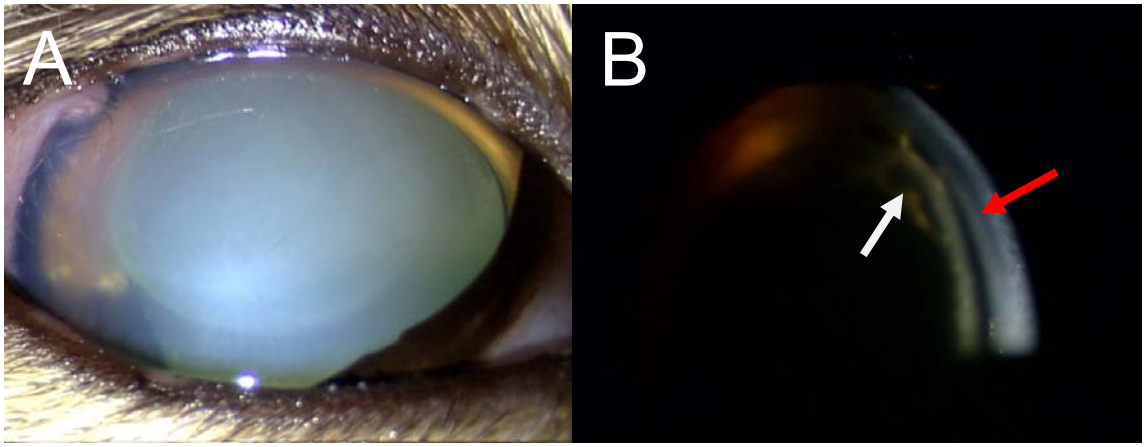

Figure 44: Second DSAEK case; Slit lamp photos four days after transplantation (final exam) showing opaque graft with stromal edema (A), graft detachment (red arrow) with fibrin attaching to the graft (white arrow) (B).

It's possible that fibrin strands pulled the graft when they condensed and contracted causing graft detachment.

5.4.3.2.3 DSAEK case 3 (xenogeneic human native cornea):

Intracameral formation of fibrin was observed postoperatively and it was directed to the edge of the graft where was the naked stroma of the donor. Four days postoperatively, subconjunctival betamethazone (3mg/0.5ml) and intracameral recombinant tissue plasminogen activator (rtPA) (150µg/0.3ml) were injected in order to digest the existing fibrin. Seven days after transplantation, the graft was clear. Central corneal thickness was 742 µm. Graft was fully attached to the stromal bed. Cells (+3) and flare (+3) were observed in the anterior chamber along with residual particles of fibrin attaching to the graft's borders (Figure 45).

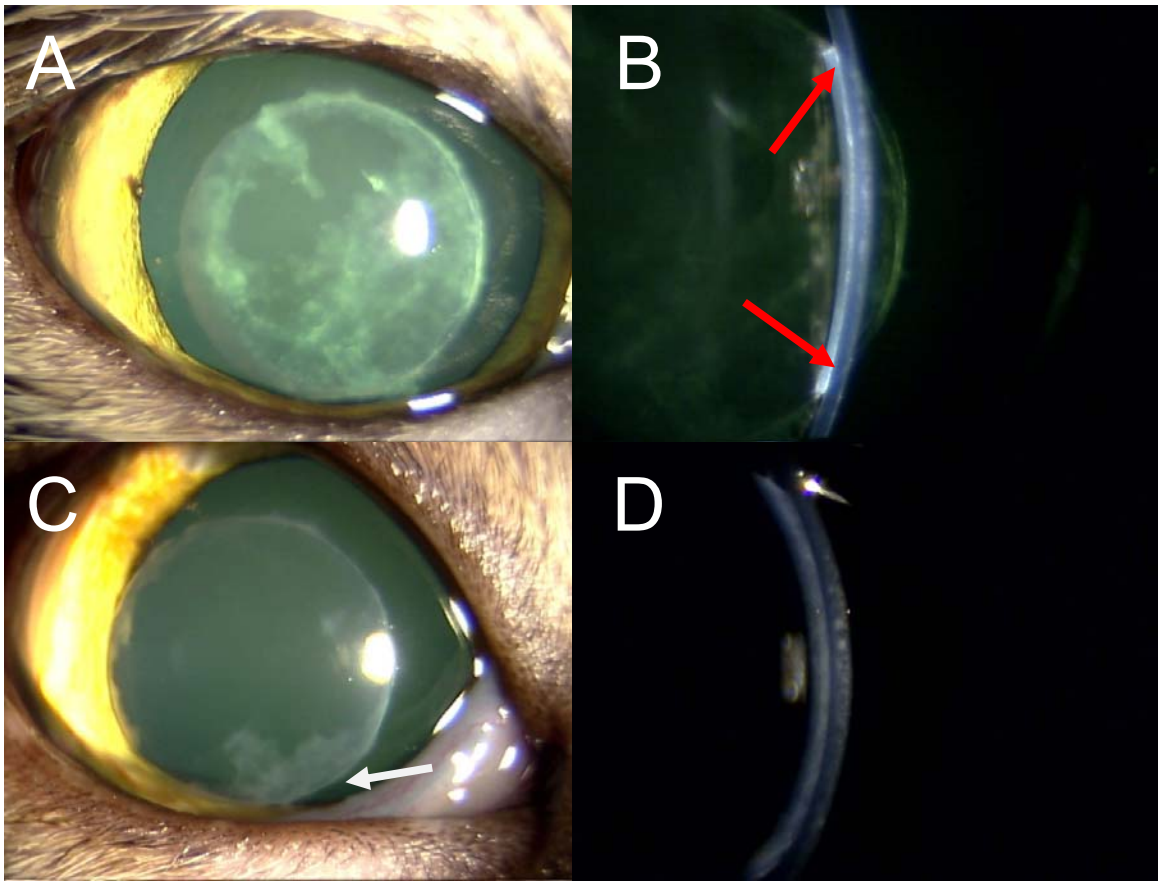

Figure 45: Third DSAEK case; Slit lamp photos: (A-B) four days after transplantation showing fibrin formation attached to the edge of the graft (red arrow). (C-D) Seven days after transplantation (final exam) showing clear graft with residual digested fibrin (white arrow) after rtPA injection.

This case showed that rtPA injection yielded a relatively successful dissolve of fibrin strands allowing better clinical outcomes.

5.4.3.2.4 DSAEK case 4 (xenogeneic human native cornea):

One day post transplantation, the graft was partially detached and severe recipient corneal edema was observed leading to opaque cornea. Severe intraocular inflammation was seen. Fibrin was attached to the graft posteriorly. Two days post transplantation, the cornea was totally opaque. The graft dropped in the anterior chamber inferiorly. Corneal thickness was over device range of measurement (Figure 46).

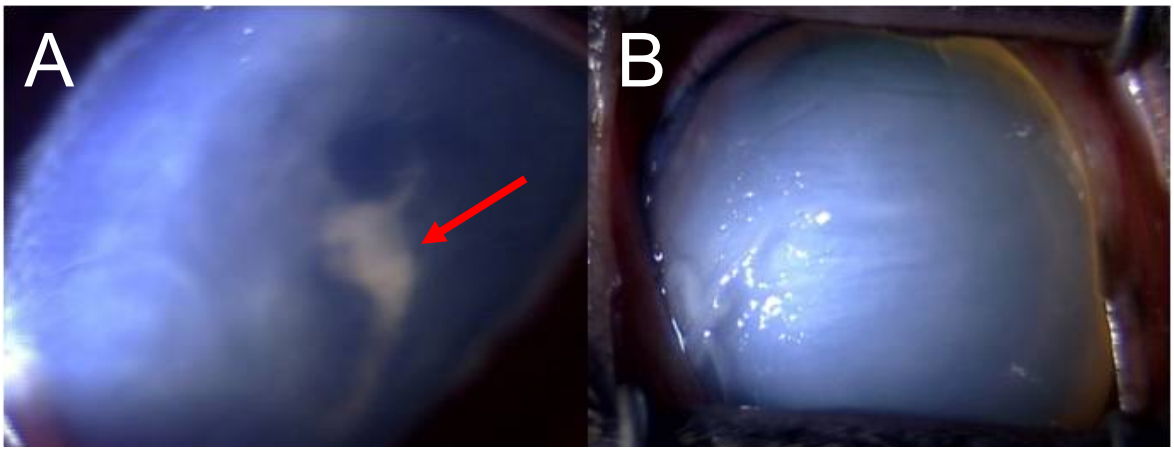

Figure 46: Fourth DSAEK case; Slit lamp photos one (A) and two (B) days after transplantation showing opaque cornea with severe stromal edema. Graft detachment with fibrin attaching to the graft was observed (red arrow).

The cause of severe intraocular inflammation was unclear. It's possible that fibrin strands caused graft detachment, which in turn increased the inflammatory reaction.

5.4.3.2.5 DSAEK case 5 (xenogeneic human native cornea):

Four days after transplantation, the graft was clear and attached. Central corneal thickness was 923 µm. Moderate fibrin was seen attaching to the edge of the graft. Seven days after transplantation, the graft was crystal clear and attached. Central corneal thickness was 692 µm. Multiple dendritic ulcers were observed. Moderate fibrin was seen (Figure 47).

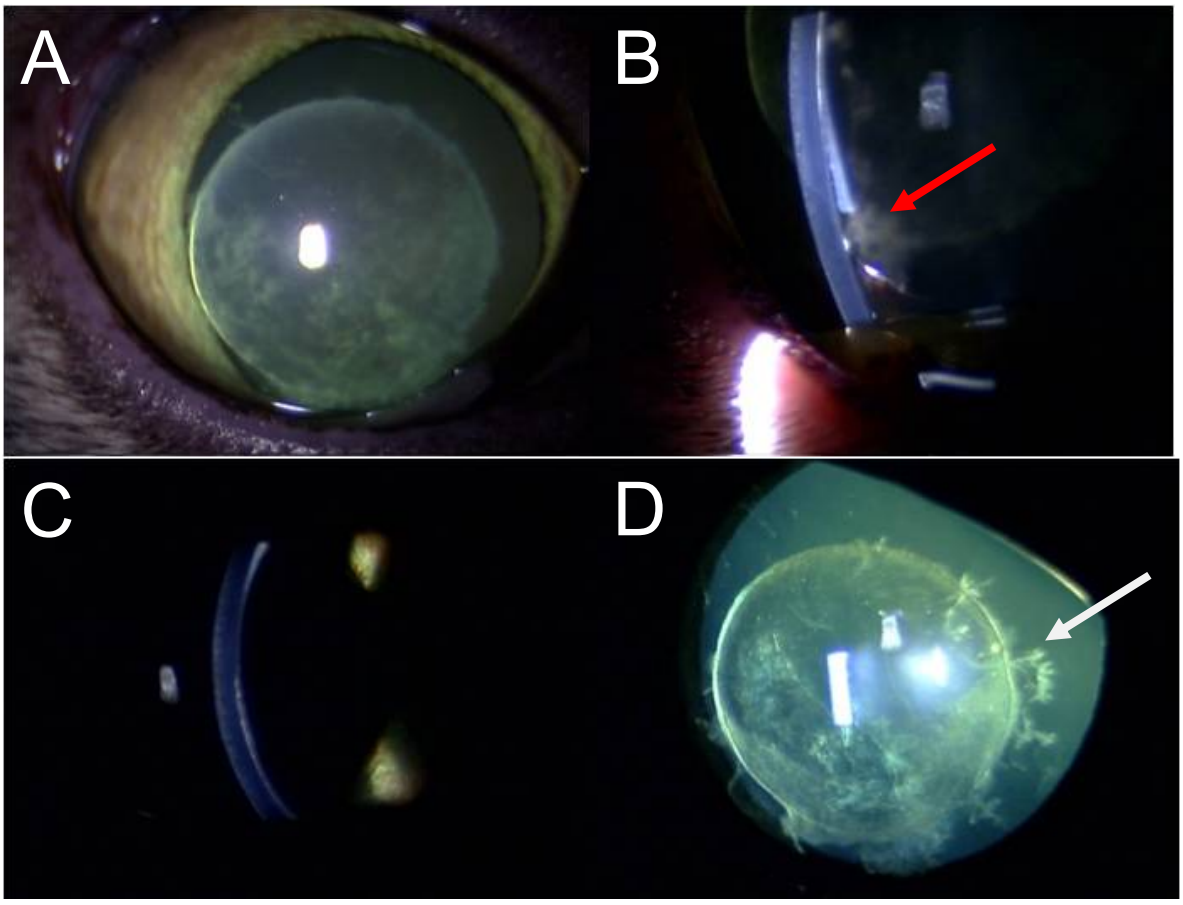

Figure 47: Fifth DSAEK case; Slit lamp photos: (A-B) four days after transplantation showing clear graft and fibrin formation attached to the edge of the graft (red arrow). (C-D) Seven days after transplantation showing clear graft with dendritic ulcers (white arrow).

This case showed an optimal clinical outcome without any unusual intervention.

5.4.4 DISCUSSION

Although DSAEK has replaced PKP in the treatment of endotheliopathies in humans, few studies have reported DSAEK in the living animal.[129, 142] To the best of my knowledge, this is the first study that assesses the feasibility of DSAEK in the feline model.

Honda et al.[129] investigated the feasibility of DSAEK using cultured human corneal endothelial cells (HCECs) in the rabbit model. Fourteen rabbits were enrolled in the study. They were divided into 2 groups:

- Seven rabbits received a cultured-graft DSAEK group (c-DSAEK) in which a stromal disc with cultured HCECs was transplanted.
- Seven rabbits received a stromal disc without HCECs (control group).

Corneal edema developed after surgery in both groups. The edema decreased and transparency recovered gradually in the c-DSAEK group, whereas the edema persisted for 28 days in the control group. Honda et al.[129] demonstrated a slow recovery of the cDSAEK group over 4 weeks of observation, so DSAEK could be reliable in the medium and long term. However, his figure showing a slit lamp photo of a graft of cDSAEK group didn't demonstrate a thin and clear graft 21 days after transplantation (Figure 48B). Furthermore, how the stromal disc without endothelial cells was hold in its place without being detached raises a big question mark.

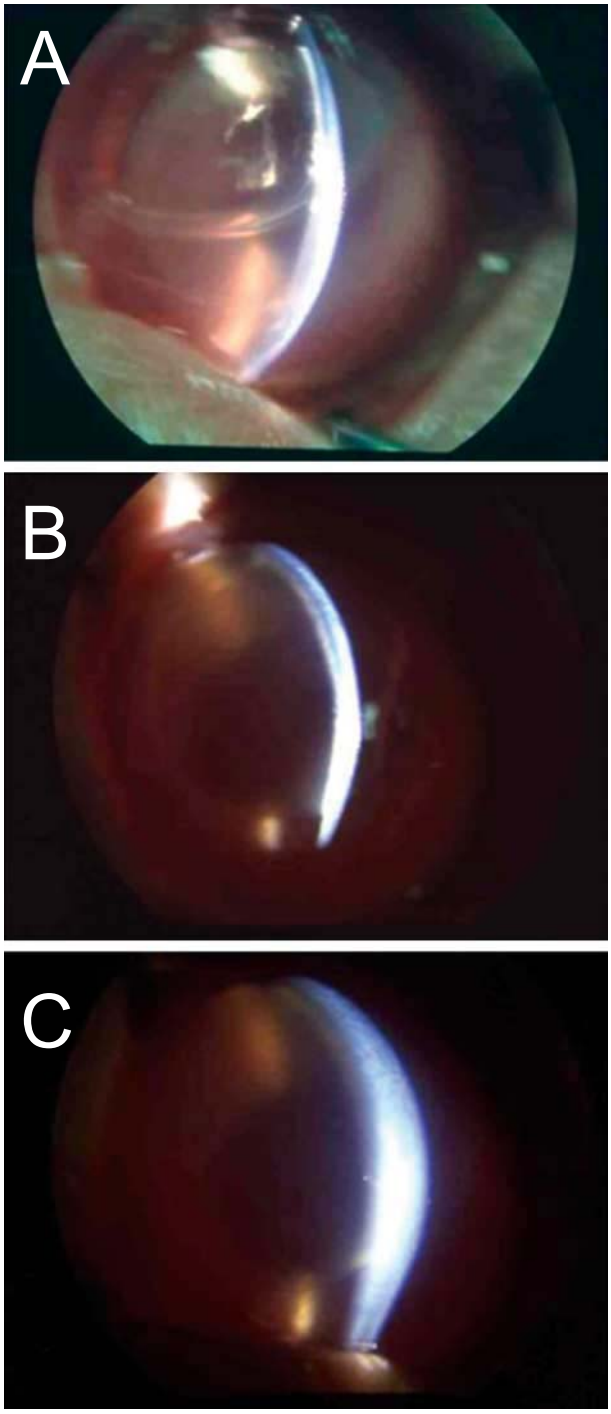

Figure 48: Descemet stripping automated endothelial keratoplasty (DSAEK) in the rabbit model. Slit lamp photo of the cultured-graft (DSAEK) group at day 1 after surgery (A), the DSAEK graft attached to the posterior surface of the cornea and corneal edema persisted.

At day 21 after surgery, corneal edema was less severe in the cultured-graft DSAEK group (B) than in the control group (C).[129]

In our study, although DSAEK technique requires a learning curve, surgery was technically difficult to perform in the feline eye. Reaching the endothelium through a limbal incision in the feline model proved to be difficult. The anterior chamber of the cat is deeper than that of the human. However, the use of curved instruments can compensate in part for this difficulty. Feline's Descemet's layer is more adherent to the underlying stroma than that in human, which made stripping more difficult. Descemet's adherence was such that pulling on it induced significant traction and distortion to the surrounding tissues with subsequent edema. In our cases, Descemet's membrane was not peeled off in a single piece as it is the case in humans. We had to strip Descemet's membrane piece by piece. The use of a blunt stripper made stripping of Descemet's membrane easier, while sharp instruments such as Sinsky hook weren't of much help. Furthermore, rapid fibrin formation inside the feline eye during surgery made manipulating the graft inside the eye difficult to perform. Mechanical removal of fibrin strands attached to the graft caused additional trauma. Intracameral injection of recombinant tissue plasminogen activator (rtPA) can partially help to resolve fibrin strands. Another limitation of DSAEK is the relative intolerance of the feline model to air in the anterior chamber.[168]

Although significantly advantageous in humans over the traditional penetrating keratoplasty, DSAEK still has some limitations. The endothelial cell attrition in DSAEK may persist for years after surgery, with a cumulative endothelial cell loss of 67% of preoperative value and a continued risk of late endothelial failure 10 years after surgery.[177] Furthermore, endothelial cell loss is significantly higher using DSAEK compared to PKP technique 6 and 12 months postoperatively with comparable graft survival and comparable donor and recipient characteristics in humans. Price et al. attributed cell loss principally to greater surgical manipulation and trauma to the graft in the DSAEK procedure.[20] Corneal endothelial immune rejection also occurs in about 27% of grafts, ultimately causing irreversible failure.[22] In our DSAEK experiments in the feline model, postoperative observation showed moderate to severe intraocular inflammation with fibrin membrane

directed to the naked stroma of the donor. Suboptimal transparency of the tissue-engineered grafts was also observed. On the other hand, crystal clear transparency was achieved with the same tissue-engineered tissue with the PKP technique, with mild inflammatory reaction in some cases.[29] Excessive surgical trauma and possible sensitivity towards naked donor stroma could be a possible explanation to this inflammatory reaction and decreased transparency in the feline model. In conclusion, our five DSAEK cases gave inconstant results in the feline model.

5.5 Other Surgical Techniques

Descemet membrane endothelial keratoplasty (DMEK)[178] and Descemet membrane automated endothelial keratoplasty (DMAEK)[179] are interesting concepts that carry better and faster visual outcomes.[180] The surgical procedure, however, is technically more challenging than DSAEK in humans, even in the hands of the most experienced surgeons. Handling a thin and fragile sheet of cells without stromal support that curls into a scroll inside the eye is an additional challenge compared to DSAEK. Quick per-operative fibrin formation inside feline eyes could make unfolding Descemet's membrane even more difficult. Postoperative endothelial cells loss and requirement of air reinjection is even higher in DMAEK than in DSAEK.[181]

For the reasons that were shown in this chapter, we chose to use the feline model and PKP technique for the *in vivo* assessment of TE-FECD corneas.

6 Chapter VI:

A Short-Term *In Vivo* Experimental Model for Fuchs Endothelial Corneal Dystrophy: *2nd Article (The Third Objective: In Vivo Assessment)*

A Short-Term *In Vivo* Experimental Model for Fuchs Endothelial Corneal Dystrophy

(Published paper in Invest Ophthalmol Vis Sci. 2012 Sep 19;53(10):6343-54)

6.1 Authors

M. Nour Haydari, MD, MSc[1,2*]

Marie-Claude Perron, MSc[1]

Simon Laprise[3]

Olivier Roy[3]

J. Douglas Cameron, MD[4]

Stéphanie Proulx, PhD[3]

Isabelle Brunette, MD, FRCSC[1,2]

*MN Haydari had the major contribution being in charge of this study including research questions and research protocols conductions, grafts transplantation, clinical follow-up and management, experiments termination, vital staining, light and transmission electron microscopy observations, all clinical and histological data analysis, writing the whole manuscript and answering the questions raised by the reviewers.

6.2 Institutional affiliation

[1]Maisonneuve-Rosemont Hospital Research Center, Montreal, QC, Canada

[2]Department of ophthalmology, University of Montreal, Montreal, QC, Canada

[3]Centre LOEX de l'Université Laval, Génie tissulaire et régénération- Centre de recherche FRSQ du Centre hospitalier *affilié* universitaire de Québec, Québec, QC, Canada and Département d'ophtalmologie et d'oto-rhino-laryngologie, Faculté de médecine, Université Laval, Québec, QC, Canada

[4]Departments of Ophthalmology and Laboratory Medicine and Pathology, Medical School, University of Minnesota, Minneapolis, MN

This work was supported by: The Canadian Institutes for Health Research, Ottawa, ON, Canada and The FRQS Research in Vision Network, Montreal, QC, Canada. IB is the recipient of the Charles-Albert Poissant Research Chair in Corneal Transplantation, University of Montreal, Canada.

Corresponding author: Isabelle Brunette, MD, FRCSC

Key words: Fuchs endothelial corneal dystrophy; corneal transplantation; tissue engineering; corneal endothelial cells; cell culture; feline model.

Word count: Abstract: **250**; Text (excluding references and figure legends): **5376**

Finance disclosure: None.

6.3 ABSTRACT

Purpose: To evaluate the *in vivo* functionality of a corneal endothelium tissue-engineered using corneal endothelial cells from human patients with Fuchs endothelial corneal dystrophy (FECD).

Methods: Fifteen healthy cats underwent full-thickness corneal transplantation. All transplants were of xenogeneic human origin and all grafts but two were tissue-engineered. In seven animals the graft corneal endothelium was tissue-engineered using cultured corneal endothelial cells from humans with FECD (TE-FECD); Two control animals were grafted with an endothelium engineered using cultured endothelial cells from normal eye bank corneas (TE-normal); Two controls received a native full-thickness corneal transplant; and four other controls were grafted with the stromal carrier only (without endothelial cells). Outcome parameters included graft transparency (0 (opaque) to 4 (clear)), pachymetry, optical coherence tomography, endothelial cell morphometry, transmission electron microscopy (TEM) and immunostaining of function-related proteins.

Results: Seven days after transplantation, 6 of 7 TE-FECD grafts, all TE-normal grafts and all normal native grafts were clear (transparency score > 3), while all carriers-only grafts were opaque (score < 1). The mean pachymetry was 772 ± 102 μm for TE-FECD, 524 ± 11 μm for TE-normal, 555 ± 48 for normal native and 1188 ± 223 μm for carriers only. TEM showed subendothelial loose fibrillar material deposition in all TE-FECD grafts. The TE endothelium expressed Na^{+}-K^{+}/ATPase and Na^{+}/$HCO3^{-}$.

Conclusion: Restoration of transparency and corneal thickness demonstrated that the TE-FECD grafts were functional *in vivo*. This novel FECD seven day living model suggests a potential role for tissue engineering leading to FECD cell rehabilitation.

6.4 INTRODUCTION

Fuchs endothelial corneal dystrophy (FECD) is responsible for more than a quarter of the corneal transplantations performed in North America (28% of the 42,642 corneal grafts performed in the United-States in 2010).[19] The pathophysiology of this inherited disease,[91-93] however, is still poorly understood. Corneal edema is thought to result from decreased endothelial cell density, increased endothelial permeability and decreased endothelial pump function,[7-12] and there is mounting evidence that oxidative stress, DNA damage and protein unfolding response leading to apoptosis may play a role in FECD pathogenesis.[13-18] Very few experimental models are available to study FECD. A collagen VIII α2 Q455K knock-in mouse model has recently successfully been developed by Jun et al.[182] for a rare type of early onset FECD. He et al.[183] have cultured FECD corneal endothelial cells transfected with the human papilloma virus type 16 genes E6/E7 to expand their lifespan. Culture of FECD cells has proven to be difficult without transfecting oncogenes.

Human corneal endothelial cells are arrested in the G1-phase of the cell cycle[23] and do not proliferate *in vivo*. However, they can proliferate *in vitro* in response to growth-promoting agents.[24-26] Our laboratory has shown that normal corneal endothelial cells can be cultured and can retain function *in vitro* and *in vivo*.[27-29] We demonstrated the first evidence of successful culture, without viral transduction, of corneal endothelial cells from patients with FECD.[30] These cells were also successfully used to tissue engineer a corneal endothelium.[184]

In this study, we evaluated the functionality of a corneal endothelium tissue-engineered (TE) using corneal endothelial cells from human subjects with FECD, that were cultured on a devitalized human stromal carrier and transplanted in a living feline eye. This short-term in vivo experimental model for FECD was assessed and characterized.

6.5 MATERIALS AND METHODS

All experiments were conducted in accordance with the Declaration of Helsinki and the ARVO Statement for the Use of Animals in Ophthalmic and Vision Research. The research protocol was approved by the Maisonneuve-Rosemont Hospital Animal Protection and Ethics for Clinical Research committees.

6.5.1 Tissue Preparation

Consenting patients with FECD undergoing DSAEK or penetrating keratoplasty (PKP) for symptomatic non-reversible corneal endothelial failure at the Maisonneuve-Rosemont Hospital (Montreal) between October 2009 and September 2010 were enrolled in this study (four women, three men, aged from 58 to 74 years, mean ±SEM= 66 ± 6 years). At the time of DSAEK, the diseased Descemet's membrane (DM) and overlying endothelium were removed from the eye as described previously.[30] No viscoelastic agent was used. The specimen was put in Optisol-GS (Bausch and Lomb, Rochester, NY) and sent on ice to the laboratory for cell isolation. For PKP, the full thickness corneal specimen was sent in Optisol-GS and DM was stripped upon arrival in the laboratory.

FECD specimens were processed on the day following surgery. Endothelial cells were isolated as described by Zhu and Joyce[26]. In five cases, the cells were cryopreserved at P0 in 90% fetal bovine serum (Hyclone) /10% dimethylsulfoxide (DMSO; Sigma). The corneal endothelial cells were cultured as described previously[184](Figure 49A) and seeded at P1 (n=1) or P2 (n=6) (initial seeding of $2.42 \times 10^5 \pm 0.34 \times 10^5$ cells) on a devitalized human stroma, on which they were grown for 1 to 2 weeks (10.9 ± 1 days, range from 8 to 15 days). The tissue-engineered corneas were then preserved in transport medium[29] for 1 to 3 days (2.5 ±1 days, range from 1 to 3) prior to transplantation.

Thirteen eye bank corneas from 13 donors were used to produce stromal carriers (mean age ±SEM: 62 ± 10 years (34 to 80 years)). Native cells were killed through three freeze (-20^{o}C) /thaw cycles and the devitalized corneas were stored at -20^{o}C until used (mean delay of 70 ± 77 days, from 8 to 531 days). The carriers to be transplanted without

endothelium were prepared in the exactly same manner, but without endothelial cell seeding.

For comparison purposes, two corneas were also engineered using the endothelial cells of normal eye bank corneas. The two donors were aged 68 and 47 years. Central Descemet's membrane was stripped using a circular biopsy punch (Acuderm, Dormer Laboratories, Toronto, ON, Canada) and fine forceps. Besides endothelial cell origin and isolation technique, all steps for tissue engineering of the normal and FECD corneas were identical.

Ultrastructure studies of mate non-transplanted, tissue-engineered corneas confirmed the previously reported similarity between the TE-FECD and the TE-normal corneas in culture.[184] The endothelial monolayer was attached to DM, with well preserved nuclei, mitochondria, and rough endoplasmic reticulum, all suggestive of healthy cellular activity (Figure 49B). DM was normal, without guttae or subendothelial deposition of loose fibrillar material. The stroma was acellular.

For native controls, two normal eye bank corneas harvested within 12 hours after death were preserved in Optisol at 4°C and transplanted within 10 days after death. All eye bank tissues in this study were obtained from our local eye banks (Québec Eye Bank, Montréal, and Banque d'yeux du Centre universitaire d'ophtalmologie, Québec, QC, Canada) and were unsuitable for transplantation in humans.

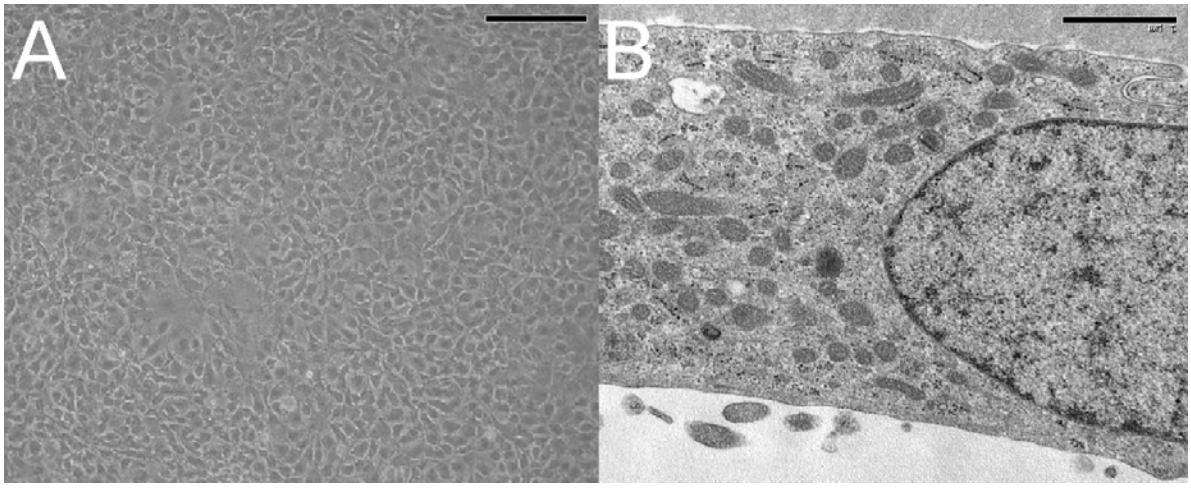

Figure 49: Corneal endothelial engineered using FECD endothelial cells. (A) FECD endothelial cells in culture. (B) Transmission electron microscopy view of a mate non-transplanted cornea engineered by seeding FECD endothelial cells on a devitalized stromal carrier. The endothelial cell is attached to DM and shows well preserved nucleus, numerous mitochondria and the presence of rough endoplasmic reticulum, all signs of healthy cellular activity. Note the absence of subendothelial deposition of loose fibrillar material. Scale bars: (A) 200 µm, (B) 1 µm.

6.5.2 Tissue Assignment

Fifteen animals underwent full-thickness corneal transplantation. All transplants were of xenogeneic human origin and all grafts but two were tissue-engineered. Seven animals were grafted with a corneal endothelium tissue-engineered using endothelial cells from patients with FECD, cultured on a devitalized stromal carrier (TE-FECD grafts). Two control animals were grafted with a corneal endothelium tissue-engineered using endothelial cells from normal eye bank corneas, cultured on a devitalized stromal carrier (TE-normal grafts). Two control animals received a normal native human cornea (normal native grafts). Four other controls were grafted with the stromal carrier only, without endothelial cells (carrier-only). One eye per animal was randomly assigned to surgery, and the contralateral unoperated eye was used as a control.

6.5.3 Preoperative Management of the Animals

Healthy animals aged 8 to 27 months (mean ± SEM: 13 ± 4 months) were obtained from a certified supplier. Standard ophthalmic examination of the animals included biomicroscopy (Haag-Streit, Bern, Switzerland), intraocular pressure measurement with a handheld veterinary tonometer (Tonovet, TV01; Tiolat Oy, Helsinki, Finland), and central corneal pachymetry (Ultrasound Pachymeter SP 3000; Tomey, Nagoya, Japan). Prophylactic famciclovir (Famvir, PMS, Montreal, QC) 125 mg/day per os was started on admission and continued over the entire study period.

6.5.4 Corneal Transplantation

Surgery was performed under general anesthesia, using the premedication and systemic and topical medication described previously.[141] The donor cornea was warmed at room temperature over 2 hours prior to transplantation. It was cut with a 9-mm Hanna punch (Moria, Antony, France). The recipient cornea was cut with an 8-mm trephine Weck (Solan Medtronics, Jacksonville, FL) and the anterior chamber was filled with viscoelastic (Healon, AMO, Santa Ana, CA). The donor tissue was gently rinsed with BSS and secured to the recipient bed with four cardinal sutures, followed by a 10–0 nylon single running suture (CU-1 10–0 nylon; Alcon Surgical, Fort Worth, TX). The viscoelastic was rinsed with BSS. A recombinant tissue plasminogen activator (Alteplase, Genentech, CA) (150 µg in 0.3 ml) was injected into the anterior chamber to stimulate resorption of the gelatinous stands of fibrin which tend to form in this species when the anterior chamber is entered. Suture knots were buried and the wound was checked for leaks using a fluorescein strip (Fluorescein sodium ophthalmic strips, Chauvin laboratories, Aubenas, France).

6.5.5 Postoperative Medication

At the end of surgery, all animals received subconjunctival injections of dexamethasone (1.2 mg in 0.3 ml), betamethasone (3mg in 0.5 ml), tobramycin (10 mg in 0.25 ml) and cefazolin (55 mg in 0.25 ml), and an elizabethan collar was installed. Sodium chloride 5% (Muro 128, Bausch & Lomb, Rochester, NY), tobramycin 0.3% and dexamethasone 0.1% (Tobradex, Alcon) ointments were applied BID. Subconjunctival injections of dexamethasone (1.2 mg in 0.3 ml) or betamethasone (3mg in 0.5 ml) were repeated when an increase in intraocular inflammation was observed on two consecutive days. No systemic antibiotics were given at any time.

6.5.6 Postoperative Follow-up

Animals were examined daily by two independent observers. Graft transparency was quantified according to a subjective 0 to +4 scale: +4, clear graft; +3, slight opacity with iris/lens details easily visible; +2, mild opacity, iris/lens details still visible; +1,

moderate opacity with no iris/lens details; and 0, opaque cornea (iris not visible).[29] Anterior chamber cells and flare were quantified according to a 0 to +4 scale (for cells: in a field size of 1 mm by 1 mm slit beam: 0: no cells; +1: occasional cells; +2: 8-15 cells; +3: too many to count; +4: very dense. The flare scale was quantified as: 0: empty; +1: very slight; +2: mild to moderate (iris/lens clear); +3: moderate (iris/lens hazy); +4: severe (fibrin, plastic aqueous).[185] Intraocular pressure and central corneal thickness were measured on days 1, 2, 3, 4, and 7. When measurements exceeded the measuring limit of the pachymeter (1400 μm), this limit was arbitrary used as the corneal thickness value.

6.5.7 Post-Mortem Assessment

Animals were euthanized (pentobarbital sodium 3 ml/2.5-5 kg intravenously) on postoperative day 7 (±12 hours) to avoid the acute immune reaction known to occur 9 to 14 days after transplantation.[186] Operated and control eyes were enucleated and examined. Optical coherence tomography (OCT) was performed (OCT III or Visante 1000; Carl Zeiss Meditec, Dublin, CA) to assess graft thickness and to document the fine structures in the anterior chamber susceptible to be washed out during tissue processing for histology.

6.5.8 Corneal Endothelial Cell Density

Non-contact specular microscopy (Konan Medical INC., Nishinomiya, Hyogo, Japan) was performed on all eyes before surgery, while the postoperative cell counts were obtained from all eyes by vital staining of part of the excised corneas. The endothelium was stained with trypan blue (Sigma) and alizarin red S (Sigma)[187] and photographed (SteREO Discovery V12, Carl Zeiss Canada, Toronto, ON, Canada). Endothelial morphometric analyses were made using the KSS-409SP software (version 2.10; Cellchek XL; Konan Medical Inc.). Three different fields were randomly selected for each corneal endothelium and a minimum of 100 cells per field were counted. The percentage of hexagonal cells was used as an index of pleomorphism and the coefficient of variation in cell area as a measure of polymegethism.[67, 135]

6.5.9 Histopathology

A portion of each cornea was fixed in 10% neutral buffered formalin and paraffin embedded by standard techniques. Sections were cut at 5 um and stained with hematoxylin & eosin. A small portion of each cornea was fixed in 2.5% glutaraldehyde for transmission electron microscopy (Hitachi H-7500, Tokyo, Japan).[27] For immunofluorescence staining, two samples of cornea were frozen in optimal cutting temperature solution (OCT) (Somagen; Edmonton, AB, Canada). Indirect immunofluorescence assay was performed on acetone fixed cryosections, as described by Proulx et al.[29] Primary antibodies consisted in mouse monoclonal anti-Na^+/K^+-ATPase α1 (Millipore, Billerica, MA) and rabbit polyclonal anti– Na^+/HCO_3^- (Chemicon, Temecula, CA). After three rinses in PBS, sections were incubated for 30 minutes at room temperature with secondary antibodies consisting in goat anti–mouse IgG or chicken anti–rabbit antibodies conjugated with Alexa 594 (Invitrogen). Negligible background was observed for controls (primary antibodies omitted). Cell nuclei were counterstained with Hoechst reagent 33258.

6.5.10 Statistical Analyses

The Kruskal-Wallis exact test was used to test for differences in medians between groups. When the Kruskal-Wallis test was significant, pairwise comparisons were carried out with the exact Wilcoxon rank-sum test. The Pearson product-moment correlation coefficient was calculated when indicated. Mean values and standard error of the mean (SEM) are reported and a p value of less than 0.05 was considered to be statistically significant. All statistical tests were two-sided. The analyses were conducted using SAS 9.2 (SAS Institute).

6.6 RESULTS

6.6.1 Surgery

Corneal transplantation was uncomplicated in all cases. In one of the carrier-only grafts, the running suture broke on the first day after surgery. It was re-sutured on the same day, but broke again on day 7. No reason could be identified for these repeated suture ruptures.

6.6.2 Post-Transplantation Follow-up

6.6.2.1 Graft Transparency

TE-FECD grafts (Figure 50A-D) and TE-normal grafts (Figure 50E-H) were clear by biomicroscopy and OCT examination, although initially not as clear as the normal native grafts (Figure 50I-L). The carrier-only controls remained opaque until the last day (Figure 50M-P). Evolution of the mean graft transparency score as a function of time after transplantation is illustrated in Figure 51A. After seven days, the mean (± SEM) score was 3.14 ± 0.76 (range from 0.5 to 4) for the TE-FECD grafts, 3.25 ± 0.25 (3 to 3.5) for the TE-normal controls, 3.5 ± 0 for the normal native controls and 0.56±0.09 (0.5 to 0.75) for the carrier-only controls. The clinically significant difference in graft transparency observed between groups tended to be statistically significant (Kruskal-Wallis: p=0.094).

One of TE-FECD grafts behaved differently from the others. On the first day after surgery, a 360 degrees posterior wound gap was noticed between the graft and the recipient cornea, leading to recipient stromal edema at the wound. At day 4, the graft transparency score was 3 and the epithelium covered 60% of the graft surface. During the next following days, however, the epithelium was progressively lost and the exposed stroma rapidly became edematous, ulcerated and necrotic, reducing the transparency score to 0.5 at day 7.

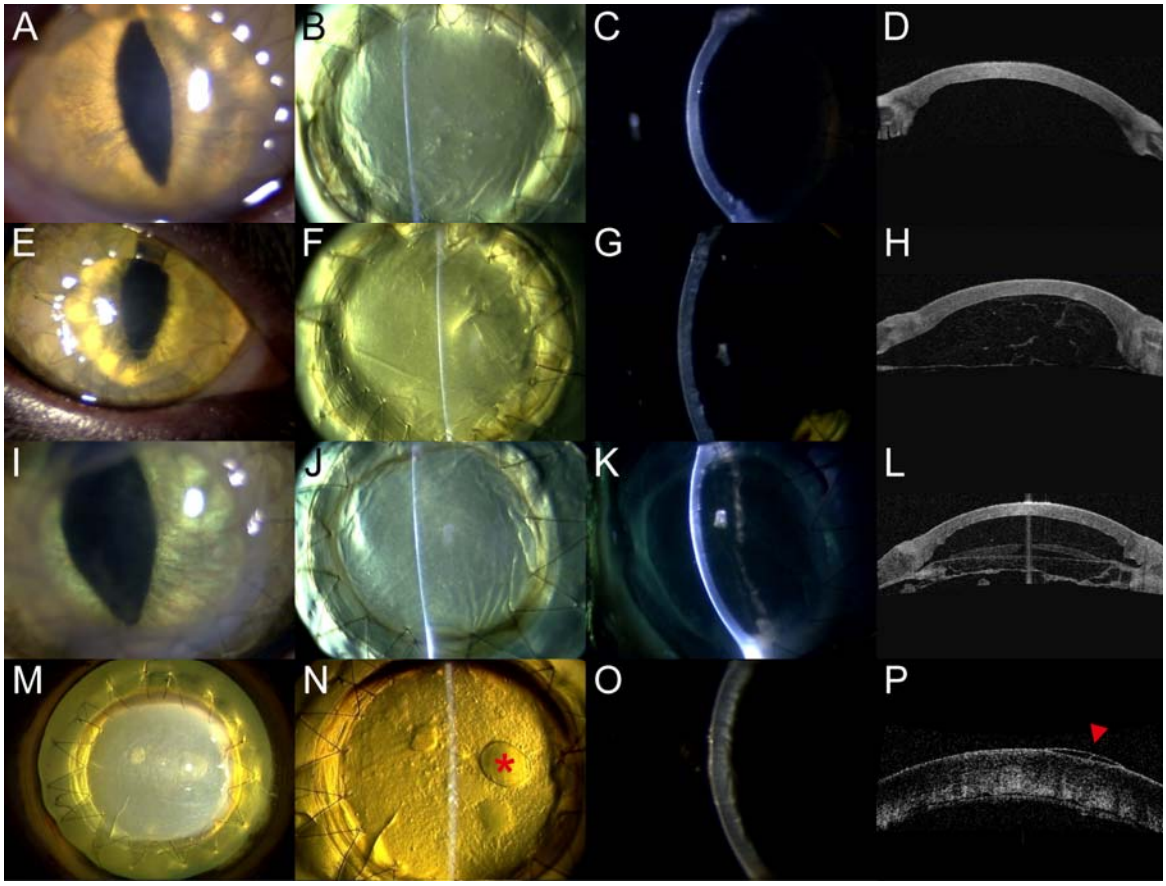

Figure 50: Corneal grafts 7 days after transplantation. Representative slit lamp (columns 1-3) and OCT (column 4) photos are shown. (A-D) Tissue-engineered graft with endothelial cells from a patient with Fuchs dystrophy. The graft is clear and thin allowing visualization of fine iris structure. Our transparency score in this case was 3.75/4 and the central corneal thickness was 659 µm. (E-H) Corneal transplant tissue-engineered from normal human endothelial cells. The graft is clear and thin (Transparency score = 3.5/4; Thickness = 513 µm). A fine membrane of loose fibrin can be seen in the anterior chamber (H). (I-L) Normal native human corneal transplant. The graft is clear and thin (Transparency score = 3.5/4; Thickness = 507 µm). A fibrin membrane can be seen in the anterior chamber (K-L). (M-P) Tissue-engineered corneal transplant consisting in a devitalized carrier without endothelial cells. The graft is opaque and edematous, with large sub-epithelial bullae (asterisk) and no detailed view of the iris (Transparency score = 0.5/4; Thickness = 1400 µm).

6.6.2.2 Pachymetry

The TE-normal grafts thinned continuously until their thickness reached that of the normal native controls (Figure 51B). The TE-FECD grafts also thinned progressively, although not as completely as the TE-normal grafts. The normal native controls remained thin and the carriers-only remained thick throughout the entire study period. On post-operative day 7, the mean central thickness was 772 ± 102 μm (659 to 1023 μm) for the TE-FECD grafts, 524 ± 11 (513 to 535 μm) for TE-normal controls, 555 ± 48 μm (507 to 603 μm) for normal native controls and 1188 ± 223 μm (742 to 1400 μm) for carriers only. The Kruskal-Wallis test confirmed an overall significant difference in corneal thickness median values among the four groups at day 7 ($p=0.0048$). Paired comparisons between TE-FECD and TE-normal grafts thicknesses tended to be statistically significant ($p=0.07$), as did paired comparisons between TE-FECD and native grafts thicknesses ($p=0.07$).

6.6.2.3 Reepithelialization

None of the tissue-engineered grafts were epithelialized at the time of transplantation. On day 7, six of the seven TE-FECD grafts were fully or almost fully reepithelialized (mean coverage of 97.3 ± 3 %) (Figure 51C). The case of corneal ulceration described above had practically no remaining epithelium at day 7. One of the two TE-normal grafts was fully reepithelialized at day 7, while the epithelium of the other one remained fragile and edematous, covering only 25% of the graft surface at day 7. In one of the two normal native controls, the epithelium was removed during surgery but grew back rapidly to achieve full coverage at day 7, and in the other case, the epithelium remained intact throughout the study period. The carrier-only controls were reepithelialized at 97 ± 4 % at day 7 in 3 cases out of 4. In the 4^{th} case, epithelial coverage reached 50% at day 4 and decreased to 20% at day 7.

6.6.2.4 Intraocular Pressure

Before surgery, the mean intraocular pressure for both operated and non-operated eyes was 31 ± 9 mm Hg. No significant increase in intraocular pressure was observed after surgery (Figure 51D).

6.6.2.5 Intraocular Inflammation

All eyes were quiet prior to surgery. On the first postoperative day, mild intraocular inflammation was present in the anterior chamber of all eyes. The number of inflammatory cells decreased progressively during the following 3 to 4 days, with a tendency to increase again by the end of the week in all four groups (Figure 51E). As the flare progressively diminished (Figure 51F), condensation of a fine fibrin formation reached its maximum at day 7. The fibrin deposition was characterized by spider-shaped filaments attaching to the edge of the graft and spreading over the graft posterior surface. The host cornea remained free of fibrin. Reactive inflammation is well known to be greater in the animal model than in human subjects.[188] Neovascularization was not present in any transplanted tissue.

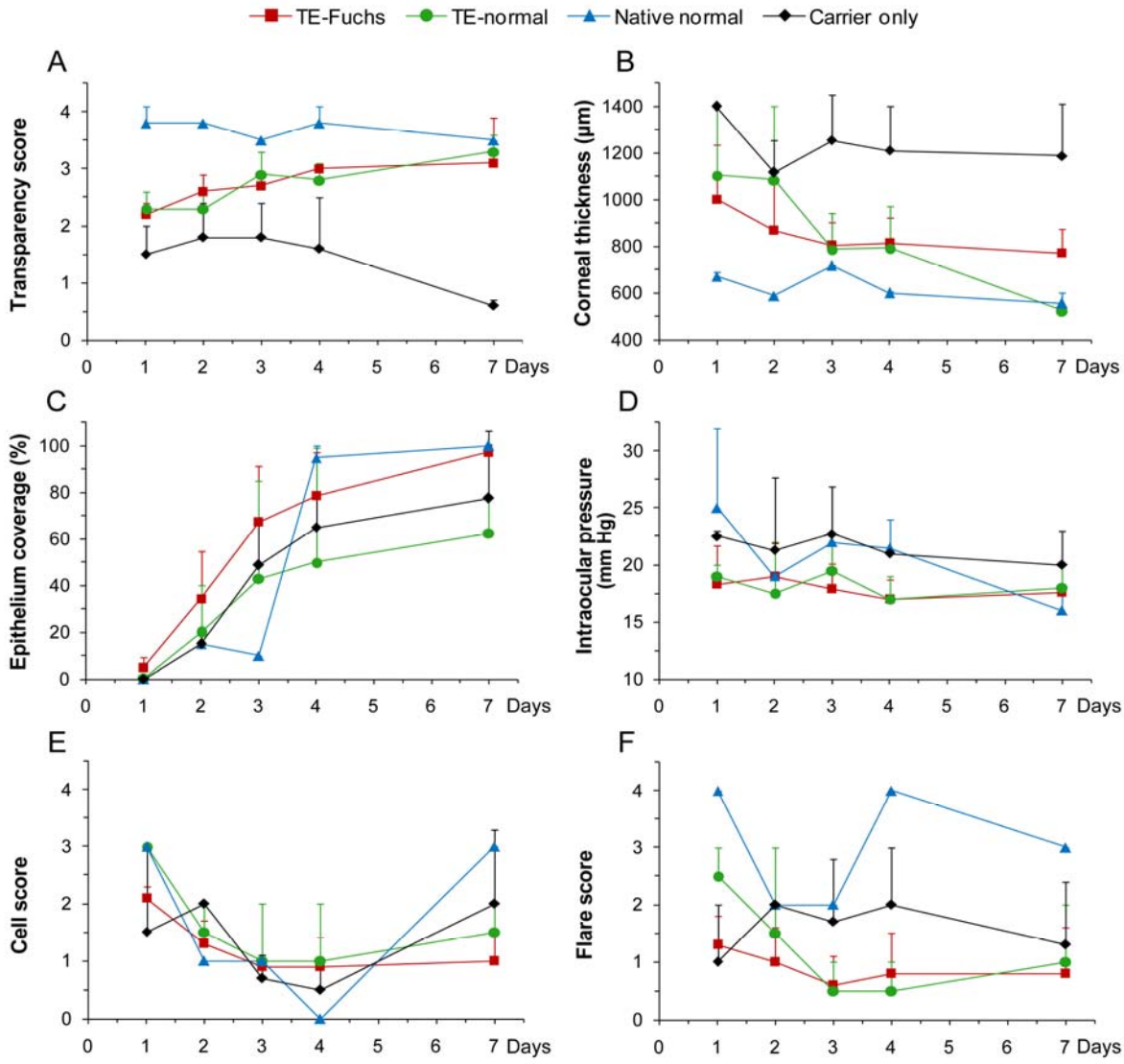

Figure 51: Clinical evolution of the operated eyes in the TE-FECD, TE-normal, normal native and carrier-only groups. (A) Transparency score. (B) Corneal thickness. (C) Epithelial coverage. (D) Intraocular pressure. (E) Anterior chamber cell score, (F) Anterior chamber flare score. All study cases are represented in these graphs, except for epithelial coverage, cells and flare at day 7 for the TE-FECD complicated case with stromal ulceration. Mean values are reported and error bars represent standard error of the mean.

6.6.3 Endothelial Cell Counts and Morphometry

Tissue-engineered cells with an endothelial polygonal morphology in culture (as shown in Figure 49A) maintained their morphology on the stromal carrier in culture and in vivo. Alizarin red and trypan blue vital staining 7 days after transplantation showed full coverage of DM by polygonal cells in the TE and native grafts (Figure 52). Signs of endothelial stabilization and maturation of cell attachment were observed, with less space between cells than previously seen in culture. No endothelial cells were seen in any of the carrier-only controls (n=4).

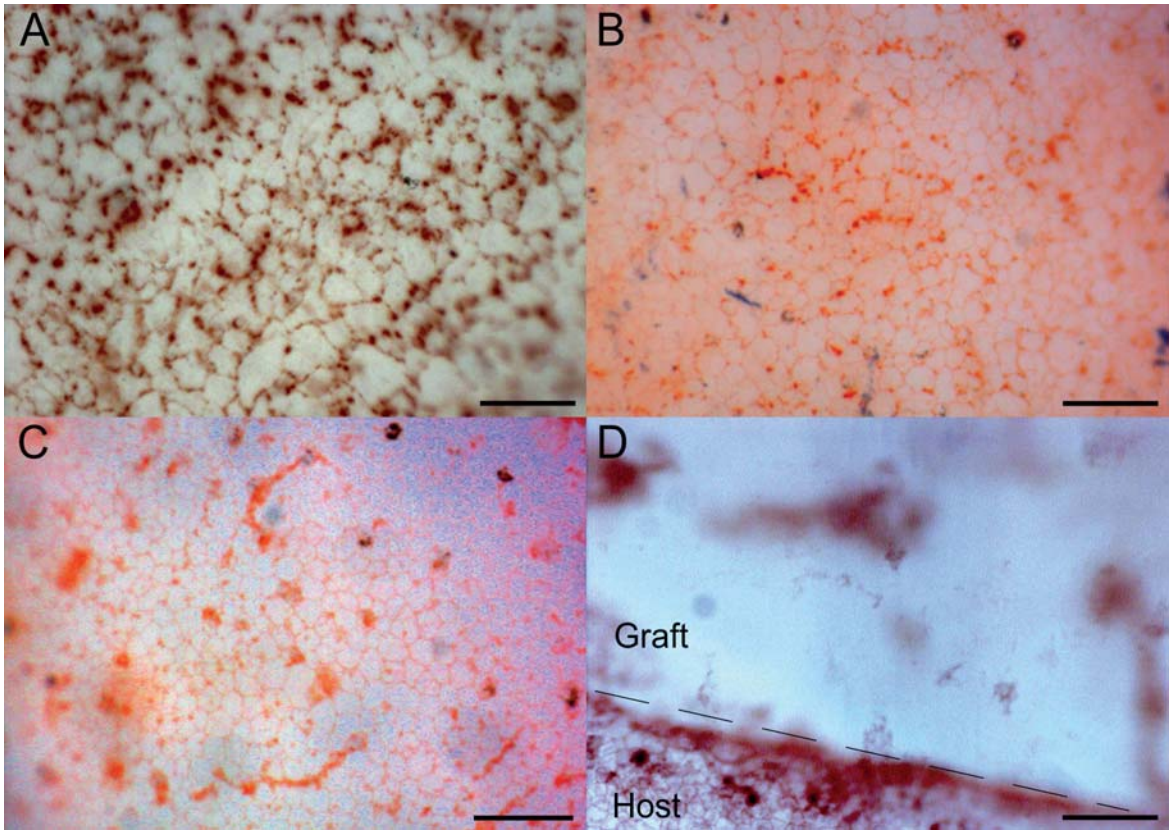

Figure 52: Alizarin red and trypan blue vital staining 7 days after transplantation. (A) TE-FECD living endothelial cells covering Descemet's Membrane (DM) surface. The cells have already developed a polygonal contour. Some inter-cellular spaces can be seen (dark spots) (Average± SD cell count was 942±445 cells/mm², average cell area was 1062 µm², CV was 42, 6-sided cells was 50%). (B) TE-normal endothelial cells seemed to be smaller

with fewer inter-cellular spaces (Average± SD cell count was 1645±336 cells/mm², average cell area was 608 µm², CV was 55, 6-sided cells was 55%). (C) Normal native endothelial cells were small, polygonal with no inter-cellular space (Average± SD cell count was 2198±168 cells/mm², average cell area was 456 µm², CV was 37, 6-sided cells was 53%). (D) In the carrier-only controls, no endothelial cells were seen. Scale bars: 100 µm.

Seven days after transplantation, the average endothelial cell count was 966 ± 165 cells/mm^2 for TE-FECD grafts (n=5), 1929 ± 200 cells/mm^2 for TE-normal controls (n=2) and 2371 ± 44 cells/mm^2 for the normal native control (n=1) (Table 5). Cell morphometric analyses could not be obtained in two TE-FECD grafts, i.e. in one case because of the presence of a fibrin membrane masking the endothelial cells, and in the other case because cells could not be seen due to stromal opacification (case of corneal necrosis described above). The Kruskal-Wallis test confirmed an overall significant difference in postoperative endothelial median cell counts between the three groups (p=0.036). Interestingly, a strong negative correlation was observed between postoperative cell densities and central graft thickness at day 7 (r=-0.914; p=0.004), all three groups being considered together.

As a corollary, TE-FECD endothelial cells were larger than TE-normal and normal native controls. The Kruskal-Wallis test confirmed a significant difference in median cell area between the three groups at day 7 (p=0.036). It was also interesting to notice that when the three groups were considered all together, cell area was positively correlated with graft thickness (r=0.785; p=0.037) and tented to be negatively correlated with graft transparency (r=-0.685; p=0.061) at day 7.

Seven days after transplantation, the tissue-engineered endothelial cells reached a pattern closer to hexagonality than that observed in culture. Hexagonality is a sign of stability (contrary to endothelial mosaic disorganization, pleomorphism (differences in cell shape) and polymegethism (differences in cell sizes)). In the TE-FECD group, 41 ± 5 % of endothelial cells were hexagonal, compared with 41 ± 4 % for the TE-normal and 51 ± 5 % for the normal native grafts (Table 5). The cell area coefficient of variation was 53 ± 10 %

for TE-FECD grafts, 51 ± 7 % for TE-normal grafts and 38 ± 3 % for the normal native graft.

	TE-FECD (n=5)	TE-normal (n=2)	Normal native (n=1)	Carrier only (n=4)
Cell count (cells/mm^2)	966 ± 165	1929 ± 200	2371 ± 44	0
Cell area (µm^2)	1110 ± 248	528 ± 56	422 ± 8	N/A
SD of cell area	594 ± 157	268 ± 41	161 ± 13	N/A
CV of cell area	53 ± 10	51 ± 7	38 ± 3	N/A
6-sided cells (%)	41 ± 5	41 ± 4	51 ± 5	N/A

Table 5: Endothelial cell counts and morphology. Average ± SEM are reported; N/A: not applicable.

6.6.4 Histopathology

6.6.4.1 Light Microscopy

The corneal endothelial cells formed a monolayer in TE-FECD grafts in 6 cases (Figure 53A). No guttae were seen in any cases. The stroma was acellular, except in the periphery of the grafts where the keratocytes had started to migrate from the host stroma to the peripheral stroma of the graft. A small number of inflammatory cells were present in the stroma of three grafts. The restored epithelium consisted of 2 to 6 layers of cells that were well attached to graft Bowman's membrane in 6 cases. In the case with corneal ulceration, the anterior stroma of the graft was massively infiltrated with inflammatory cells, with foci of anterior corneal necrosis. No microorganisms were identified.

By light microscopy, TE-normal and TE-FECD grafts were very similar. In TE-normal grafts, the endothelial monolayer was well attached to DM (Figure 53B), the host's keratocytes had started to migrate into the graft periphery, a few inflammatory cells were

observed in the stroma of one of the grafts, and the regenerated epithelium consisted of 2 to 4 layers of cells well attached to Bowman's membrane.

The native controls showed a regular endothelial monolayer well attached to the underlying DM (Figure 53C) and normal keratocytes present across the entire stroma. The epithelium consisted of 1 to 5 layers of cells well attached to Bowman's membrane.

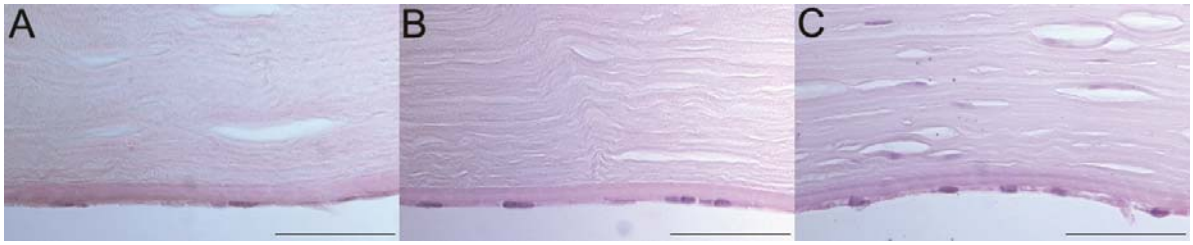

Figure 53: Histological observations 7 days after transplantation. (A) TE-FECD graft (B) TE-normal graft showing endothelium consisting of a continuous monolayer endothelial cells firmly adherent to DM. The stroma is acellular. (C) Normal endothelium of a native graft with native keratocytes in the stroma. Hematoxylin & eosin staining. Scale bars: 50 μm.

In the carrier-only controls, no endothelial cells were seen. The otherwise acellular graft stroma had been partially repopulated by the host keratocytes in the periphery. Numerous inflammatory cells were observed within the stroma of two grafts and the epithelium consisted of only 1 to 3 layers of cells attached to Bowman's membrane. No neovascularization was seen in any of the 15 grafts.

6.6.4.2 Transmission Electron Microscopy

Overall, post-mortem TEM confirmed the progression of tissue-engineered endothelial monolayer stabilization, with a maturation of the cell-cell attachments, fewer and narrower intercellular gaps and more developed tight junctions than routinely seen in culture prior to transplantation.[184]

In the TE-FECD grafts, the endothelium consisted of a 1.5 to 2.5 μm thick monolayer of cells (Figure 54A). Normal-appearing tight junctions were present (Figure 54B). The endothelial cells generally were intact except that intercellular attachments were not always complete. Occasional apical V-shape separations of the cells (Figure 54C) or a

mid-height intercellular focal gaps (Figure 54D) were present laterally. The endothelial nuclei were unremarkable (Figure 54A, C, E). Numerous mitochondria were present (Figure 54F). Rough endoplasmic reticulum (RER) was generally prominent (Figure 54G). Vacuoles were present in some cells, as well as electron dense bodies consistent with lyzosomes (Figure 54H). A focal zone of dense intra-cytoplasmic filaments was seen in one case (Figure 54I). No pigment granules were present in any of the cases. Cytoplasmic processes were observed projecting either towards DM (Figure 54J), towards the anterior chamber (microvilli) (Figure 54E) or towards a neighboring cell (Figure 54D - arrows). The endothelium was attached to DM in all cases. Subendothelial deposition of loose fibrillar material was a consistent finding (Figure 54K). The carrier's DM consisted in two normal anterior and posterior layers in all cases. No guttae were found in any of the cases. A few striated bodies (with a periodicity of 110 nm) were seen in the carrier's DM of one TE-FECD graft.

No apparently viable keratocytes were observed in TEM specimens, which is not surprising as TEM samples were cut from the center of the grafts. Non-viable keratocyte material was observed across the entire stroma (Figure 54L), as remnants of the devitalization process. The space between stromal collagen fibers varied from 20 to 40 nm (Figure 55A).

In the corneal ulceration case, the stroma was massively infiltrated with polymorphonuclear leukocytes and monocytes. Scattered degenerated endothelial cells were seen on the posterior surface of the graft.

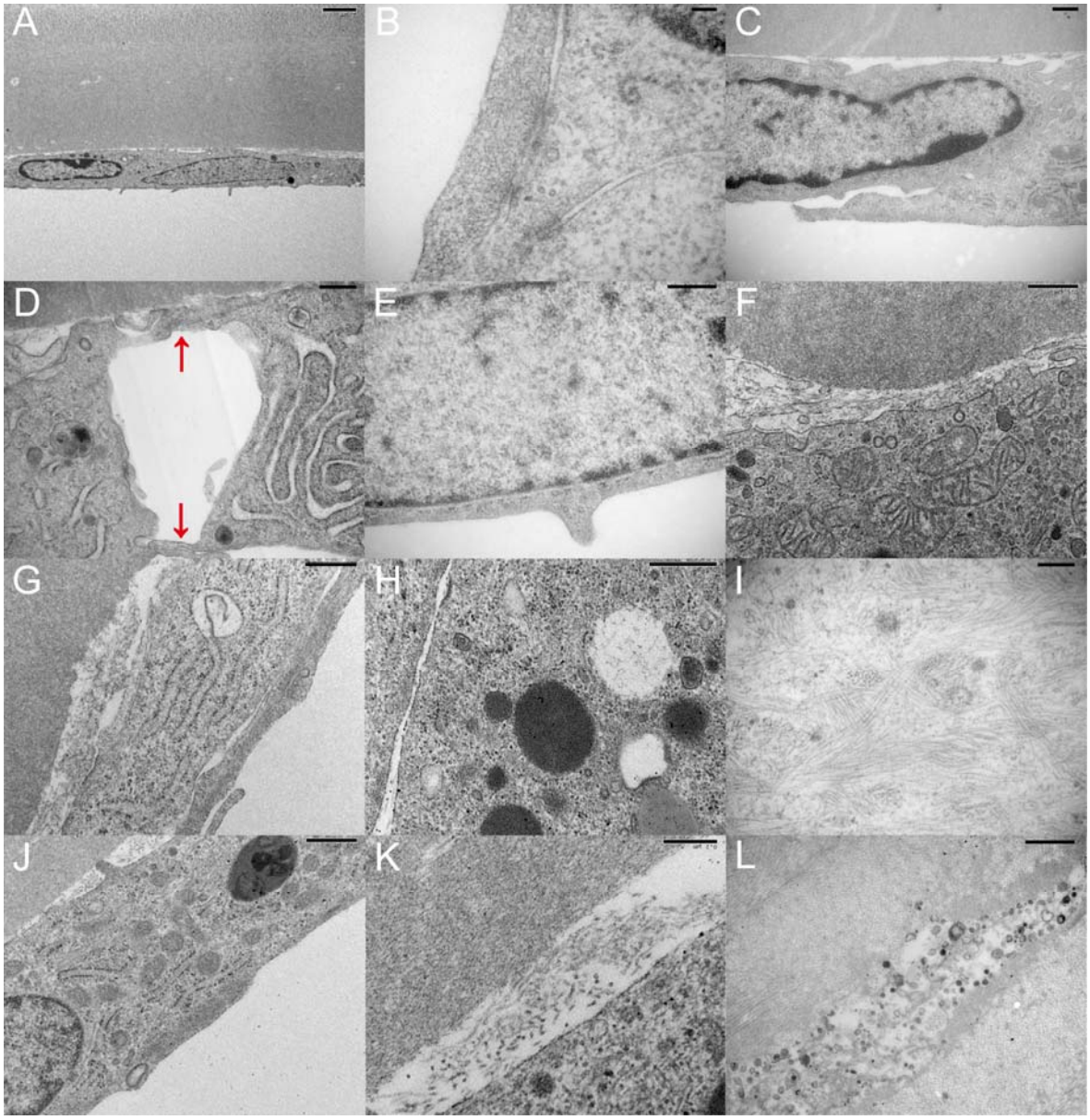

Figure 54: Transmission electron microscopy. Ultrastructure of the TE-FECD grafts 7 days after transplantation. (A) Continuous monolayer of endothelial cells with intact nuclei. Normal DM. No guttata were present. (B) Complete cell-cell attachment showing tight junctions. (C) Incomplete apical cell-cell attachment. (D) Incomplete cell-cell attachment with intercellular residual gap. Arrows indicate basal and apical cytoplasmic projections attaching two adjacent cells. (E) Microvillus oriented toward the anterior chamber. (F) Normal appearing mitochondria. (G) Prominent RER with electron dense inclusion in Golgi apparatus. (H) Vacuoles and electron dense bodies consistent with lyzosomes. (I)

Intracytoplasmic filaments. (J) Cytoplasmic processes projecting towards DM. (K) Deposits of subendothelial fibrillar material. (L) Residual keratocyte debris in the devitalized stroma. Scale bars: (A) 2 μm, (B) 0.1 μm, (C-H, J) 0.5 μm, (I, K) 0.2 μm, (L) 1 μm.

In the TE-normal controls, the endothelium consisted of a 2.5 to 3.5 μm thick monolayer of cells (Figure 56A). The attachment between adjacent endothelial cells was generally intact (Figure 56B). Gaps between endothelial cells were occasionally seen, and when present, these gaps were less prominent than in the TE-FECD grafts. The endothelium was well attached to DM in all cases. Small amounts of subendothelial loose fibrillar material were observed in focal areas in one case. Small cytoplasmic processes were observed in one case projecting towards DM (Figure 56C). Nuclei were intact. Vacuoles were seen, as well as electron dense bodies consistent with lyzosomes. No pigment granules were seen. Mitochondria were unremarkable. RER was prominent (Figure 56B). No intra-cellular filaments were seen. DM consisting of normal anterior and posterior layers was present in all the cases. No guttae were found. Residual non-viable keratocytes were observed in the stroma and the mean space between stromal collagen fibers was 25 nm (Figure 55B).

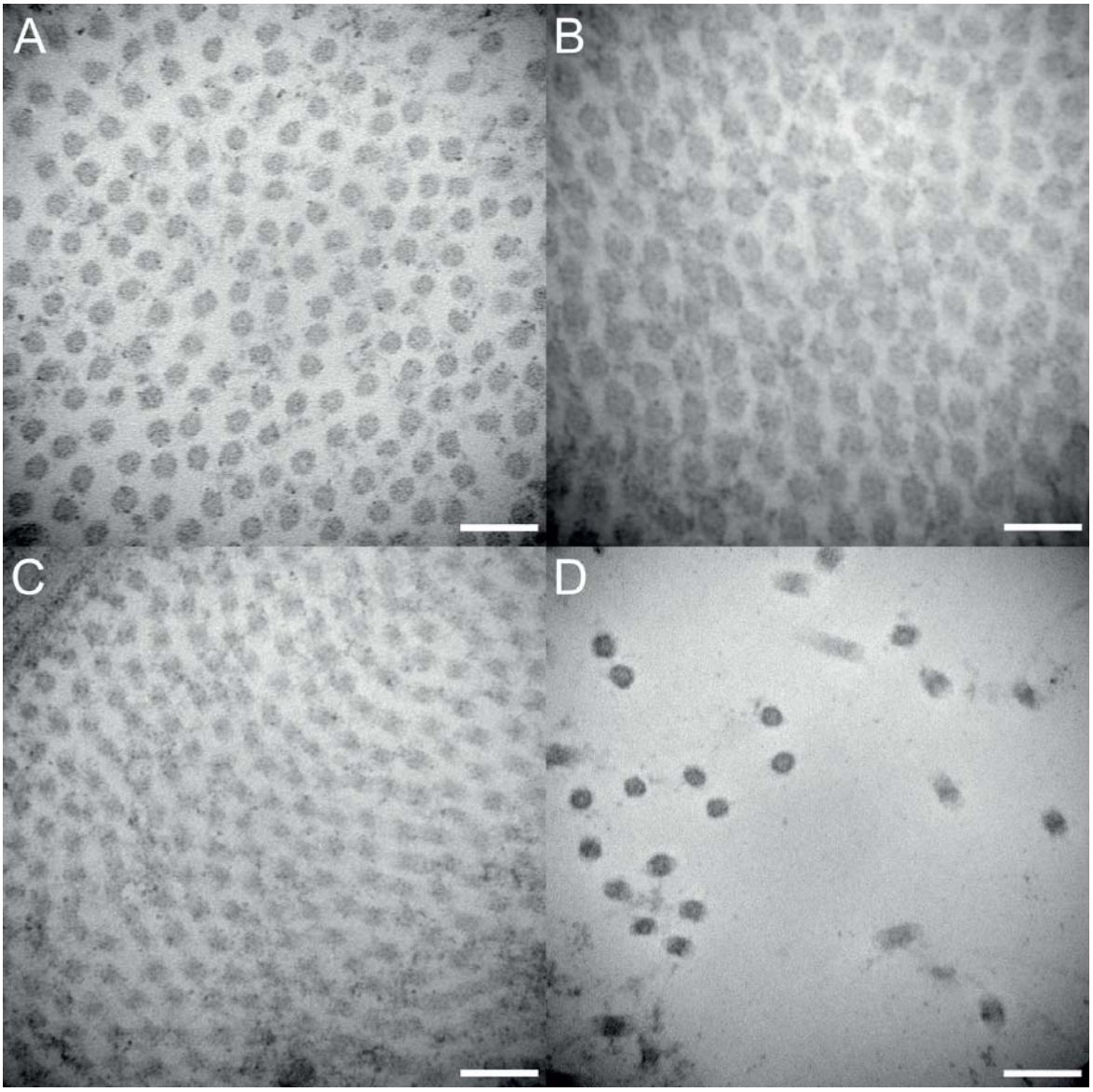

Figure 55: Transmission electron microscopy. Stromal collagen fibers arrangement 7 days after transplantation. (A) TE-FECD graft showing a slightly irregular arrangement of the stromal collagen fibers. TE-normal graft (B) and normal native graft (C) showing a regular arrangement. (D) Carrier-only (without endothelial cells) grafts showing very irregular arrangement due to severe stromal edema. Scale bars: 100 nm.

In the normal native controls, the endothelium consisted of a 3.5 µm-thick monolayer of cells (Figure 56D). Adjacent endothelial cells were fully attached to each other and to underlying DM (Figure 56E). Cell nuclei, mitochondria and RER appeared normal (Figure 56F). Vacuoles and lyzosomes were observed. No cytoplasmic processes, pigment granules, intra-cellular filaments, or guttae were observed. DM consisted of normal anterior and posterior layers. Normal keratocytes were present throughout the stroma. The mean space between stromal collagen fibers was 15 nm (Figure 55C).

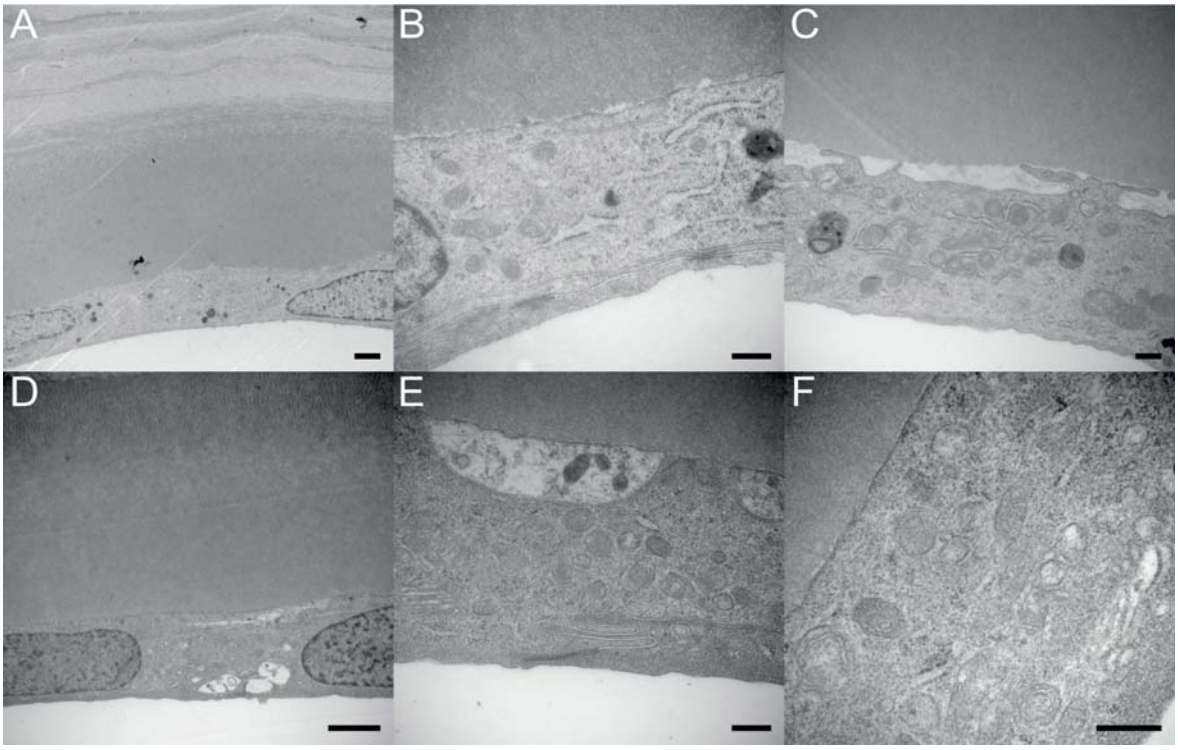

Figure 56: Transmission electron microscopy. Ultrastructure of the TE-normal (A-C) and normal native (D-F) grafts 7 days after transplantation. (A) Continuous monolayer of endothelial cells with intact nuclei. (B-C) Complete cell-cell attachment with normal tight junctions. Prominent RER, normal appearing mitochondria, electron dense bodies consistent with lyzosomes, and cytoplasmic processes. Little subendothelial fibrillar material deposition. (D) Continuous monolayer of endothelial cells with normal nuclei. (E) Complete cell-cell attachment with mature tight junctions. Large vacuole-filled with cell debris. (F) Normal appearing mitochondria and RER. Absence of cytoplasmic processes

and subendothelial fibrillar material deposition. Scale bars: (A, D) 2 µm, (B-C, E-F) 0.5 µm.

TEM confirmed the absence of endothelial cells in the carrier-only controls. The DM was normal, without guttae. Residual non-viable keratocytes were observed in the stroma and the space between stromal collagen fibers was much larger, varying between 50 and 100 nm (Figure 55D).

6.6.4.3 Immunofluorescence

Immunofluorescence detection of the sodium-potassium pump Na^+/K^+-ATPase α1 and the Na^+/HCO_3^- cotransporter revealed the presence of these proteins in all three types of endothelialized grafts. However, staining was less intense in TE grafts than in the normal native grafts (Figure 57).

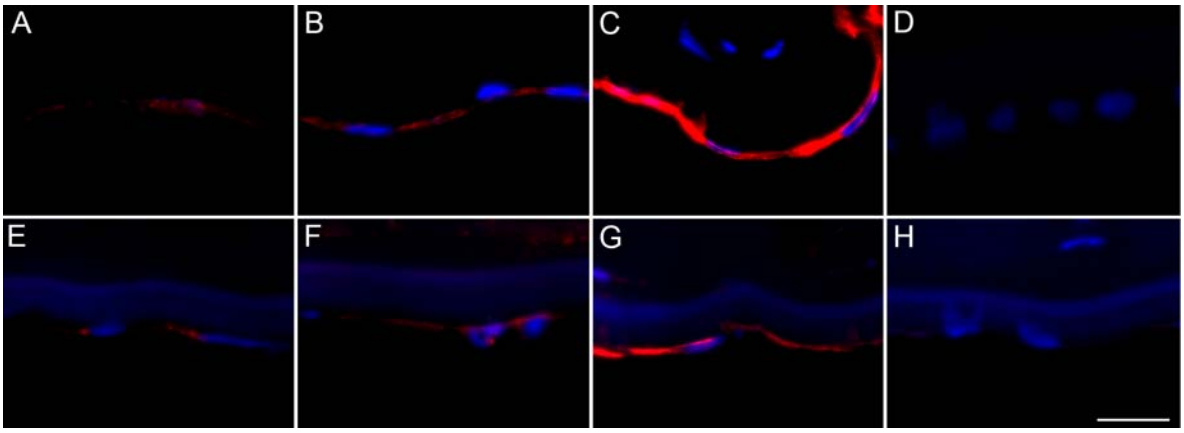

Figure 57: Immunofluorescence labeling of function-related proteins. Immunofluorescence detection of the sodium-potassium pump Na^+/K^+-ATPase α1 (A-D) and the Na^+/HCO_3^- cotransporter (E-H) in a TE-FECD graft (A, E), a TE-normal graft (B, F), a normal native graft (C, G), and in negative controls (incubated with secondary antibody only) (D, H). Cell nuclei were counterstained with Hoechst (blue). Scale bar: 20 µm.

6.7 DISCUSSION

To the best of our knowledge, this study presents the first successful living model for FECD generated using untransformed human cells. We also demonstrated the first evidence that the sick endothelial cells of clinically decompensated FECD corneas, when cultured and seeded on a devitalized stromal carrier, can recover active pump function and restore and maintain corneal transparency for 7 days after transplantation in the living feline eye.

6.7.1 Partial rehabilitation

Overall, the tissue-engineered FECD endothelium seemed to perform better in the cat eye than in the patient's eye. TE-FECD grafts progressively became thinner and clearer. Rare trypan blue staining of the nuclei, TEM observation of a well structured TE-FECD endothelial monolayer, with developed tight junction complexes, normal mitochondria, enlarged RER (sign of active protein production), lyzosomes and vacuoles, as well as the presence of endothelial pump sites observed by immunofluorescence, were all signs of healthy cellular activity.

Explanations for this partial rehabilitation can only be hypothesized, since not specifically investigated in the present study. Proposed hypotheses include the beneficial effect of the culture conditions and/or the natural selection of the healthiest cells in culture. Removal of the diseased thickened DM may also have a played a role in the recovery of these endothelial cells.

Partial rehabilitation of these end stage FECD endothelial cells and the demonstration of their *in vivo* functionality opens the door to an entirely new horizon.

6.7.2 A clinical performance suggestive of early FECD

However, despite this functional improvement, the TE-FECD corneas still did not perform normally in vivo and these corneas rapidly developed signs of mild to moderate Fuchs dystrophy. While considerably clearer and thinner than the negative controls without

endothelium, the TE-FECD grafts remained thicker than the TE-normal and the native controls. Endothelial cell density was also lower in TE-FECD grafts.

6.7.3 TEM signs observed in native and tissue-engineered FECD corneas

Several of the TEM signs typically reported in native FECD corneas were observed in this study. Subendothelial deposition of a layer of loose fibrillar material was systematically observed in TE-FECD grafts. Some subendothelial amorphous or fibrillary material was also seen in one of the TE-normal grafts, but in focal areas only and in smaller amounts than in the TE-FECD grafts. This excessive basement membrane like material production may reflect the known predisposition of FECD cells for excessive production of DM material. An abnormal thickening of DM is characteristic of native FECD, the normal anterior banded (fetal) and nonbanded layers being typically lined by two abnormal layers consisting in a posterior banded layer and a fibrillar layer.[64, 66, 69, 71]

Incomplete closure of the cell-cell attachments, fewer and shorter tight junctions, residual gaps between adjacent cells, and an overall lower cell density were observed in the TE-FECD grafts. This may suggest that FECD endothelial cells were more susceptible to death, the remaining cells spreading to reach the next available cell in order to cover the area left by dying cells. This process would be very similar to that described in native FECD, where degenerating endothelial cells loosen their junctional complexes and disintegrate, leaving large intercellular gaps.[66]

Intracytoplasmic filaments have been described by Iwamoto and DeVoe as a sign of transformation of the FECD endothelial cell into fibroblast-like cells,[66] but they can also be occasionally seen in the normal endothelium.[189] In our TEM specimens, endothelial intracytoplasmic filaments were only seen once in a TE-FECD graft.

The pigment granules[66, 68] seen in the patients' specimens were not recovered in any of the engineered endothelia. Pigment granules have been reported to originate from the iris pigmented epithelium and to normally be phagocyted by the corneal endothelial cells.[137] The absence of pigment in the tissue-engineered endothelium is not surprising in the absence of an active source (such as the iris pigmented epithelium). The pigment granules

seen in the DSAEK specimens were probably either rinsed off or eliminated with the loss of the most dysfunctional cells.

Striated bodies of various periodicity, size and distribution are typically seen in the DM abnormal posterior banded layer and guttae of native corneas with FECD.[30, 40, 69-71] In this short-term study, no striated bodies were observed in the new DM-like material secreted by the engineered endothelium. No guttae formation were observed in this study, which was also compatible with the short duration of the follow-up.

In summary, in the absence of a single pathognomonic sign, the diagnosis of FECD is usually based on a combination of signs typical of the disease. In the present study, all of the TE-FECD cells carried the genetic signature of the patient from whom they were harvested, and in all cases, these patients had a confirmed diagnosis of end-stage clinical FECD. Once transplanted back to a native living environment, this TE-FECD endothelium rapidly developed a combination of signs typical of FECD, including low endothelial cell counts, corneal edema, incomplete cell-cell attachments, and the accelerated and excessive production of DM-like subendothelial material. After only 7 days in the living eye, this short-term model, which carries the genetic background of FECD, gathered the key descriptors for early FECD.

6.7.4 Characteristics of the proposed FECD model

The FECD model we describe offers several significant advantages: **(1)** It is a living model; **(2)** it offers clinical and TEM quantifiable parameters for the characterization of TE-FECD endothelial function and structure. Clinical parameters include corneal transparency and corneal thickness (corneal transparency is still considered as the only real proof of endothelial functionality). TEM and histology parameters include a subendothelial layer of loose fibrillar material, which here appears to be the most specific sign of FECD, and less specific signs such as a decreased endothelial cell density, incomplete cell-cell attachment, and intracytoplasmic filaments. These parameters are very similar to those used to assess severity of the disease in native FECD; **(3)** it is polyvalent in that it is not limited to one specific mutation or cell line. In this paper, no selection was made in the choice of

FECD patients; **(4)** it allows for the in vivo selective investigation of FECD endothelial cell behavior in the absence of sick DM and guttae; **(5)** it allows for correlations between the FECD endothelial cells behavior in cell culture, in tissue culture, and *in vivo*, which can be very useful for the translational development of new therapies; and finally, **(6)** it was developed in the feline eye, which is functionally similar to the human eye in several aspects. Feline corneal endothelial cells do not replicate *in vivo*,[138] contrary to species such as the rat[153] or rabbit,[138, 140] and the feline endothelium repairs by cell spreading and migration,[138] as in humans.[156] Endothelial cell density [158, 160] and corneal thickness values are comparable to human values.[163, 165] The large corneal diameter of the cat cornea (15.5-18 mm)[160, 167] permits full size grafts, using the same instrumentation and techniques as for human subjects. These large grafts also yield large amounts of tissue for postmortem analyses. And finally, short term human-to-cat corneal xenografts are well tolerated.[146, 169]

Additional improvements to this model could include a longer follow-up. A 7 day follow-up period was chosen here to avoid xenograft rejection. A longer follow-up would require immunosuppression.

6.7.5 Potential applications of this model

The living experimental model for FECD we describe suggests many novel research opportunities with a goal of better understanding of FECD cell dysfunction, molecular pathophysiology and apoptosis. It offers the opportunity to test new therapeutic approaches at different stages of the disease.

In addition to the development of a new living model for FECD, this study confirms the regenerative potential of FECD corneal endothelial cells in culture, making conceivable surgical therapeutic approaches in which the diseased corneal endothelial cells of Fuchs patients would be biopsied, cultured, treated, and used to engineer a healthy endothelium to be transplanted back to the patient (autograft). This would eliminate the risk of allograft rejection and constitute an exciting additional step toward a better management of this endothelial dystrophy.

In conclusion, we demonstrated herein the first evidence that the sick endothelial cells of clinically decompensated FECD corneas still retain proliferative capacity, allowing tissue engineering of a functional endothelium without transfection. Whether permitted by the favorable effect of the culture conditions or by the natural selection of the healthiest cells in culture, rehabilitation of end stage FECD endothelial cells and the demonstration of their *in vivo* functionality opens the door to an entirely new horizon of medical and surgical therapies.

Acknowledgements: The authors would like to thank Patricia-Ann Laughrea for obtaining FECD endothelial specimens; Myriam Bareille, Danièle Caron, Patrick Carrier, André Deveault, Angèle Halley, Vivianne Leduc, Catherine Mauger Labelle, Aristide Pusterla, Olivier Rochette-Drouin and the HMR-Rosemont and CUO operating room nurses for their technical assistance; Élodie Samson for the statistical analysis consultation; the LOEX research assistants for the histology preparations, Fayrouz Barkat for histology photography assistance; and Steve Breault for the electron microscopy preparations and photography assistance.

7 Chapter VII:

General Discussion, Conclusions and Perspectives

7.1 General Discussion and Conclusions

This thesis shows the first evidence of the feasibility of tissue engineering a corneal endothelium using endothelial cells from patients with Fuchs endothelial corneal dystrophy (FECD). These FECD tissue-engineered corneas were similar to tissue-engineered corneas using healthy endothelial cells *in vitro* at all studied levels (morphology, cell density, ultrastructure and protein expression). In fact, we could not differentiate the TE-FECD corneas from the TE-normal ones in aspect. The beneficial effect of the culture conditions, the natural selection of the healthiest cells in culture and/or the removal of the diseased thickened DM and guttae could explain the observed "normalization" of the TE-FECD corneas.

To the best of my knowledge, this is the first tissue model of FECD. Only few *in vitro* cellular models have been reported for FECD.[183, 190] He et al.[183] cultured FECD endothelial cells transduced with the human papilloma virus type 16 genes E6/E7 to expand their lifespan. Transduced FECD endothelial cells were similar to healthy in cell proliferation, morphology and two-dimensional gel protein electrophoretic patterns. The *in vitro* cellular model of He was recently used to study FECD pathogenesis. FECD endothelial cells were found to be more susceptible to oxidative DNA damage and oxidative-stress-induced apoptosis than normal.[16] Kelliher et al.[190] described a cellular model for FECD using Chinese hamster ovary cells transfected with collagen VIII α2 mutations resulting in abnormal intracellular accumulation of collagen VIII. This ovary cellular model represents collagen VIII α2 mutations rather than FECD. Potential risks inherent to cell lines established by transfection, however, include latent potency for tumorigenicity, genetic instability and abnormal phenotypes. The transfer of genes into a cell modulates the cell's protein expression, which can affect cell behavior. This may influence the effectiveness of studies on disease pathogenesis and may interfere with the treatment of these cells. The tissue model presented in this thesis is representative of any kind of FECD and is not restricted to any mutation or cell line.

We used a devitalized human stroma as a carrier for corneal tissue engineering. The advantages of this carrier are multiple. Native human corneas unsuitable for transplantation are frequently available in eye banks. Devitalization method is not complicated. Biocompatibility, physiological curvature, preservation of stromal collagen fibers arrangement and preservation of optical transparency property of the devitalized carrier have been previously demonstrated.[29] The devitalized stromal carriers would be technically compatible with any corneal transplantation technique that is used for the treatment of endotheliopathies (PKP, DSAEK or DMEK). Besides, devitalized stromal carriers (free of living cells) seeded with autologous tissue-engineered endothelial cells are not expected to stimulate an immune reaction in the host.[191] However, assessing mechanical compatibility is still needed. It's important to demonstrate that this carrier is capable of providing the strength needed to help maintaining the shape of the cornea under the pressure of aqueous humor over time.

Over the past 30 years, scientists made a remarkable progress of optimization and development of corneal endothelial cell isolation techniques and culture media.[106] However, not all endothelial specimens initiate culture and if they do, not all of them have typical endothelial morphology in culture.[25, 26, 30] In the presented studies, only cultured endothelial cells with endothelial-like morphology (polygonal to slightly elongated shapes) were used for corneal tissue engineering. Developments in culture medium are still needed. Ideally, all biopsied endothelial specimens should initiate a culture regardless of the patient's age, his chronic illness or his endothelial cell illness stage. Furthermore, all endothelial cells should have the typical endothelial cell morphology in culture. Recently, a serum free culture medium (SFM) was showed to protect endothelial cells from apoptosis and necrotic cell death.[192] Rho-associated kinase (ROCK) inhibitor (Y-27632) was also showed to promote adhesion, increase proliferation and inhibit apoptosis of cultured endothelial cells.[193, 194]

This thesis shows the first report of the DSAEK procedure in the feline model. Although the DSAEK procedure is currently the treatment of choice for endotheliopathies in humans,[20, 195] it gave inconsistent clinical results in the feline model. The limitations of

DSAEK in my study were mostly related to technical difficulties and rapid fibrin formation in the feline model. Technical difficulties arise from the fact that cats have a large cornea, a deep anterior chamber, a DM that is attached firmly to the stroma and rapid fibrin formation during and after surgery. Using customized surgical tools designed for cats and mechanical scraping of the endothelium only leaving DM in place could solve part of the problem. Fibrin formation, however, is still a challenge. In our hands, fibrin strands attached to the graft once inserted inside the feline eye, acting like glue, making intraocular manoeuvres difficult to perform, which in turn caused additional trauma to the transplanted endothelium. rtPA injection helped partially in digesting the strands. After surgery, fibrin persisted to form strands targeting the naked stroma of the graft. Similar fibrin formation was also reported by Mohay[120] and Bahn[186] in the feline model after corneal transplantation. Honda et al.[129] reported DSAEK in the rabbit model. The clinical outcome, however, was suboptimal (see section 5.4.4). Koizumi et al.[142] recently reported a successful DSAEK in the monkey model. The clarity of the cornea was recovered by the second week after DSAEK. Minimal steroid treatment (ointment applied once daily for one month) was required. The monkey primitive model seems to have less inflammatory reaction than the feline model.

This thesis presents the first successful *in vivo* model for FECD using tissue engineering. The TE-FECD corneas, that were tissue-engineered using endothelial cells from patients with clinical end-stage FECD, recovered an active pump function and restored and maintained corneal transparency for 7 days after transplantation in the living feline eye. This successful clinical performance suggests a potential role of tissue engineering for FECD cell rehabilitation. The TE-FECD corneas, however, showed a clinical performance suggestive of early FECD. While considerably clearer and thinner than the negative controls without endothelium, the tissue-engineered FECD grafts remained thicker than the tissue-engineered normal and the native normal controls. Endothelial cell density was also lower in the tissue-engineered FECD grafts. After only seven days of transplantation, there was a continuous deposition of loose fibrillar material under the endothelium in the tissue engineered FECD grafts which reflected the velocity of FECD endothelial cells in producing ECM, i.e. Descemet's membrane.

To the best of my knowledge, only one *in vivo* experimental model has been reported for FECD.[182] A collagen VIII α2 Q455K knock-in mouse model has recently been reported by Jun et al.[182] This mutation caused a decrease in endothelial cell density, formation of guttae, dilated RER, unfolded protein response and apoptosis. Using this model, Matthaei et al.[196] recently demonstrated that p21 is upregulated in FECD suggesting a premature senescence in FECD. This model, however, represents a rare type of early onset FECD, while our model is not limited to any mutation (see section 6.8.4).

The postoperative follow-up period of our *in vivo* model was short. Following the animals for more than 7 days after surgery, however, is possible. It would necessitate immunosuppression, which was not possible with our set-up. Systemic immunosuppression requires special animal facilities, isolation, positive pressure rooms, Antibody Defined animals free of pathogens, and dedicated instrumentation. Shortness of follow-up could also be considered as an advantage. Within a period of only a few weeks, our model is combining the advantages of both *in vitro* and *in vivo* experimentation. Cell and tissue culture offers an initial period during which cell growth can be modulated within the controlled environment of the laboratory, followed by transplantation in the living eye, which still represents the only reliable test for corneal endothelial functionality.

7.2 Perspectives

To the best of my knowledge, this thesis shows the first successful *in vitro* and *in vivo* models for FECD using tissue engineering. This model opens the way to entirely new research perspectives for a better understanding of FECD cell dysfunction, pathophysiology and apoptosis. It offers the opportunity of testing new drugs at different stages of the disease. These could include, for instance, anti-oxidants against DNA oxidative damage;[13, 15, 16] Rho-associated kinase (ROCK) inhibitor (Y-27632) to promote adhesion, increase proliferation and inhibit apoptosis of cultured endothelial cells and to promote endothelial wound healing;[142, 193, 194] and gene therapy that could induce endothelial cell proliferation and/or enhanced survival.[197, 198]

In addition to the development of a new living model for FECD, this thesis confirms the regenerative potential of FECD endothelial cells in culture, making conceivable surgical

therapeutic approaches in which the diseased endothelial cells of Fuchs patients would be biopsied, cultured, treated, and used to engineer a healthy endothelium to be transplanted back in the patient (autograft). This would eliminate the risk of allograft rejection, reduce requirement for postoperative steroid therapy with its associated complications,[191] and constitute an exciting additional step toward a better management of this common, painful and blinding disease. I believe that tissue engineering has the potential to be a useful tool in the future management of corneal endothelial diseases.

References

1. Fuchs E. Dystrophia epithelialis corneae. *Albrecht Von Graefes Arch Klin Exp Ophthalmol* 1910;76:478-508.
2. Waring GO, 3rd, Bourne WM, Edelhauser HF, Kenyon KR. The corneal endothelium. Normal and pathologic structure and function. *Ophthalmology* 1982;89:531-590.
3. Adamis AP, Filatov V, Tripathi BJ, Tripathi RC. Fuchs' endothelial dystrophy of the cornea. *Surv Ophthalmol* 1993;38:149-168.
4. Waring GO, 3rd, Rodrigues MM, Laibson PR. Corneal dystrophies. II. Endothelial dystrophies. *Surv Ophthalmol* 1978;23:147-168.
5. Wilson SE, Bourne WM. Fuchs' dystrophy. *Cornea* 1988;7:2-18.
6. Elhalis H, Azizi B, Jurkunas UV. Fuchs endothelial corneal dystrophy. *Ocul Surf* 2010;8:173-184.
7. Burns RR, Bourne WM, Brubaker RF. Endothelial function in patients with cornea guttata. *Invest Ophthalmol Vis Sci* 1981;20:77-85.
8. Geroski DH, Matsuda M, Yee RW, Edelhauser HF. Pump function of the human corneal endothelium. Effects of age and cornea guttata. *Ophthalmology* 1985;92:759-763.
9. Wilson SE, Bourne WM, O'Brien PC, Brubaker RF. Endothelial function and aqueous humor flow rate in patients with Fuchs' dystrophy. *Am J Ophthalmol* 1988;106:270-278.
10. McCartney MD, Robertson DP, Wood TO, McLaughlin BJ. ATPase pump site density in human dysfunctional corneal endothelium. *Invest Ophthalmol Vis Sci* 1987;28:1955-1962.
11. McCartney MD, Wood TO, McLaughlin BJ. Immunohistochemical localization of ATPase in human dysfunctional corneal endothelium. *Curr Eye Res* 1987;6:1479-1486.
12. McCartney MD, Wood TO, McLaughlin BJ. Moderate Fuchs' endothelial dystrophy ATPase pump site density. *Invest Ophthalmol Vis Sci* 1989;30:1560-1564.
13. Jurkunas UV, Bitar MS, Funaki T, Azizi B. Evidence of oxidative stress in the pathogenesis of Fuchs endothelial corneal dystrophy. *Am J Pathol* 2010;177:2278-2289.
14. Jurkunas UV, Bitar MS, Rawe I, Harris DL, Colby K, Joyce NC. Increased clusterin expression in Fuchs' endothelial dystrophy. *Invest Ophthalmol Vis Sci* 2008;49:2946-2955.
15. Jurkunas UV, Rawe I, Bitar MS, et al. Decreased expression of peroxiredoxins in Fuchs' endothelial dystrophy. *Invest Ophthalmol Vis Sci* 2008;49:2956-2963.
16. Azizi B, Ziaei A, Fuchsluger T, Schmedt T, Chen Y, Jurkunas UV. p53-Regulated Increase in Oxidative-Stress-Induced Apoptosis in Fuchs Endothelial Corneal Dystrophy: A Native Tissue Model. *Invest Ophthalmol Vis Sci* 2011;52:9291-9297.

17. Engler C, Kelliher C, Spitze AR, Speck CL, Eberhart CG, Jun AS. Unfolded protein response in fuchs endothelial corneal dystrophy: a unifying pathogenic pathway? *Am J Ophthalmol* 2010;149:194-202 e192.
18. Borderie VM, Baudrimont M, Vallee A, Ereau TL, Gray F, Laroche L. Corneal endothelial cell apoptosis in patients with Fuchs' dystrophy. *Invest Ophthalmol Vis Sci* 2000;41:2501-2505.
19. EBAA. 2010 Eye Banking Statistical Report. Washington, DC; 2011:18.
20. Price MO, Gorovoy M, Benetz BA, et al. Descemet's stripping automated endothelial keratoplasty outcomes compared with penetrating keratoplasty from the Cornea Donor Study. *Ophthalmology* 2010;117:438-444.
21. Lee WB, Jacobs DS, Musch DC, Kaufman SC, Reinhart WJ, Shtein RM. Descemet's stripping endothelial keratoplasty: safety and outcomes: a report by the American Academy of Ophthalmology. *Ophthalmology* 2009;116:1818-1830.
22. Thompson RW, Jr., Price MO, Bowers PJ, Price FW, Jr. Long-term graft survival after penetrating keratoplasty. *Ophthalmology* 2003;110:1396-1402.
23. Joyce NC, Meklir B, Joyce SJ, Zieske JD. Cell cycle protein expression and proliferative status in human corneal cells. *Invest Ophthalmol Vis Sci* 1996;37:645-655.
24. Joyce NC. Proliferative capacity of the corneal endothelium. *Prog Retin Eye Res* 2003;22:359-389.
25. Joyce NC, Zhu CC. Human corneal endothelial cell proliferation: potential for use in regenerative medicine. *Cornea* 2004;23:S8-S19.
26. Zhu C, Joyce NC. Proliferative response of corneal endothelial cells from young and older donors. *Invest Ophthalmol Vis Sci* 2004;45:1743-1751.
27. Proulx S, Audet C, Uwamaliya J, et al. Tissue engineering of feline corneal endothelium using a devitalized human cornea as carrier. *Tissue Eng Part A* 2009;15:1709-1718.
28. Proulx S, d'Arc Uwamaliya J, Carrier P, et al. Reconstruction of a human cornea by the self-assembly approach of tissue engineering using the three native cell types. *Mol Vis* 2010;16:2192-2201.
29. Proulx S, Bensaoula T, Nada O, et al. Transplantation of a tissue-engineered corneal endothelium reconstructed on a devitalized carrier in the feline model. *Invest Ophthalmol Vis Sci* 2009;50:2686-2694.
30. Zaniolo K, Bostan C, Rochette Drouin O, et al. Culture of human corneal endothelial cells isolated from corneas with Fuchs endothelial corneal dystrophy. *Exp Eye Res* 2012;94:22-31.
31. DelMonte DW, Kim T. Anatomy and physiology of the cornea. *J Cataract Refract Surg* 2011;37:588-598.
32. Sanchis-Gimeno JA, Sanchez-Zuriaga D, Martinez-Soriano F. White-to-white corneal diameter, pupil diameter, central corneal thickness and thinnest corneal thickness values of emmetropic subjects. *Surg Radiol Anat* 2012;34:167-170.
33. Hanna C, Bicknell DS, O'Brien JE. Cell turnover in the adult human eye. *Arch Ophthalmol* 1961;65:695-698.

34. Li W, Hayashida Y, Chen YT, Tseng SC. Niche regulation of corneal epithelial stem cells at the limbus. *Cell Res* 2007;17:26-36.
35. Wiley L, SundarRaj N, Sun TT, Thoft RA. Regional heterogeneity in human corneal and limbal epithelia: an immunohistochemical evaluation. *Invest Ophthalmol Vis Sci* 1991;32:594-602.
36. Boote C, Dennis S, Newton RH, Puri H, Meek KM. Collagen fibrils appear more closely packed in the prepupillary cornea: optical and biomechanical implications. *Invest Ophthalmol Vis Sci* 2003;44:2941-2948.
37. Maurice DM. The transparency of the corneal stroma. *Vision Res* 1970;10:107-108.
38. Meek KM, Boote C. The organization of collagen in the corneal stroma. *Exp Eye Res* 2004;78:503-512.
39. Jester JV, Moller-Pedersen T, Huang J, et al. The cellular basis of corneal transparency: evidence for 'corneal crystallins'. *J Cell Sci* 1999;112 (Pt 5):613-622.
40. Gottsch JD, Zhang C, Sundin OH, Bell WR, Stark WJ, Green WR. Fuchs corneal dystrophy: aberrant collagen distribution in an L450W mutant of the COL8A2 gene. *Invest Ophthalmol Vis Sci* 2005;46:4504-4511.
41. Johnson DH, Bourne WM, Campbell RJ. The ultrastructure of Descemet's membrane. I. Changes with age in normal corneas. *Arch Ophthalmol* 1982;100:1942-1947.
42. Kabosova A, Azar DT, Bannikov GA, et al. Compositional differences between infant and adult human corneal basement membranes. *Invest Ophthalmol Vis Sci* 2007;48:4989-4999.
43. Bourne WM. Corneal endothelium--past, present, and future. *Eye Contact Lens* 2010;36:310-314.
44. Yee RW, Matsuda M, Schultz RO, Edelhauser HF. Changes in the normal corneal endothelial cellular pattern as a function of age. *Curr Eye Res* 1985;4:671-678.
45. Bourne WM, Nelson LR, Hodge DO. Central corneal endothelial cell changes over a ten-year period. *Invest Ophthalmol Vis Sci* 1997;38:779-782.
46. Verkman AS, Ruiz-Ederra J, Levin MH. Functions of aquaporins in the eye. *Prog Retin Eye Res* 2008;27:420-433.
47. Jun AS. One hundred years of Fuchs' dystrophy. *Ophthalmology* 2010;117:859-860 e814.
48. EBAA. *2011 Eye Banking Statistical Report*. Washington D.C; 2012:1-70.
49. Borboli S, Colby K. Mechanisms of disease: Fuchs' endothelial dystrophy. *Ophthalmol Clin North Am* 2002;15:17-25.
50. Laing RA, Leibowitz HM, Oak SS, Chang R, Berrospi AR, Theodore J. Endothelial mosaic in Fuchs' dystrophy. A qualitative evaluation with the specular microscope. *Arch Ophthalmol* 1981;99:80-83.
51. Kopplin LJ, Przepyszny K, Schmotzer B, et al. Relationship of Fuchs endothelial corneal dystrophy severity to central corneal thickness. *Arch Ophthalmol* 2012;130:433-439.
52. Lipman RM, Rubenstein JB, Torczynski E. Keratoconus and Fuchs' corneal endothelial dystrophy in a patient and her family. *Arch Ophthalmol* 1990;108:993-994.

53. Rao GP, Kaye SB, Agius-Fernandez A. Central corneal endothelial guttae and age-related macular degeneration: is there an association? *Indian J Ophthalmol* 1998;46:145-147.
54. Olsen T. Is there an association between Fuchs' endothelial dystrophy and cardiovascular disease? *Graefes Arch Clin Exp Ophthalmol* 1984;221:239-240.
55. Pitts JF, Jay JL. The association of Fuchs's corneal endothelial dystrophy with axial hypermetropia, shallow anterior chamber, and angle closure glaucoma. *Br J Ophthalmol* 1990;74:601-604.
56. Hodgkins PR, Vardy S, Teye-Botchway L, Morrell AJ, Baxter R. Blepharospasm and Fuchs' endothelial dystrophy. *Eye (Lond)* 1993;7 (Pt 6):808-809.
57. Buxton JN, Preston RW, Riechers R, Guilbault N. Tonography in cornea guttata. A preliminary report. *Arch Ophthalmol* 1967;77:602-603.
58. Roberts CW, Steinert RF, Thomas JV, Boruchoff SA. Endothelial guttata and facility of aqueous outflow. *Cornea* 1984;3:5-9.
59. Nagarsheth M, Singh A, Schmotzer B, et al. Relationship Between Fuchs Endothelial Corneal Dystrophy Severity and Glaucoma and/or Ocular Hypertension. *Arch Ophthalmol* 2012;1-5.
60. Kuwabara T, Quevedo AR, Cogan DG. An experimental study of dichloroethane poisoning. *Arch Ophthalmol* 1968;79:321-330.
61. Waring GO, Font RL, Rodrigues MM, Mulberger RD. Alterations of Descemet's membrane in interstitial keratitis. *Am J Ophthalmol* 1976;81:773-785.
62. Sekundo W, Lee WR, Kirkness CM, Aitken DA, Fleck B. An ultrastructural investigation of an early manifestation of the posterior polymorphous dystrophy of the cornea. *Ophthalmology* 1994;101:1422-1431.
63. McCartney AC, Kirkness CM. Comparison between posterior polymorphous dystrophy and congenital hereditary endothelial dystrophy of the cornea. *Eye (Lond)* 1988;2 (Pt 1):63-70.
64. Waring GO, 3rd. Posterior collagenous layer of the cornea. Ultrastructural classification of abnormal collagenous tissue posterior to Descemet's membrane in 30 cases. *Arch Ophthalmol* 1982;100:122-134.
65. Johnson BL, Brown SI. Posterior polymorphous dystrophy: a light and electron microscopic study. *Br J Ophthalmol* 1978;62:89-96.
66. Iwamoto T, DeVoe AG. Electron microscopic studies on Fuchs'combined dystrophy. I. Posterior portion of the cornea. *Invest Ophthalmol* 1971;10:9-28.
67. McCarey BE, Edelhauser HF, Lynn MJ. Review of corneal endothelial specular microscopy for FDA clinical trials of refractive procedures, surgical devices, and new intraocular drugs and solutions. *Cornea* 2008;27:1-16.
68. Bergmanson JP, Sheldon TM, Goosey JD. Fuchs' endothelial dystrophy: a fresh look at an aging disease. *Ophthalmic Physiol Opt* 1999;19:210-222.
69. Yuen HK, Rassier CE, Jardeleza MS, et al. A morphologic study of Fuchs dystrophy and bullous keratopathy. *Cornea* 2005;24:319-327.
70. Kayes J, Holmberg A. The Fine Structure of the Cornea in Fuchs' Endothelial Dystrophy. *Invest Ophthalmol* 1964;3:47-67.

71. Bourne WM, Johnson DH, Campbell RJ. The ultrastructure of Descemet's membrane. III. Fuchs' dystrophy. *Arch Ophthalmol* 1982;100:1952-1955.
72. Rodrigues MM, Krachmer JH, Hackett J, Gaskins R, Halkias A. Fuchs' corneal dystrophy. A clinicopathologic study of the variation in corneal edema. *Ophthalmology* 1986;93:789-796.
73. Kenney MC, Labermeier U, Hinds D, Waring GO, 3rd. Characterization of the Descemet's membrane/posterior collagenous layer isolated from Fuchs' endothelial dystrophy corneas. *Exp Eye Res* 1984;39:267-277.
74. Levy SG, Moss J, Sawada H, Dopping-Hepenstal PJ, McCartney AC. The composition of wide-spaced collagen in normal and diseased Descemet's membrane. *Curr Eye Res* 1996;15:45-52.
75. Jurkunas UV, Bitar M, Rawe I. Colocalization of increased transforming growth factor-beta-induced protein (TGFBIp) and Clusterin in Fuchs endothelial corneal dystrophy. *Invest Ophthalmol Vis Sci* 2009;50:1129-1136.
76. Riazuddin SA, Eghrari AO, Al-Saif A, et al. Linkage of a mild late-onset phenotype of Fuchs corneal dystrophy to a novel locus at 5q33.1-q35.2. *Invest Ophthalmol Vis Sci* 2009;50:5667-5671.
77. Shousha MA, Perez VL, Wang J, et al. Use of ultra-high-resolution optical coherence tomography to detect in vivo characteristics of Descemet's membrane in Fuchs' dystrophy. *Ophthalmology* 2010;117:1220-1227.
78. Johnson DH, Bourne WM, Campbell RJ. The ultrastructure of Descemet's membrane. II. Aphakic bullous keratopathy. *Arch Ophthalmol* 1982;100:1948-1951.
79. Bell KD, Campbell RJ, Bourne WM. Pathology of late endothelial failure: late endothelial failure of penetrating keratoplasty: study with light and electron microscopy. *Cornea* 2000;19:40-46.
80. Kenney MC, Atilano SR, Zorapapel N, Holguin B, Gaster RN, Ljubimov AV. Altered expression of aquaporins in bullous keratopathy and Fuchs' dystrophy corneas. *J Histochem Cytochem* 2004;52:1341-1350.
81. Ahuja Y, Baratz KH, McLaren JW, Bourne WM, Patel SV. Decreased corneal sensitivity and abnormal corneal nerves in Fuchs endothelial dystrophy. *Cornea* 2012;31:1257-1263.
82. Bramsen T, Stenbjerg S. Fibrinolytic factors in aqueous humour and serum from patients with Fuchs' dystrophy and patients with cataract. *Acta Ophthalmol (Copenh)* 1979;57:470-476.
83. Reiss GR, Bourne WM. Fuchs' dystrophy and serum fibrinogen degradation products. *Am J Ophthalmol* 1985;100:615-616.
84. Rosenthal WN, Blitzer M, Insler MS. Aqueous amino acid levels in Fuchs' corneal dystrophy. *Am J Ophthalmol* 1986;102:570-574.
85. Wilson SE, Bourne WM, Maguire LJ, et al. Aqueous humor composition in Fuchs' dystrophy. *Invest Ophthalmol Vis Sci* 1989;30:449-453.
86. Robinson MR, Streeten BW. Energy dispersive x-ray analysis of the cornea. Application to paraffin sections of normal and diseased corneas. *Arch Ophthalmol* 1984;102:1678-1682.

87. Szentmary N, Szende B, Suveges I. Epithelial cell, keratocyte, and endothelial cell apoptosis in Fuchs' dystrophy and in pseudophakic bullous keratopathy. *Eur J Ophthalmol* 2005;15:17-22.
88. Li QJ, Ashraf MF, Shen DF, et al. The role of apoptosis in the pathogenesis of Fuchs endothelial dystrophy of the cornea. *Arch Ophthalmol* 2001;119:1597-1604.
89. Miyake H, Hara I, Gleave ME, Eto H. Protection of androgen-dependent human prostate cancer cells from oxidative stress-induced DNA damage by overexpression of clusterin and its modulation by androgen. *Prostate* 2004;61:318-323.
90. Tuberville AW, Wood TO, McLaughlin BJ. Cytochrome oxidase activity of Fuchs' endothelial dystrophy. *Curr Eye Res* 1986;5:939-947.
91. Rosenblum P, Stark WJ, Maumenee IH, Hirst LW, Maumenee AE. Hereditary Fuchs' Dystrophy. *Am J Ophthalmol* 1980;90:455-462.
92. Afshari NA, Li YJ, Pericak-Vance MA, Gregory S, Klintworth GK. Genome-wide linkage scan in fuchs endothelial corneal dystrophy. *Invest Ophthalmol Vis Sci* 2009;50:1093-1097.
93. Louttit MD, Kopplin LJ, Igo RP, Jr., et al. A multicenter study to map genes for Fuchs endothelial corneal dystrophy: baseline characteristics and heritability. *Cornea* 2012;31:26-35.
94. Magovern M, Beauchamp GR, McTigue JW, Fine BS, Baumiller RC. Inheritance of Fuchs' combined dystrophy. *Ophthalmology* 1979;86:1897-1923.
95. Weiss JS, Moller HU, Lisch W, et al. The IC3D classification of the corneal dystrophies. *Cornea* 2008;27 Suppl 2:S1-83.
96. Gottsch JD, Sundin OH, Liu SH, et al. Inheritance of a novel COL8A2 mutation defines a distinct early-onset subtype of fuchs corneal dystrophy. *Invest Ophthalmol Vis Sci* 2005;46:1934-1939.
97. Aldave AJ, Rayner SA, Salem AK, et al. No pathogenic mutations identified in the COL8A1 and COL8A2 genes in familial Fuchs corneal dystrophy. *Invest Ophthalmol Vis Sci* 2006;47:3787-3790.
98. Wilson SE, Bourne WM, Brubaker RF. Effect of dexamethasone on corneal endothelial function in Fuchs' dystrophy. *Invest Ophthalmol Vis Sci* 1988;29:357-361.
99. Li JY, Terry MA, Goshe J, Shamie N, Davis-Boozer D. Graft rejection after Descemet's stripping automated endothelial keratoplasty: graft survival and endothelial cell loss. *Ophthalmology* 2012;119:90-94.
100. Proulx S, Haydari MN, Goyer B, et al. Reconstruction of a corneal endothelium using cells from patients with Fuchs endothelial corneal dystrophy. The Association for Research in Vision and Ophthalmology (ARVO) annual meeting 2012; 2012.
101. Engelmann K, Bednarz J, Valtink M. Prospects for endothelial transplantation. *Exp Eye Res* 2004;78:573-578.
102. Chen KH, Azar D, Joyce NC. Transplantation of adult human corneal endothelium ex vivo: a morphologic study. *Cornea* 2001;20:731-737.
103. Li W, Sabater AL, Chen YT, et al. A novel method of isolation, preservation, and expansion of human corneal endothelial cells. *Invest Ophthalmol Vis Sci* 2007;48:614-620.

104. Yokoo S, Yamagami S, Yanagi Y, et al. Human corneal endothelial cell precursors isolated by sphere-forming assay. *Invest Ophthalmol Vis Sci* 2005;46:1626-1631.
105. Ishino Y, Sano Y, Nakamura T, et al. Amniotic membrane as a carrier for cultivated human corneal endothelial cell transplantation. *Invest Ophthalmol Vis Sci* 2004;45:800-806.
106. Peh GS, Beuerman RW, Colman A, Tan DT, Mehta JS. Human corneal endothelial cell expansion for corneal endothelium transplantation: an overview. *Transplantation* 2011;91:811-819.
107. Blake DA, Yu H, Young DL, Caldwell DR. Matrix stimulates the proliferation of human corneal endothelial cells in culture. *Invest Ophthalmol Vis Sci* 1997;38:1119-1129.
108. Yue BY, Sugar J, Gilboy JE, Elvart JL. Growth of human corneal endothelial cells in culture. *Invest Ophthalmol Vis Sci* 1989;30:248-253.
109. Miyata K, Drake J, Osakabe Y, et al. Effect of donor age on morphologic variation of cultured human corneal endothelial cells. *Cornea* 2001;20:59-63.
110. Amano S. Transplantation of cultured human corneal endothelial cells. *Cornea* 2003;22:S66-74.
111. Pistsov MY, Sadovnikova E, Danilov SM. Human corneal endothelial cells: isolation, characterization and long-term cultivation. *Exp Eye Res* 1988;47:403-414.
112. Engelmann K, Friedl P. Optimization of culture conditions for human corneal endothelial cells. *In Vitro Cell Dev Biol* 1989;25:1065-1072.
113. Engelmann K, Friedl P. Growth of human corneal endothelial cells in a serum-reduced medium. *Cornea* 1995;14:62-70.
114. Choi JS, Williams JK, Greven M, et al. Bioengineering endothelialized neo-corneas using donor-derived corneal endothelial cells and decellularized corneal stroma. *Biomaterials* 2010;31:6738-6745.
115. Merjava S, Neuwirth A, Mandys V, Jirsova K. Cytokeratins 8 and 18 in adult human corneal endothelium. *Experimental eye research* 2009;89:426-431.
116. Lange TM, Wood TO, McLaughlin BJ. Corneal endothelial cell transplantation using Descemet's membrane as a carrier. *J Cataract Refract Surg* 1993;19:232-235.
117. Lai JY, Chen KH, Hsiue GH. Tissue-engineered human corneal endothelial cell sheet transplantation in a rabbit model using functional biomaterials. *Transplantation* 2007;84:1222-1232.
118. Yoeruek E, Saygili O, Spitzer MS, Tatar O, Bartz-Schmidt KU, Szurman P. Human anterior lens capsule as carrier matrix for cultivated human corneal endothelial cells. *Cornea* 2009;28:416-420.
119. Madden PW, Lai JN, George KA, Giovenco T, Harkin DG, Chirila TV. Human corneal endothelial cell growth on a silk fibroin membrane. *Biomaterials* 2011;32:4076-4084.
120. Mohay J, Lange TM, Soltau JB, Wood TO, McLaughlin BJ. Transplantation of corneal endothelial cells using a cell carrier device. *Cornea* 1994;13:173-182.
121. Griffith M, Osborne R, Munger R, et al. Functional human corneal equivalents constructed from cell lines. *Science* 1999;286:2169-2172.

122. Koizumi N, Sakamoto Y, Okumura N, et al. Cultivated corneal endothelial cell sheet transplantation in a primate model. *Invest Ophthalmol Vis Sci* 2007;48:4519-4526.
123. Engelmann K, Drexler D, Bohnke M. Transplantation of adult human or porcine corneal endothelial cells onto human recipients in vitro. Part I: Cell culturing and transplantation procedure. *Cornea* 1999;18:199-206.
124. Patel SV, Bachman LA, Hann CR, Bahler CK, Fautsch MP. Human corneal endothelial cell transplantation in a human ex vivo model. *Invest Ophthalmol Vis Sci* 2009;50:2123-2131.
125. Mimura T, Yamagami S, Usui T, et al. Long-term outcome of iron-endocytosing cultured corneal endothelial cell transplantation with magnetic attraction. *Exp Eye Res* 2005;80:149-157.
126. Amano S, Mimura T, Yamagami S, Osakabe Y, Miyata K. Properties of corneas reconstructed with cultured human corneal endothelial cells and human corneal stroma. *Jpn J Ophthalmol* 2005;49:448-452.
127. Wencan W, Mao Y, Wentao Y, et al. Using basement membrane of human amniotic membrane as a cell carrier for cultivated cat corneal endothelial cell transplantation. *Curr Eye Res* 2007;32:199-215.
128. Koizumi N, Sakamoto Y, Okumura N, et al. Cultivated corneal endothelial transplantation in a primate: possible future clinical application in corneal endothelial regenerative medicine. *Cornea* 2008;27 Suppl 1:S48-55.
129. Honda N, Mimura T, Usui T, Amano S. Descemet stripping automated endothelial keratoplasty using cultured corneal endothelial cells in a rabbit model. *Arch Ophthalmol* 2009;127:1321-1326.
130. Hogan MJ, Alvarado JA, Weddel JE. The cornea. In: Saunders WBC (ed), *Histology of the human eye: an Atlas and textbook.* Philadelphia.; 1971:55-111.
131. Maurice DM. The cornea and sclera. In: Davson H (ed), *The Eye.* Orlando, Florida: Academic Press; 1984.
132. Barfort P, Maurice D. Electrical potential and fluid transport across the corneal endothelium. *Experimental eye research* 1974;19:11-19.
133. Bonanno JA. Identity and regulation of ion transport mechanisms in the corneal endothelium. *Prog Retin Eye Res* 2003;22:69-94.
134. Proulx S, Bourget JM, Gagnon N, et al. Optimization of culture conditions for porcine corneal endothelial cells. *Molecular vision* 2007;13:524-533.
135. Matsuda M, Bourne WM. Long-term morphologic changes in the endothelium of transplanted corneas. *Arch Ophthalmol* 1985;103:1343-1346.
136. Klintworth GK. Corneal dystrophies. *Orphanet journal of rare diseases* 2009;4:7.
137. Bloomfield SE, Jakobiec FA, Iwamoto T, Harrison WG. Retrocorneal pigmentation secondary to iris stromal melanocytic proliferation. *Ophthalmology* 1981;88:1274-1280.
138. Van Horn DL, Sendele DD, Seideman S, Buco PJ. Regenerative capacity of the corneal endothelium in rabbit and cat. *Invest Ophthalmol Vis Sci* 1977;16:597-613.
139. Von Sallmann L, Caravaggio LL, Grimes P. Studies on the corneal endothelium of the rabbit. I. Cell division and growth. *Am J Ophthalmol* 1961;51:955-969.

140. Nakahori Y, Katakami C, Yamamoto M. Corneal endothelial cell proliferation and migration after penetrating keratoplasty in rabbits. *Jpn J Ophthalmol* 1996;40:271-278.
141. Brunette I, Rosolen SG, Carrier M, et al. Comparison of the pig and feline models for full thickness corneal transplantation. *Vet Ophthalmol* 2011;14:365-377.
142. Koizumi N, Okumura N, Kinoshita S. Development of new therapeutic modalities for corneal endothelial disease focused on the proliferation of corneal endothelial cells using animal models. *Exp Eye Res* 2012;95:60-67.
143. Insler MS, Lopez JG. Extended incubation times improve corneal endothelial cell transplantation success. *Invest Ophthalmol Vis Sci* 1991;32:1828-1836.
144. Insler MS, Lopez JG. Heterologous transplantation versus enhancement of human corneal endothelium. *Cornea* 1991;10:136-148.
145. Reichard M, Hovakimyan M, Wree A, et al. Comparative in vivo confocal microscopical study of the cornea anatomy of different laboratory animals. *Curr Eye Res* 2010;35:1072-1080.
146. Ohno K, Nelson LR, Mitooka K, Bourne WM. Transplantation of cryopreserved human corneas in a xenograft model. *Cryobiology* 2002;44:142-149.
147. Oh JY, Kim MK, Ko JH, et al. Histological differences in full-thickness vs. lamellar corneal pig-to-rabbit xenotransplantation. *Vet Ophthalmol* 2009;12:78-82.
148. Ohno K, Mitooka K, Nelson LR, Hodge DO, Bourne WM. Keratocyte activation and apoptosis in transplanted human corneas in a xenograft model. *Invest Ophthalmol Vis Sci* 2002;43:1025-1031.
149. Bahn CF, Grosserode R, Musch DC, et al. Effect of 1% sodium hyaluronate (Healon) on a nonregenerating (feline) corneal endothelium. *Invest Ophthalmol Vis Sci* 1986;27:1485-1494.
150. Lee SS, Kim H, Wang NS, et al. A pharmacokinetic and safety evaluation of an episcleral cyclosporine implant for potential use in high-risk keratoplasty rejection. *Invest Ophthalmol Vis Sci* 2007;48:2023-2029.
151. Huang PT, Nelson LR, Bourne WM. The morphology and function of healing cat corneal endothelium. *Invest Ophthalmol Vis Sci* 1989;30:1794-1801.
152. Petroll WM, Ma L, Jester JV, Cavanagh HD, Bean J. Organization of junctional proteins in proliferating cat corneal endothelium during wound healing. *Cornea* 2001;20:73-80.
153. Tuft SJ, Williams KA, Coster DJ. Endothelial repair in the rat cornea. *Invest Ophthalmol Vis Sci* 1986;27:1199-1204.
154. Ling TL, Vannas A, Holden BA. Long-term changes in corneal endothelial morphology following wounding in the cat. *Invest Ophthalmol Vis Sci* 1988;29:1407-1412.
155. Rao GN, Shaw EL, Arthur E, Aquavella JV. Morphological appearance of the healing corneal endothelium. *Arch Ophthalmol* 1978;96:2027-2030.
156. Joyce NC, Meklir B, Neufeld AH. In vitro pharmacologic separation of corneal endothelial migration and spreading responses. *Invest Ophthalmol Vis Sci* 1990;31:1816-1826.

157. Doughty MJ. Are there geometric determinants of cell area in rabbit and human corneal endothelial cell monolayers? *Tissue Cell* 1998;30:537-544.
158. Giasson CJ, Gosselin L, Masella A, Forcier P. Does endothelial cell density correlate with corneal diameter in a group of young adults? *Cornea* 2008;27:640-643.
159. Jackson AJ, Gardiner T, Archer DB. Morphometric analysis of corneal endothelial giant cells in normal and traumatized corneas. *Ophthalmic Physiol Opt* 1995;15:305-310.
160. Bahn CF, Glassman RM, MacCallum DK, et al. Postnatal development of corneal endothelium. *Invest Ophthalmol Vis Sci* 1986;27:44-51.
161. Franzen AA, Pigatto JA, Abib FC, Albuquerque L, Laus JL. Use of specular microscopy to determine corneal endothelial cell morphology and morphometry in enucleated cat eyes. *Vet Ophthalmol* 2010;13:222-226.
162. Kafarnik C, Fritsche J, Reese S. In vivo confocal microscopy in the normal corneas of cats, dogs and birds. *Vet Ophthalmol* 2007;10:222-230.
163. Gonzalez-Perez J, Gonzalez-Meijome JM, Rodriguez Ares MT, Parafita MA. Central corneal thickness measured with three optical devices and ultrasound pachometry. *Eye Contact Lens* 2011;37:66-70.
164. Hao GS, Zeng L, Li YR, Shui D. Agreement and repeatability of central corneal thickness measurement using the Pentacam and ultrasound pachymetry. *Zhonghua Yan Ke Za Zhi* 2011;47:142-145.
165. Bourne WM, Nelson LR, Buller CR, Huang PT, Geroski DH, Edelhauser HF. Long-term observation of morphologic and functional features of cat corneal endothelium after wounding. *Invest Ophthalmol Vis Sci* 1994;35:891-899.
166. Moodie KL, Hashizume N, Houston DL, et al. Postnatal development of corneal curvature and thickness in the cat. *Vet Ophthalmol* 2001;4:267-272.
167. Carrington SD, Woodward EG. Corneal thickness and diameter in the domestic cat. *Ophthalmic Physiol Opt* 1986;6:385-389.
168. Landry H, Aminian A, Hoffart L, et al. Corneal Endothelial Toxicity of Air and SF6. *Invest Ophthalmol Vis Sci* 2010.
169. Bahn CF, Meyer RF, MacCallum DK, et al. Penetrating keratoplasty in the cat. A clinically applicable model. *Ophthalmology* 1982;89:687-699.
170. Gospodarowicz D, Greenburg G, Alvarado J. Transplantation of cultured bovine corneal endothelial cells to species with nonregenerative endothelium. The cat as an experimental model. *Arch Ophthalmol* 1979;97:2163-2169.
171. Melles GR, Eggink FA, Lander F, et al. A surgical technique for posterior lamellar keratoplasty. *Cornea* 1998;17:618-626.
172. Melles GR, Lander F, van Dooren BT, Pels E, Beekhuis WH. Preliminary clinical results of posterior lamellar keratoplasty through a sclerocorneal pocket incision. *Ophthalmology* 2000;107:1850-1856; discussion 1857.
173. Terry MA, Ousley PJ. Deep lamellar endothelial keratoplasty in the first United States patients: early clinical results. *Cornea* 2001;20:239-243.
174. Terry MA, Ousley PJ. Replacing the endothelium without corneal surface incisions or sutures: the first United States clinical series using the deep lamellar endothelial keratoplasty procedure. *Ophthalmology* 2003;110:755-764; discussion 764.

175. EBAo -A. Eye Banking Statistical Report. 2007.
176. Terry MA, Shamie N, Chen ES, Hoar KL, Friend DJ. Endothelial keratoplasty a simplified technique to minimize graft dislocation, iatrogenic graft failure, and pupillary block. *Ophthalmology* 2008;115:1179-1186.
177. Ing JJ, Ing HH, Nelson LR, Hodge DO, Bourne WM. Ten-year postoperative results of penetrating keratoplasty. *Ophthalmology* 1998;105:1855-1865.
178. Melles GR, Ong TS, Ververs B, van der Wees J. Descemet membrane endothelial keratoplasty (DMEK). *Cornea* 2006;25:987-990.
179. McCauley MB, Price FW, Jr., Price MO. Descemet membrane automated endothelial keratoplasty: hybrid technique combining DSAEK stability with DMEK visual results. *J Cataract Refract Surg* 2009;35:1659-1664.
180. Guerra FP, Anshu A, Price MO, Price FW. Endothelial keratoplasty: fellow eyes comparison of Descemet stripping automated endothelial keratoplasty and Descemet membrane endothelial keratoplasty. *Cornea* 2011;30:1382-1386.
181. McCauley MB, Price MO, Fairchild KM, Price DA, Price FW, Jr. Prospective study of visual outcomes and endothelial survival with Descemet membrane automated endothelial keratoplasty. *Cornea* 2011;30:315-319.
182. Jun AS, Meng H, Ramanan N, et al. An alpha 2 collagen VIII transgenic knock-in mouse model of Fuchs endothelial corneal dystrophy shows early endothelial cell unfolded protein response and apoptosis. *Hum Mol Genet* 2011.
183. He Y, Weng J, Li Q, Knauf HP, Wilson SE. Fuchs' corneal endothelial cells transduced with the human papilloma virus E6/E7 oncogenes. *Exp Eye Res* 1997;65:135-142.
184. Goyer B, Haydari MN, Drouin OR, et al. Tissue engineering of a corneal endothelium using cells from patients with Fuchs endothelial corneal dystrophy. Tissue Engineering; 2012.
185. Schlaegel TJ. *Essentials of Uveities*. Boston: Brown & Co; 1969.
186. Bahn CF, MacCallum DK, Lillie JH, Meyer RF, Martonyi CL. Complications associated with bovine corneal endothelial cell-lined homografts in the cat. *Invest Ophthalmol Vis Sci* 1982;22:73-90.
187. Taylor MJ, Hunt CJ. Dual staining of corneal endothelium with trypan blue and alizarin red S: importance of pH for the dye-lake reaction. *Br J Ophthalmol* 1981;65:815-819.
188. Short BG. Safety evaluation of ocular drug delivery formulations: techniques and practical considerations. *Toxicol Pathol* 2008;36:49-62.
189. Iwamoto T, Smelser GK. Electron Microscopy of the Human Corneal Endothelium with Reference to Transport Mechanisms. *Invest Ophthalmol* 1965;4:270-284.
190. Kelliher C, Chakravarti S, Vij N, et al. A cellular model for the investigation of Fuchs' Endothelial Corneal Dystrophy. *Exp Eye Res* 2011;93:880-888.
191. Arnalich-Montiel F, Dart JK. Ipsilateral rotational autokeratoplasty: a review. *Eye (Lond)* 2009;23:1931-1938.
192. Jackel T, Knels L, Valtink M, Funk RH, Engelmann K. Serum-free corneal organ culture medium (SFM) but not conventional minimal essential organ culture medium

(MEM) protects human corneal endothelial cells from apoptotic and necrotic cell death. *Br J Ophthalmol* 2011;95:123-130.

193. Okumura N, Koizumi N, Ueno M, et al. The new therapeutic concept of using a rho kinase inhibitor for the treatment of corneal endothelial dysfunction. *Cornea* 2011;30 Suppl 1:S54-59.
194. Okumura N, Ueno M, Koizumi N, et al. Enhancement on primate corneal endothelial cell survival in vitro by a ROCK inhibitor. *Invest Ophthalmol Vis Sci* 2009;50:3680-3687.
195. Gorovoy MS. Descemet-stripping automated endothelial keratoplasty. *Cornea* 2006;25:886-889.
196. Matthaei M, Meng H, Meeker AK, Eberhart CG, Jun AS. Endothelial Cdkn1a (p21) overexpression and accelerated senescence in a mouse model of Fuchs endothelial corneal dystrophy. *Invest Ophthalmol Vis Sci* 2012;53:6718-6727.
197. Kampik D, Ali RR, Larkin DF. Experimental gene transfer to the corneal endothelium. *Exp Eye Res* 2011.
198. Fuchsluger TA, Jurkunas U, Kazlauskas A, Dana R. Anti-apoptotic gene therapy prolongs survival of corneal endothelial cells during storage. *Gene Ther* 2011;18:778-787.